



**Aus der Klinik für Dermatologie, Allergologie und Venerologie
der Universität zu Lübeck
Direktor: Prof. Dr. med. D. Zillikens**

**Die Rolle des zellulären Metabolismus in der
Epidermolysis bullosa acquisita**

INAUGURALDISSERTATION

zur

Erlangung der Doktorwürde
der Universität zu Lübeck

- Aus der Sektion Medizin -

vorgelegt von

Aleksandra Derenda-Hell

aus Bydgoszcz, Polen

Lübeck 2021

1. Berichtstatter: Prof. Dr. med. Christian Sadik
2. Berichtstatter: Priv.-Doz. Dr. Yves Laumonier
Tag der mündlichen Prüfung: 20.04.2022
Zum Druck genehmigt. Lübeck, den 20.04.2022
-Promotionskommission der Sektion Medizin-

ABSTRACT

Bullous pemphigoid-like epidermolysis bullosa acquisita (EBA) is an autoimmune disease characterized by autoantibodies directed against type VII collagen, resulting in the formation of mucocutaneous blisters. Commonly used therapy with immunosuppressants and corticosteroids is nonspecific and prone to side effects and remissions. The EBA pathogenesis is predominantly neutrophil-driven, however their metabolism as the potential therapeutic target is still unexplored.

Previous work from our group demonstrated that treatment with metformin and 2-deoxy-glucose attenuated disease in the antibody-transfer induced EBA model. However, what mechanism of action was responsible for this amelioration was still unknown. Therefore, this thesis aimed to elucidate the underlying mechanism and extend research on that observation.

This thesis describes evidence that neutrophils stimulation with immune complexes (ICs) enhances aerobic glycolysis, which in turn leads to the release of reactive oxygen species (ROS) and leukotriene B₄ (LTB₄). Additionally, 2-deoxy-glucose and other inhibitors of glycolysis, such as heptelidic acid, gallofalvin and TEPP-46, inhibited the response of activated neutrophils. Furthermore, only a supra-pharmacological dose of metformin decreased the rate of oxidative phosphorylation (OXPHOS) and blunted neutrophil response to the stimulation with immune complexes, potentially as a result of low expression of organic cation transporters, which transport metformin into the cells. Likewise, the neutrophil response was inhibited by oligomycin, an OXPHOS inhibitor, suggesting that intact mitochondrial membrane potential is required for neutrophil response. An additional unexpected finding was that moxifloxacin, a fluoroquinolone antibiotic, suppressed the neutrophil response in the same way.

Moreover, the effect of 5' adenosine monophosphate-activated protein kinase (AMPK) activation, which is considered to be the major mechanism of action of metformin, was examined both *in vitro* and *in vivo* using nucleoside 5-aminoimidazole-4-carboxamide-1- β -D-ribofuranoside (AICAR), a direct activator of AMPK. In the *in vitro* experiments, AICAR demonstrated a trend towards stimulation of glycolysis and decreased OXPHOS. AICAR inhibited not only the release of ROS and LTB₄ from IC-activated neutrophils, but also the

formation of neutrophil extracellular traps (NETs). Moreover, AICAR inhibited C5a-mediated migration of neutrophils. Despite the evident *in vitro* effects of AICAR on IC-activated neutrophils, in the antibody-transfer induced EBA model AICAR induced only subtle improvement of BP-like EBA symptoms.

Collectively, this thesis highlights that modulating neutrophil metabolism may be a promising therapeutic target in BP-like EBA. More importantly, the compounds investigated in this work may serve as a foundation for further research and new treatment options not only for EBA, but also for other neutrophil-driven autoimmune diseases.

ZUSAMMENFASSUNG

Die Epidermolysis bullosa acquisita (EBA), eine dem bullösem Pemphigoid ähnliche Autoimmundermatose, die durch Autoantikörper charakterisiert ist, welche gegen Kollagen Typ VII gerichtet sind und zur Bildung von mukokutanen Blasen führen. Die derzeit am häufigsten verwendete Therapie basiert auf unspezifischen Immunsuppressiva und Kortikosteroiden, mit vielen Nebenwirkungen und höherer Wahrscheinlichkeit von Remissionen. Die EBA-Pathogenese wird überwiegend von neutrophilen Granulozyten dominiert, deren Metabolismus als potenzielles therapeutisches Ziel jedoch noch weitgehend unerforscht ist.

Vorhergegangene Studien in der Klinik für Dermatologie am UKSH in Lübeck haben gezeigt, dass im Mausmodell der Antikörpertransfer-induzierten EBA die Behandlung mit Metformin und 2-Deoxy-Glukose die Krankheit abschwächt. Welcher Wirkmechanismus für diese Krankheitslinderung verantwortlich ist, ist jedoch noch unbekannt. Ziel dieser Arbeit war es, diesen Mechanismus zu untersuchen und die Forschung auf dem Gebiet des Immunmetabolismus zu erweitern.

In dieser Arbeit konnte gezeigt werden, dass die Stimulation von Neutrophilen mit Immunkomplexen die aerobe Glykolyse steigert und gleichzeitig zur Freisetzung von reaktiven Sauerstoffspezies (ROS) und Leukotrien B₄ (LTB₄) führt. 2-Deoxy-Glukose und andere Inhibitoren der Glykolyse, wie Heptelidsäure, Gallofalvin und TEPP-46, hemmten dagegen die Reaktion der aktivierten Neutrophilen. Darüber hinaus war es nur mittels einer supra-pharmakologische Dosis von Metformin möglich die Rate der oxidativen Phosphorylierung (OXPHOS) zu senken und die Reaktion der neutrophilen Granulozyten auf die Stimulation mit Immunkomplexen abzuschwächen. Die hohe Dosis war möglicherweise auf Grund der schwachen Expression von organischen Kationentransportern, welche Metformin in die Zellen transportieren, notwendig. Gleichmaßen wurde die Zellaktivierung der neutrophilen Granulozyten durch Oligomycin, einem OXPHOS-Inhibitor, gehemmt, was darauf hindeutet, dass ein intaktes mitochondriales Membranpotential für die neutrophile Antwort erforderlich ist. Ein zusätzliches unerwartetes Ergebnis war, dass Moxifloxacin, ein Fluorchinolon-Antibiotikum, die Zellaktivierung der neutrophilen Granulozyten auf die gleiche Weise unterdrückte.

Zudem wurde die Wirkung der 5'-Adenosinmonophosphat-aktivierten Proteinkinase (AMPK)-Aktivierung, welche als Hauptwirkungsmechanismus von Metformin angesehen wird, sowohl *in vitro* als auch *in vivo* untersucht, unter Verwendung des Nukleosids 5-Aminoimidazol-4-carboxamid-1- β -D-ribofuranosid (AICAR), einem direkten Aktivator der AMPK. In *in-vitro*-Experimenten konnte in dieser Arbeit gezeigt werden, dass AICAR eine Tendenz zeigte die Glykolyse zu stimulieren und die OXPHOS zu senken. Gleichzeitig hemmte AICAR nicht nur die Freisetzung von ROS und LTB₄ aus aktivierten neutrophilen Granulozyten, sondern auch die Bildung von neutrophilen extrazellulären Fallen (NETs, neutrophil extracellular traps). Trotz der eindeutigen *in vitro* Effekte von AICAR auf aktivierte neutrophile Granulozyten, konnte im Antikörper-Transfermodell der EBA nur eine subtile Verbesserung der Krankheitssymptome durch Behandlung mit AICAR gemessen werden. Schlussendlich dient diese Arbeit und die darin untersuchten Substanzen als Grundlage für weitere Forschungen und neue Behandlungsmöglichkeiten, nicht nur für EBA, sondern auch für andere neutrophil getriebene Autoimmunerkrankungen.

TABLE OF CONTENTS

ABSTRACT	III
ZUSAMMENFASSUNG	V
TABLE OF CONTENTS	VII
LIST OF FIGURES.....	X
LIST OF TABLES.....	XI
ABBREVIATIONS.....	XII
1 INTRODUCTION	1
1.1 Autoimmune bullous skin diseases	1
1.2 Epidermolysis bullosa acquisita (EBA)	1
1.2.1 Pathophysiology	2
1.2.2 Clinical presentation	9
1.2.3 Diagnosis.....	12
1.2.4 Treatment	12
1.3 Experimental models of EBA	15
1.3.1 Immunization-induced EBA	15
1.3.2 Antibody transfer-induced EBA	15
1.4 Immunometabolism	16
1.4.1 Neutrophils and their role in immunometabolism	18
1.5 Metformin.....	19
1.5.1 Mechanisms of action.....	20
1.6 Aim of the study.....	23
2 MATERIALS AND METHODS	24
2.1 Materials.....	24
2.1.1 Mice	24
2.1.2 Laboratory equipment.....	24
2.1.3 Disposable materials.....	25

2.1.4	Chemicals.....	26
2.1.5	Comercial buffers and solutions.....	28
2.1.6	Antibodies.....	28
2.1.7	Primers used for RT-qPCR.....	29
2.1.8	Kits and others.....	30
2.1.9	Self-made buffers and solutions.....	30
2.2	Methods.....	31
2.2.1	Generation of affinity purified rabbit anti-murine COL7C IgG.....	31
2.2.2	Induction of antibody transfer EBA mouse model.....	31
2.2.3	Evaluation of disease severity in antibody transfer EBA mouse model.....	32
2.2.4	Flow cytometry analysis of skin samples.....	33
2.2.5	Isolation of murine bone marrow.....	34
2.2.6	Isolation of neutrophils using MACS.....	34
2.2.7	ROS Release assay upon stimulation with fixed immune complexes.....	36
2.2.8	LTB ₄ competitive enzyme immunoassay.....	36
2.2.9	Metabolic analysis of murine neutrophils.....	37
2.2.10	Sytox Green.....	38
2.2.11	Immunohistochemistry.....	39
2.2.12	RNA isolation from skin samples.....	40
2.2.13	RNA isolation from cells.....	41
2.2.14	cDNA synthesis.....	41
2.2.15	Real time quantitative PCR (RT-qPCR).....	42
2.2.16	Migration Assay.....	42
2.2.17	Cytotoxicity Assay.....	43
2.2.18	Statistical analysis.....	46
3	RESULTS	47
3.1	Mechanisms of metformin and 2-DG action in the BP-like EBA mouse model ..	47
3.2	Gene expression of metformin and glucose receptors in murine neutrophils ..	50

3.3	Metabolic activity of neutrophils in response to ICs and metformin.....	51
3.3.1	The effect of immune complexes and metformin on the glycolytic activity of murine bone marrow-derived neutrophils.....	52
3.3.2	The effect of immune complexes and metformin on the mitochondrial respiration of murine bone marrow-derived neutrophils.....	54
3.4	The effect of metformin, 2-DG and oligomycin on the IC-triggered release of ROS and LTB ₄ from murine neutrophils.....	56
3.5	Pharmacological targeting of aerobic glycolysis.....	58
3.6	The inhibitory effect of moxifloxacin on the IC-triggered release of ROS and LTB ₄ from murine neutrophils	61
3.7	Neutrophil metabolic activity in response to ICs and AICAR.....	63
3.8	The effect of AICAR on the IC-triggered release of ROS and LTB ₄ from murine neutrophils.....	66
3.9	The effect of AICAR on NETs.....	69
3.10	Stimulus dependent inhibition on neutrophil migration by AICAR.....	71
3.11	The effect of AICAR in the antibody transfer model of BP-like EBA.....	72
4	DISCUSSION.....	75
4.1	Neutrophil glucose metabolism as a target in BP-like EBA	75
4.2	The role of activated AMPK in the EBA	84
4.3	Summary.....	89
5	REFERENCES	91
6	APPENDIX.....	109
6.1	Publications.....	109
6.2	Approvals	109
7	ACKNOWLEDGEMENTS	110
8	CURRICULUM VITAE.....	111

LIST OF FIGURES

Figure 1. Clinical characteristics of Epidermolysis bullosa acquisita (EBA).....	11
Figure 2. Metformin and 2-DG ameliorate BP-like EBA.	20
Figure 3. Representative murine bone marrow-derived neutrophils purity after isolation using MACS.	35
Figure 4. Drugs used in in vitro experiments are not cytotoxic.	45
Figure 5. Cellular infiltration of the perilesional skin and expression of the genes involved in the skin inflammation.....	49
Figure 6. mRNA expression of select genes in murine neutrophils, liver, and kidney tissue.	51
Figure 7. Stimulation of neutrophils with ICs enhances aerobic glycolysis, whereas metformin does not affect it.	53
Figure 8. Metformin reduces mitochondrial respiration in murine BM-derived neutrophils.	55
Figure 9. Metformin, 2-DG and oligomycin inhibit the release of ROS and LTB ₄ from murine BM-derived neutrophils.....	57
Figure 10. Aerobic glycolysis contributes to the response of neutrophils to immune complexes.....	60
Figure 11. Moxifloxacin inhibits ROS and LTB ₄ release in a dose-dependent manner from murine BM-derived neutrophils.....	62
Figure 12. AICAR affects murine BM-derived neutrophil metabolism.	65
Figure 13. AICAR inhibits the release of ROS and LTB ₄ from murine BM-derived neutrophils.....	68
Figure 14. AICAR inhibits murine NETs formation.	70
Figure 15. AICAR inhibits C5a-mediated, but does not alter LTB ₄ -mediated, migration of murine BM-derived neutrophils.....	71
Figure 16. AICAR treatment does not ameliorate disease in the antibody transfer model of BP-like EBA.....	74

LIST OF TABLES

Table 1. Other cell types involved in the effector phase	8
Table 2. New therapeutic options that have been successful in mouse models of epidermolysis bullosa acquisita.....	13
Table 3. Effects of AMPK activation on cellular metabolism.	22
Table 4. Scoring table used to determine the disease severity in antibody-transfer EBA (ery: erythema; cru: crusts; alo: alopecia; ero: erosions).	33

ABBREVIATIONS

12/15-LO	Leukocyte-type 12/15-lipoxygenase
2-DG	2-deoxy-D-glucose
AAb	autoantibody
Ab; Abs	antibody; antibodies
ABSA	affected body surface area
ACC	acetyl-CoA carboxylase
ADP	adenosine diphosphate
AIBD(s)	autoimmune blistering skin disease (s)
AICAR	5-Aminoimidazole-4-carboxamide-1- β -D-ribofuranoside
Akt	protein kinase B
ALDOA	aldolase A
AMP	adenosine monophosphate
AMPK	5' AMP-activated protein kinase
APC	allophycocyanin
APCs	antigen-presenting cells
ATGL	adipose triglyceride lipase
ATP	adenosine triphosphate
AUC	area under curve
BLT1	leukotriene receptor 1
BM	bone marrow
BMZ	basement membrane zone
BP	bullous pemphigoid
BSA	bovine serum albumin
C3	complement component 3
C5a	complement component 5 a
C5aR	complement 5 a receptor 1
cAMP	cyclic adenosine monophosphate
CARD9	caspase recruitment domain-containing protein 9
CCL	C-C chemokine ligand
CD	cluster of differentiation
CEJ	cementoenamel junction
CL	chemiluminescence
COL7	type VII collagen
COL7A1	collagen type VII alpha 1 chain
CPT-1	carnitine palmitoyltransferase I
CRTC2	CREB regulated transcription coactivator 2
CXCL	C-X-C motif chemokine ligand
CXCR	C-X-C chemokine receptor
DDW	double distilled water
DEJ	dermal-epidermal junction
DF	dimethyl fumarate
DIF	direct immunofluorescence
EBA	epidermolysis bullosa acquisita
ECAR	cellular acidification rate

eEF2	eukaryotic elongation factor 2
ELISA	enzyme-linked immunosorbent assay
ERK	extracellular-signal-regulated kinase
FA	fatty acid
FACS	fluorescence-activated cell sorting
FADH	flavin adenine dinucleotide
Fc	fragment crystallizable region
FC	flow cytometry
FCCP	Carbonyl cyanide-p-trifluoromethoxyphenylhydrazone
FcRn	neonatal Fc receptor
FCS	fetal calf serum
FcγR(s)	Fc gamma receptor(s)
FITC	Fluorescein isothiocyanate
Fli1	actin-remodeling protein flightless I
FoxP3	forkhead box protein P3
GAPDH	glyceraldehyde 3-phosphate dehydrogenase
GF	galloflavin
GLUT	glucose transporter
GM-CSF	granulocyte-macrophage colony-stimulating factor
GPAT	glycerol-3-phosphate acyltransferase
HA	heptelidic acid
HCA2	hydroxycarboxylic acid receptor 2
HCK	hematopoietic cell kinase
HLA	human leukocyte antigen
HMG-CoA	β-Hydroxy β-methylglutaryl-CoA
HNF	hepatocyte nuclear factor
HSA	human serum albumin
Hsp90	heat-shock protein 90
i.p.	intraperitoneal
IC(s)	immuno-complex(es)
IF	immunofluorescence
IFN	interferon
Ig	immunoglobulin
IHC	immunohistochemistry
IIF	indirect immunofluorescence
IL	interleukin
IVIG	intravenous immunoglobulins
LDH	lactate dehydrogenase
LO	lipoxygenase
LPS	lipopolysaccharide
LTB4	leukotriene LTB4
Ly6G	lymphocyte antigen 6 complex locus G6D
MAPK	mitogen activated protein kinase
MHC	major histocompatibility complex
MM-EBA	mucous membrane EBA
MMP	matrix metalloproteinase
mRNA	messenger RNA

mTOR	mechanistic target of rapamyci
NADH	nicotinamide adenine dinucleotide
NADPH	nicotinamide adenine dinucleotide phosphate
NC	non-collagenous domain
NETs	neutrophil extracellular traps
NFκB	nuclear factor kappa-light-chain-enhancer of activated B cells
NGS	normal goar serum
NK cells	natural killer cells
NOX2	NADPH oxidase 2
OCR	oxygen consumption rate
OCTs	organic cation transporters
OXPHOS	oxidative phosphorylation
PBS	phosphate-buffered saline
PCK2	phosphoenolpyruvate carboxykinase 2
PCR	polymerase chain reaction
PDE4	phosphodiesterase 4
PDH	pyruvate dehydrogenase
PDs	pemphigoid diseases
PE	phycoerythrin
PerCP	peridinin chlorophyll protein
PFK	phosphofructokinase
PG(s)	prostaglandin(s)
PGC	peroxisome proliferator-activated receptor gamma coactivator
PGI	phosphoglucose isomerase
PI3Kβ	phospho inositol 3 kinase β
PKC	protein kinase C
PKM2	pyruvate kinase M2
PMNs	polymorphonuclear leukocytes
RA	rheumatoid arthritis
RFU	relative fluorescent units
RORα	retinoid-related orphan nuclear receptor alpha
ROS	reactive oxygen species
RT	room temperature
RT-qPCR	Real time quantitative PCR
s.c.	subcutaneous
SEM	standard error of mean
SIRT	sirtuin
SYK	spleen tyrosine kinase
TCA cycle	tricarboxylic acid cycle
TGF-β	transforming growth factor-β
Th cells	T helper cells
TIF	transcription intermediary factor
TNF	tumour necrosis factor
Tregs	regulatory T cells
TSC2	tuberous Sclerosis Complex 2
TXNIP	thioredoxin Interacting Protein
ULK1	unc-51 like autophagy activating kinase

WT	wild-type
YT-1	2-Phenyl-4-quinolone
ZMP	5-amino-4-imidazolecarboxamide riboside 5'-monophosphate

1 INTRODUCTION

1.1 Autoimmune bullous skin diseases

Autoimmune bullous skin diseases (AIBDs) are a group of rare, organ-specific, usually chronic conditions, characterized by autoantibodies (AABs) directed against structural proteins of the skin and/or mucous membranes (Saschenbrecker et al., 2019). Clinically, AIBDs manifest predominantly as blisters and erosions on the skin and mucous membranes (Schmidt and Zillikens, 2011). AIBDs pathogenesis is based on specific autoantibodies, which bind to adhesion molecules of the skin, leading to the loss of epidermal interkeratinocyte or dermo-epidermal adhesion. Consequently, the adhesive functions are disrupted, resulting in splitting and blister formation (Saschenbrecker et al., 2019). Depending on whether the skin has been affected within the epidermis or the dermal-epidermal junctions, blistering skin diseases can be divided into two groups (Damoiseaux, 2013). In the pemphigus group (including pemphigus vulgaris, pemphigus foliaceus, paraneoplastic pemphigus, and IgA pemphigus), autoantibodies are directed against desmosomal proteins, which results in the loss of connection between adjacent keratinocytes, resulting in the formation of loose and delicate intraepidermal blisters (Schmidt and Zillikens, 2011). In the pemphigoid group, the autoantibodies target hemidesmosomal proteins and type VII collagen, occurring in a de-adhesion of basal keratinocytes from the basement membrane and creation of tense subepidermal blisters (Damoiseaux, 2013). The pemphigoid group includes many disease entities, of which the most important representative for this dissertation is epidermolysis bullosa acquisita (EBA).

1.2 Epidermolysis bullosa acquisita (EBA)

Epidermolysis bullosa acquisita (EBA) is a rare, severe, acquired autoimmune bullous dermatosis that affects the skin and mucous membrane and is characterized by subepidermal blistering. The first patient with a non-hereditary variant of EBA was described by Elliot over a century ago (Koga et al., 2019). The prevalence of EBA worldwide is estimated between 0.2 and 0.5 per million inhabitants per year (Bertram et al., 2009; Gupta et al., 2012; Hübner et al., 2016). In recent years, the incidence of EBA in Germany has been reported to be 2.84 per million inhabitants (Hübner et al., 2016). EBA can occur

at any age, but the average age of onset is estimated to be between 40 and 50 years of age (Gupta et al., 2012; Hübner et al., 2016). There is no gender or racial predilection, although higher prevalence in African and Korean populations has been reported (Lee, 1998; Schmidt and Zillikens, 2013).

Like many autoimmune diseases, EBA is associated with other systemic disorders. The most frequently correlated condition with EBA is inflammatory bowel disease, especially Crohn's disease (Chen et al., 2002; Hundorfean et al., 2010). It has been reported the coexistence of other various diseases such as psoriasis, systemic or cutaneous lupus erythematosus, rheumatoid arthritis, diabetes mellitus, Hashimoto's thyroiditis, amyloidosis (Gupta et al., 2012; Ishii et al., 2010a; Lee, 1998). However, due to the rare incidence of EBA, these data are anecdotal.

The direct cause of most autoimmune diseases is unidentified. As to EBA, the collected data suggest that the combination of genetic and environmental factors may trigger the disease (Koga et al., 2019).

1.2.1 Pathophysiology

1.2.1.1 Type VII Collagen as the autoantigen in EBA

One of the major breakthroughs in understanding EBA's pathogenesis came via the discovery of type VII Collagen (COL7) as an autoantigen in EBA. In 1984 Woodley et al. identified a 290-kDa protein in the basement membrane of the skin and described the carboxyl terminus of COL7 four years later as the autoantigen in EBA (Woodley et al., 1988, 1984). COL7 is an extracellular adhesion molecule in the epithelial basement membrane and is the major component of anchoring fibrils which provide cohesion in dermal-epidermal junction (DEJ) (Ishii et al., 2010). Except for the basement membrane of the skin, COL7 is also expressed in the esophagus, oral mucosa, cervix, anal canal, cornea and chorioamnion (Chung and Uitto, 2010). COL7, encoded by the COL7A1 gene, is a homotrimer composed of three identical α -chains, each containing a central triple-helical collagenous domain, flanked by NC1 (145 kDa) and NC2 (34 kDa) non-collagenous domains at the amino- and carboxy-terminus, respectively (Chung and Uitto, 2010; Kasperkiewicz et al., 2016). Although, anti-COL7 IgG are the most prevalent autoantibodies in EBA, small

subset of patients present anti-COL7 IgA autoantibodies either as the only Ig class or in combination with IgG autoantibodies (Ludwig, 2013). The epitope mapping of human and murine sera from EBA, revealed that most of the antibodies bind the amino-terminal domain NC1, which initiate the recruitment of immune cells (Ludwig, 2013). Subsequently, the anchoring complexes are degraded, the adhesion between the epidermis and the dermis is disrupted, creating subepidermal blisters (Schmidt and Zillikens, 2013).

1.2.1.2 Afferent phase: generation of autoantibodies directed against COL7

1.2.1.2.1 Genetic and environmental factors

Although EBA is usually an acquired disease, data suggest that a certain genetic predisposition and environmental factors also contribute to EBA pathogenesis (Koga et al., 2019). It has been shown that a loss of tolerance to COL7 is associated with genes both inside and outside the major histocompatibility complex (MHC) locus. Specifically, an association with the MHC haplotype, in particular HLA-DR2 (Gammon et al., 1988) and HLA-DRB1 *15:03 (Zumelzu et al., 2011). Furthermore, it has been reported that black-skinned patients carrying the risk allele HLA-DRB1*15:03 seem to be more susceptible to develop EBA (Zumelzu et al., 2011). Moreover, several EBA cases have been observed within the family, suggesting a genetic control of EBA (Noe et al., 2008). The genetic predisposition has been confirmed in immunization-induced EBA, in which 75% of mice carrying MHC haplotype H2S developed symptoms of the disease (Ludwig et al., 2011). Furthermore, a quantitative trait loci mapping determined several non-MHC genes located on specific chromosomes that are linked to the onset of EBA (Ludwig et al., 2012). In addition to genetic factors, gene-microbiota interactions affect the development of symptoms in immunization-induced EBA. More specifically, a higher richness and diversity of skin microbiota before immunization is associated with the lower probability of developing symptoms of EBA after immunization (Ellebrecht et al., 2016; Srinivas et al., 2013).

1.2.1.2.2 Induction (afferent) phase: break of tolerance to COL7

In the induction phase, autoantibodies against collagen VII are produced, which leads to a loss of tolerance to COL7. Autoreactive T cells recognizing the NC1 domain of COL7 have been described in EBA patients (Müller et al., 2010). In immunization-induced EBA mouse

model, it has been shown that depletion of CD4⁺ T cells led to a delay in the production of anti-COL7 autoantibodies and thus also to disease onset, whereas CD8⁺ T cells depletion had no effect (Iwata et al., 2013). Furthermore, it has been shown that a T helper type 1 (Th1)-like cytokine profile with an increased IFN- γ /IL-4 ratio in draining lymph node is associated with a clinical manifestation of an immunization-induced EBA, while a Th2-like cytokine gene expression leads to resistance to disease induction (Hammers et al., 2011). To determine which antigen-presenting cells (APCs) are relevant for the formation of CD4⁺ T cells, certain cell subsets have been depleted in immunization-induced EBA in mice. Based on cell-depletion results of B cells, dendritic cells, and macrophages, the antigen-specific CD4⁺ T cell response was suppressed. Hence, the presence of these specific APCs is immanent for development of COL7-specific CD4⁺ T cells (Iwata et al., 2013). Additionally, scurfy mice that lacked regulatory T cells (T_{regs}) developed blisters by producing pathogenic autoantibodies (Haeberle et al., 2018; Koga et al., 2019; Muramatsu et al., 2018).

The involvement of neutrophils in the production of autoantibodies has been also evaluated. In immunization-induced EBA, neutrophil-depleted mice generated less COL7 autoantibodies which was associated with reduced neutrophils numbers in draining lymph nodes. Moreover, the same effect was observed in granulocyte-macrophage colony-stimulating factor (GM-CSF) deficient mice and more interestingly, an additive effect was observed in the absence of neutrophils (Samavedam et al., 2014).

Apart from COL7, another protein involved in the production of AAbs is heat-shock protein 90 (Hsp90). In immunization-induced EBA, the pharmacological inhibition of Hsp90 suppressed the production of AAbs. More interestingly, the injected mice with Hsp90 inhibitors prior immunization with COL7 developed significantly reduced disease symptoms (Kasperkiewicz et al., 2011).

1.2.1.2.3 Presence of autoantibodies in the vasculature

In immunization-induced EBA mouse model, autoreactive B cells differentiate into autoantibody-producing plasma cells, which form mainly IgG antibodies. Until now, COL7-specific plasma cells have been only detected in peripheral lymph nodes, as opposed to antigen-specific T cells (Tiburzy et al., 2013). The maintenance of autoantibodies occurs either through continuous activation of B cells resulting in the formation of short-lived (few

days) plasma cells or through the persistence of long-lived (month or years) plasma cells (Tiburzy et al., 2013). After the antibodies enter the blood circulation from the lymph nodes, their half-life is largely determined by the expression of the neonatal Fc receptor (FcRn), an MHC class I-like molecule which among other functions protects IgGs and albumins from catabolism (Kuo et al., 2010). In experimental EBA, the blockade of FcRn led to lowered levels of autoantibodies by stimulating their catabolism and thus, shortening IgGs half-life, which in result protected mice from tissue injury (Sesarman et al., 2008).

1.2.1.3 Effector (efferent) phase

1.2.1.3.1 Complement

The effector phase is initiated by anti-COL7 autoantibodies binding at the NC1 domain of the COL7 at the DEJ. After injecting the mice with anti-COL7 IgG antibodies, direct immunofluorescence (DIF) microscopy showed a binding of COL7-specific autoantibodies at the murine DEJ within 24 hours (Ishii et al., 2011). Later, via the Fc domain of complement-fixing antibodies, such as IgG1, IgG3 in humans (Recke et al., 2010) and IgG2a, IgG2b in mice (Sitaru et al., 2006), the complement system is activated generating a pro-inflammatory milieu. One of the most significant complement factors are C3, of which linear deposits were detected at the DEJ in immunization-induced EBA (Sitaru et al., 2006) and C5a - a chemoattractant for neutrophils, mast cells, and monocytes (Mihai et al., 2018). More interestingly, both C5a-deficient and C5aR1-deficient mice were protected from the induction of blister formation (Mihai et al., 2018; Sitaru et al., 2005). Furthermore, examination of another complement activation pathways has showed the following: factor B-deficient mice (alternative pathway) and less extensive C1q-deficient mice (classical pathway) showed clinically relevant amelioration of disease activity, whereas mannan-binding lectin (MBL)-deficient mice (lectin pathway) developed a similar EBA phenotype to the wild-type (WT) controls (Mihai et al., 2007).

1.2.1.3.2 Neutrophils

Studies on BP-like EBA have shown that neutrophils are the main factor responsible for blister formation (Sezin et al., 2017). It has been suggested that cleavage products of complement activation, such as C5a, mediate CD18-dependent neutrophil recruitment into

the skin (Ludwig, 2013). In antibody transfer-induced EBA, the CD18 (integrin $\beta 2$)-deficient mice were completely resistant to skin blistering due to the lack of neutrophil extravasation to the site of inflammation (Chiriac et al., 2007). Moreover, it has been shown recently, that CD18 plays a central role in regulating neutrophil adhesion, more specifically inhibition of $\beta 2$ -integrins and thus the inhibition of neutrophil adhesion, which prevents tissue damage, both in the *in vitro* and *ex vivo* models of EBA (Yu et al., 2018). Additionally, the up-regulation of GM-CSF, CXCL1/2, TNF- α , HSP90, IL-1 α/β and LTB $_4$ is linked to neutrophil-induced blister formations in experimental EBA (Hirose et al., 2013, 2016; Sadeghi et al., 2015; Samavedam et al., 2014; Sezin et al., 2017; Tukaj et al., 2015), whereas IL-10 show anti-inflammatory activity by inhibiting neutrophil migration (Kulkarni et al., 2016).

After neutrophils are recruited to the skin, they are activated via an Fc γ receptors (Fc γ R) – dependent process. Activation of C5aR induces the upregulation of activating Fc γ Rs and downregulation of inhibitory Fc γ RIIB on neutrophils (Karsten and Köhl, 2012). When IgG autoantibodies bind to NC1 domain of the COL7 at the DEJ, an immune complex is created, to which neutrophil bind via Fc γ R. Fc γ Rs belong to the family of Fc receptors for IgG, they are expressed by innate immune effector cells such as basophils, mast cells, monocytes, macrophages and neutrophils. In mice neutrophils express mainly the inhibitory Fc γ RIIB and the activating Fc γ RIII and Fc γ RIV (Nimmerjahn and Ravetch, 2008). In the transfer model of EBA in mice lacking the common γ -chain of all the activating Fc γ Rs or the Fc γ RIV – deficient mice were protected from disease induction, while the mice lacking Fc γ RIIB manifested increased skin inflammation compared to WT mice (Kasperkiewicz et al., 2012).

Once the neutrophils are activated, a signaling cascade is triggered. Neutrophil cell surface receptors initiate signal transduction pathways, in which signaling molecules crucial in the pathogenesis of EBA are involved. In detail, the depletion or pharmacological inhibition of the p38 MAPK, ERK1/2, AKT, PI3K β , Hsp90, ROR α , PDE4, Src kinases (including Hck, Fgr and Lyn), SYK and CARD9 protected mice partially or completely from blistering in antibody transfer-induced EBA (Hellberg et al., 2013; Koga et al., 2016; Kovács et al., 2014; Kulkarni et al., 2011; Németh et al., 2016, p. 9; Sadeghi et al., 2015; Samavedam et al., 2018, p. 2016; Tukaj et al., 2015).

In experimental models of EBA, it has been demonstrated that one of the key processes leading to the formation of dermal-subepidermal separation is the release of reactive oxygen species (ROS) by activated neutrophils (Kulkarni et al., 2011). Reactive oxygen species (ROS) are defined as reactive oxygen radicals as well as some nonradical derivatives of molecular oxygen (Halliwell, 2006). They are produced during the mitochondrial electron transport of aerobic respiration but also via cellular responses to xenobiotics, cytokines, and bacterial invasion (Ray et al., 2012). ROS play a multitude of roles in a number of biological processes including phagocytosis, cell signaling, apoptosis, necrosis, gene expression, activation of cell signaling cascades (Hancock et al., 2001). Additionally, the release of ROS is one of the main causes of DEJ separation and consequently the formation of blisters in the antibody-mediated EBA model (Chiriac et al., 2007). In neutrophils the majority of ROS is produced through the NADPH oxidase (NOX2). Mice lacking neutrophil cytosolic factor 1 showed absence of functional NADPH, which is an enzyme that catalyzes the production of superoxide from oxygen, resulting in skin blistering resistance (Chiriac et al., 2007).

Furthermore, lipid mediator leukotriene B₄ (LTB₄), a chemoattractant for neutrophils and eosinophils, regulates numerous cellular functions such as chemotaxis, adhesion, transmigration, and production of ROS (Woo et al., 2002). It has been shown, that LTB₄ is essential for the development of skin inflammation in the antibody transfer EBA model by recruiting neutrophils to the DEJ (Sezin et al., 2017). Neutrophils in turn produce LTB₄ themselves to recruit additional cells to the site of inflammation.

In addition to ROS and LTB₄, neutrophils have the ability to form neutrophil extracellular traps (NETs), which have immune-modulatory functions. NETs are defined as networks of extracellular fibers, built of chromatin and granule proteins, which are released by neutrophils upon activation to bind pathogens (Brinkmann, 2004). NETs are involved in the development of autoimmune diseases including cutaneous diseases such as psoriasis (Hu et al., 2016). NETs might play an important role in cutaneous host defense, as infiltration of neutrophils is a hallmark of many skin diseases.

In addition, proteases have been described as crucial factors in the split formation. The treatment with either a combination of broad-range protease inhibitors or a specific

inhibition of gelatinase B (MMP-9) and elastase (MMP-12) entirely blocked DEJ splitting induced by anti-COL7 autoantibodies *ex vivo* (Shimanovich et al., 2004).

1.2.1.3.3 Other cell types involved in the effector phase

Although it seems that neutrophils play a major role in blister formation in the EBA, other cell types are also of interest for research. The functions of other cell types in the effector phase are summarized in Table 1.

Table 1. Other cell types involved in the effector phase

Cell type	Function	Reference
Monocytes/macrophages	Are directly involved in ROS release and blister formation in human skin.	(Hirose et al., 2016)
NKT/ $\gamma\delta$ T cells	Ameliorate clinical phenotype of antibody transfer-induced EBA.	(Bieber et al., 2016)
IL-10+ B cells/plasma cells	Impair the clinical manifestation of immunization-induced EBA via suppressing neutrophil migration during plasmacytosis.	(Kulkarni et al., 2016)
T _{regs}	Inhibit an antibody transfer-induced EBA progression.	(Bieber et al., 2017)

1.2.1.4 Resolution phase

The mechanisms responsible for resolution of inflammation in EBA are still not fully understood. However, recent studies have shown that eosinophils are involved in the resolution phase (Sezin et al., 2020). By depleting the Alox15 gene, a gene encoding Leukocyte-type 12/15-lipoxygenase (12/15-LO), it was demonstrated that BP-like EBA symptoms were aggravated and disease duration was prolonged. Furthermore, Sezin et al. indicated that 12/15-LO, which is expressed on eosinophils, promotes eosinophil and T_{regs} recruitment, which in turn inhibits neutrophil activity.

Furthermore, apart from 12/15-LO, the actin-remodeling protein flightless I (Flii) modulates the resolution of skin blistering in autoantibody transfer-induced EBA (Kopecki et al., 2011). An overexpression of Flii leads not only to severe post-induction of EBA with thinner and more fragile skin but also to delayed recovery after blistering (Kopecki et al., 2014, 2011). By contrast, reduced Flii expression in Flii^{+/-} mice showed reduced blister formation

severity and increased integrin and COL7 expression. More interestingly, topical treatment with Flil-neutralizing antibodies cream had a therapeutic effect in experimental EBA, however it did not affect neutrophils or macrophages in the skin (Kopecki et al., 2013), suggesting that the effect of Flil is most likely not related to the immunological pathways per se, but rather to the mechanisms occurring in the skin during wound healing (Kasperkiewicz et al., 2016).

1.2.2 Clinical presentation

Although the clinical manifestation of EBA is very heterogeneous, two major clinical types can be distinguished: (i) the classical/mechanobullous form and (ii) the nonclassical/nonmechanobullous form. The prevalence varies in different countries, more specifically the classical type is the most common in Europe and the BP-like form in Asia. (Prost-Squarcioni et al., 2018). However, the clinical symptoms in individual patients may change during the course of disease or the same patients may present a mixed form of EBA (Gupta et al., 2012; Ludwig, 2013).

1.2.2.1 Classical/mechanobullous form

The classical/mechanobullous form of EBA is noninflammatory and it is observed in about one third of patients (Buijsrogge et al., 2011). It is characterized by skin fragility, tense blisters, vesicles, bullae or erosions. Blistering can be clear or hemorrhagic and can lead to erosions, crusts, scales, scarring alopecia, milia cysts and nail dystrophy (Gupta et al., 2012). Lesions can occur on every skin region or mucous membranes, but preferentially they are localized on trauma-prone areas, especially on the extensor skin surfaces such as elbows, knees, knuckles, back of the hands, feet, and sacral area. Typically, the lesions heal with atrophic scarring, hypo- or hyperpigmentation and pearl-like milia cysts within the scarred areas (Buijsrogge et al., 2011; Gupta et al., 2012; Ishii et al., 2010; Schmidt and Zillikens, 2013). Porphyria cutanea tarda and pseudoporphyria should be excluded in the mild form of mechanobullous variant (Vorobyev et al., 2017), whereas the severe form of classical EBA can clinically mimic the hereditary dystrophic EB with fibrosis of the hands and fingers (Ishii et al., 2010; Koga et al., 2019). Histologically, classical form is presented by minimal

inflammation and dermal-epidermal disjunction at the basement membrane (Gupta et al., 2012).

1.2.2.2 Nonclassical/nonmechanobullous form

1.2.2.2.1 Bullous pemphigoid (BP)-like EBA

BP-like EBA is the most common inflammatory nonmechanobullous form of EBA. BP-like EBA manifests with widespread pruritic tense bullae and vesicles on inflamed erythematous or urticarial skin. Commonly, the trunk, extremities and skin folds are affected, but vesiculobullous eruptions can appear in any area, including oral mucosa and face. Unlike the classical form of EBA, the lesions usually heal without atrophic scars or milia cysts (Gupta et al., 2012; Kim and Kim, 2013; Koga et al., 2019). Histology shows mononuclear cells and granulocytes (mostly neutrophils and occasionally eosinophils) (Gupta et al., 2012).

1.2.2.2.2 Mucous membrane (MM) – EBA

MM-EBA form may also be inflammatory and it affects predominantly MM lined by squamous epithelium such as the mucous membrane of mouth, pharynx, esophagus, epiglottis, conjunctiva, genitalia, anus and respiratory tract, especially the trachea and bronchi (Koga et al., 2019; Luke et al., 1999; Prost-Squarcioni et al., 2018), resulting in complications like symblepharon and/or blindness (Kim and Kim, 2013), ankyloglossia, perforation of the nasal septum and/or stenosis of nostrils, choanal, pharynx and larynx, esophageal stenosis (Delgado et al., 2011; Luke et al., 1999) and tracheal stenosis (Alexandre et al., 2006). Unlike the classical form of EBA, the occurrence of skin lesions does not depend on the injury, the skin is not significantly fragile and the blisters are normally intact (Gupta et al., 2012; Koga et al., 2019). Histologically, a mixed inflammatory infiltrate is presented with fewer inflammatory findings than in BP form (Gupta et al., 2012; Kamaguchi and Iwata, 2019).

1.2.2.2.3 IgA – EBA

The IgA-EBA may also be inflammatory and it is presented with linear IgA deposits in the basement membrane zone (BMZ) that can be witnessed by direct immunofluorescence (DIF) (Prost-Squarcioni et al., 2018). The IgA-EBA may resemble linear IgA bullous

dermatosis (LABD) with tense blisters, erythematous and urticated plaques in an annular form, so called “string of pearls” (Vodegel et al., 2002; Vorobyev et al., 2017). Normally scarring and milia are not observed. However, IgA-EBA can manifest with more severe clinical symptoms, including involvement of mucous membranes, scarring and/or milia formation and ocular lesions (Vodegel et al., 2002). Histology shows mainly neutrophils infiltrate, occasionally accompanied by eosinophils (Vodegel et al., 2002).

1.2.2.2.4 Brunsting – Perry Type EBA

Brunsting-Perry Type EBA is usually a noninflammatory form of EBA that is defined as a chronic recurrent blistering dermatosis restricted to the head and neck region with minimal or no mucosal involvement (Asfour et al., 2017; Prost-Squarcioni et al., 2018). Skin lesions are characterized by pruritic vesiculobullous eruptions resulting in significant atrophic scarring. Histology shows a subepidermal blister formation containing numerous eosinophils and neutrophils with the predominance of the latter (Asfour et al., 2017; Tanaka et al., 2009).

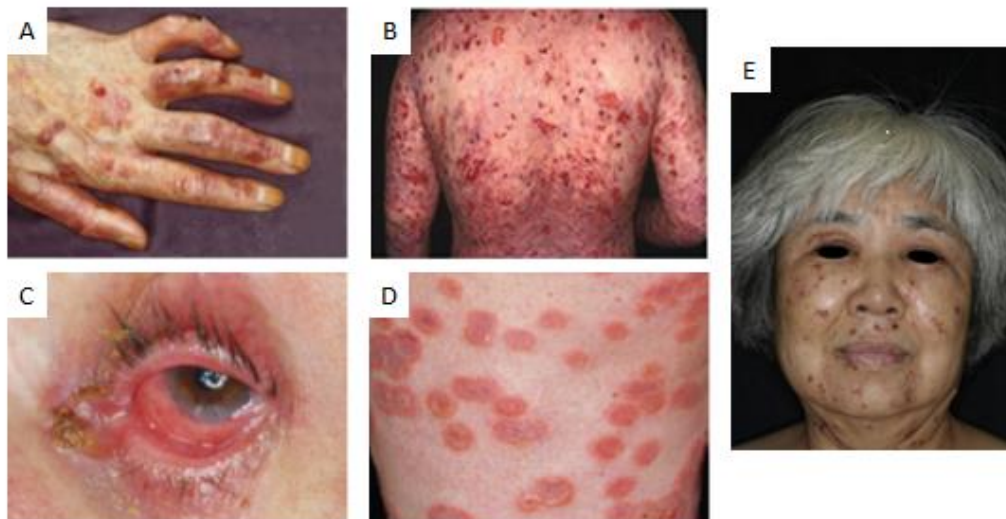


Figure 1. Clinical characteristics of Epidermolysis bullosa acquisita (EBA)

(A) Vesicles, erosions, atrophic erythematous plaques and milia on the extensor surfaces of the left hand. **(B)** Inflammatory blisters on the back and arms in BP-like EBA patient. **(C)** Conjunctival lesion, symblepharon, erosions and yellow crusts in MM-EBA patient. **(D)** IgA-EBA patient with annular erythematous plaques with blistering along the edges (“string of pearls”). **(E)** Blisters and erosions with erythematous atrophic plaques on face in Brunsting – Perry Type EBA patient. Pictures A, C, D from (Schmidt and Zillikens, 2013), picture B from (Kim and Kim, 2013) and picture E from (Tanaka et al., 2009).

1.2.3 Diagnosis

EBA is a complex autoimmune bullous skin disease with a heterogeneous clinical manifestation, therefore in case of clinical suspicion of EBA further diagnostic tests need to be implemented. Currently, a diagnostic gold standard is DIF microscopy of perilesional skin or MM with linear IgG, C3, IgA and/or IgG deposits along the DEJ or CEJ with detection of u-serrated pattern of immunoglobulin deposits along the BMZ (Prost-Squarcioni et al., 2018). Suitable alternatives for the DIF microscopy are immunoelectron microscopy and fluorescent overlay antigen mapping (FOAM), however these methods are only performed in a few centers for the diagnosis of EBA (Koga et al., 2019; Witte et al., 2018). The other tests are DIF and indirect immunofluorescence (IIF) microscopy performed on human salt-split skin using 1 M NaCl, nonetheless they provide only a probable diagnosis of EBA (Prost-Squarcioni et al., 2018). Though, serological tests for the detection of circulating autoantibodies against COL7 are not regularly conducted as a form of diagnostics, there are following serological tests available: (i) ELISA based on the NC1 domain or the combination of NC1 and NC2 domains (Saleh et al., 2011), (ii) an IIF test based on the biochip technology using human cells that express the NC1 domain (Marzano et al., 2016), (iii) immunoblotting detects autoantibodies in patient sera that bind to the COL7 (Komorowski et al., 2013). These serological tests help not only to confirm the diagnosis of EBA, but also to monitor the disease activity (Kim et al., 2013). Furthermore, although routine histopathology from a lesional skin or MM biopsy does not separate EBA from other subepidermal AIBDs, it is helpful in diagnostic by revealing (i) a subepidermal or subepithelial blister, (ii) amount and type of inflammatory infiltrate, (iii) milia cysts and fibrosis in older lesions (Prost-Squarcioni et al., 2018).

1.2.4 Treatment

EBA is a rare disease and due to the low prevalence, no randomized clinical trials have been implemented, therefore the treatment of EBA remains challenging (Ludwig, 2013). Therapy of EBA relies essentially on systemic immunosuppression. Systemic corticosteroids (e.g. prednisolone at an initial dose 0.5–2.0 mg/kg/day (Schmidt and Zillikens, 2013)) are widely used as a first choice combined with steroid-sparing agents (e.g. colchicine, dapsone, methotrexate, azathioprine, cyclosporine, mycophenolate mofetil, cyclophosphamide) to

help minimize the side effects of corticosteroid therapy (Koga et al., 2019). Some authors recommend colchicine as the first line treatment for mild cases of EBA due to the relatively mild adverse effects (Adachi et al., 2016; Cunningham et al., 1996). Other therapeutic options, such as high dose intravenous immunoglobulin (IVIG) (Ishii et al., 2010), rituximab (Schmidt et al., 2006), plasmapheresis and immunoabsorption (Furue et al., 1986; Kolesnik et al., 2014; Kubisch et al., 2010; Niedermeier et al., 2007) and extracorporeal photochemotherapy (Baroudjian et al., 2012; Gordon et al., 1997) have been also reported as a successful treatment in a combined therapy of EBA.

In recent years, the pathogenesis of EBA and the contribution of various signaling pathways involved in the development of the disease, have been the subject of intensive research. As a result, new potential promising therapeutic targets that affect the different phases of the EBA progression, have been identified (Witte et al., 2016). Due to the rarity of EBA, most of these studies were conducted either on an immunization-induced EBA or an antibody transfer-induced EBA mouse models. Successfully *in vivo* applied EBA treatments are summarized in Table 2.

Table 2. New therapeutic options that have been successful in mouse models of epidermolysis bullosa acquisita.

Drugs	Target	Main results	References
17-DMAG, TCBL-145, 17-AAG	HSP90	Inhibition of effector T cells, B cells and neutrophils; suppression of autoantibody, pro-inflammatory cytokine, and reactive oxygen species production; potential inhibition of MMPs; promotion of regulatory B cells.	(Tukaj et al., 2017; Tukaj et al., 2015)
Anti-GM-CSF	GM-CSF	Reduced neutrophils number. Reduced autoantibody serum levels in GM-CSF-deficient mice.	(Samavedam et al., 2014)
Anakinra	Il-1	Inhibited recruitment of inflammatory cells. Decreased expression of ICAM-1.	(Sadeghi et al., 2015b)
DF2156A	CXCR1/2	Impaired IL-8 induced ROS release from neutrophils. Increased cutaneous CXCL1 and CXCL2 expression.	(Hirose et al., 2013)
U0126	ERK1/2	Inhibition of IC-induced ROS release from neutrophils.	(Hellberg et al., 2013)
SB203580	p38 MAPK	Inhibition of IC-induced ROS release from neutrophils. Inhibition of neutrophil degranulation.	(Hellberg et al., 2013)

sCD32	FcγR	Inhibition of IC-induced ROS release from neutrophils. Reduction of antigen-specific autoantibodies.	(Iwata et al., 2015)
IVIg	FcγRIIB FcγRIV Dectin-1	Reduction of (i) circulating autoantibodies, (ii) complement C3 deposition, (iii) complement-fixing antibodies (IgG2b and IgG2c) at the DEJ and (iv) C5a-mediated neutrophil migration.	(Hirose et al., 2015; Karsten et al., 2012a)
Anti-FcγRIV antibody	FcγRIV	Inhibited neutrophil activation by ICs.	(Kasperkiewicz et al., 2012)
EndoS	N-linked glycans of native IgG	Inhibited recruitment of neutrophils. Reduction of inflammatory infiltrate in the lesional skin. Downregulation of activating FcγR and upregulation of inhibiting FcγRIIB.	(Hirose et al., 2012)
Etanercept	TNFα	Reduced cutaneous TNFα expression. Reduced monocytes/macrophages number. Reduced levels of IL-6, G-CSF and KC.	(Hirose et al., 2016)
Dimethylfumarate	Neutrophils	Inhibited neutrophil activation: including ROS release, NET generation and TNF-α-induced chemotaxis.	(Müller et al., 2016)
Goat anti-mouse IgD serum	IL-10 plasma cells	Suppressed IL-10-dependent neutrophil migration toward C5a.	(Kulkarni et al., 2016)
SR333	RORα	Inhibition of IC-induced ROS release from neutrophils.	(Sadeghi et al., 2015)
Calcitriol	Vitamin D	Inhibition of IC-induced ROS release from neutrophils. Promotion of regulatory T (CD4+FoxP3+) and B (CD19+IL-10) cells. Suppression of pro-inflammatory T helper 17 CD4+IL-17+ cells. Suppression of circulating anti-COL7 autoantibodies.	(Tukaj et al., 2018)
Flii-neutralizing antibodies	Flii	Decreased expression of Flii in the epidermis.	(Tukaj et al., 2017)
LAS191954	PI3Kδ	Inhibition of IC-induced ROS release from neutrophils and monocytes.	(Koga et al., 2018)
Roflumilast	PDE4	Inhibition of IC-induced ROS release from neutrophils. Impairment of CD62L shedding and decrease of CD11b expression on IC-stimulated PMNs.	(Koga et al., 2016)
Recombinant IL-6	IL-6	Increased IL-1ra and TIMP-1 expression in skin and serum. Inhibited basal keratinocyte apoptosis.	(Samavedam et al., 2013)

1.3 Experimental models of EBA

Due to the rare prevalence of the disease and the limited therapeutic possibilities, EBA animal models have been developed to better understand the mechanisms involved in the formation of the disease and to establish novel treatments with the least possible side effects. There are active and passive EBA mouse models available, which reflect the different phases of EBA pathogenesis.

1.3.1 Immunization-induced EBA

In the immunization-induced EBA, also known as an active model, the induction and the effector phases of EBA are reproduced. To obtain this, mice are immunized subcutaneously in the footpads or at the tail bases with recombinant peptide fragment from the immunogenic NC-1 domain of murine COL7 (mCOL7) emulsified in adjuvant Titermax™ in order to abolish the self-tolerance against the protein of the skin components. As a result, T and B cells are activated and the complement-fixing IgG2a/b autoantibodies are generated (Sitaru, 2007). Subsequently, four weeks after the first injection the mice develop disease symptoms (Sitaru et al., 2006). The main advantage of this method is that it reflects both the loss of tolerance to COL7 and the effector phase, which allows to examine not only all aspects of the mechanisms involved in the disease's formation, but also to evaluate long-term therapeutic effects. However, this system is relatively time-consuming and almost completely murine therefore it is possible that findings in mice will not correspond to humans (Bieber et al., 2017).

1.3.2 Antibody transfer-induced EBA

In the antibody transfer-induced EBA, which is the passive model, only the effector phase of EBA is recreated. To reproduce the effector phase, rabbits are immunized with recombinant peptides derived from the NC1 domain of the (i) murine COL7 (Sitaru et al., 2005), (ii) human COL7 (Woodley et al., 2005) or (iii) COL7 from EBA patients (Woodley et al., 2006). Subsequently, mice are repeatedly injected with affinity purified IgG antibodies from the rabbit sera. The development of skin lesions ensues 2-4 days after the first injection. Reproducing only the effector phase of EBA serves as both an advantage and disadvantage of this model. Testing the therapeutic effects of drugs is easily feasible

because clinical symptoms in mice are visible after only a few days (Bieber et al., 2017). However, this model does not recreate an autoimmune response to COL7 (Sitaru, 2007) and, as in most animal models, the patient's situation may not correspond to findings of this model.

1.4 Immunometabolism

Immunometabolism, a term first used in 2011, is still a developing field of science, which explores the interaction of two seemingly distinct disciplines of immunology and metabolism (Mathis and Shoelson, 2011). In recent years, the surprising discovery has been made, that immune cell metabolism is not only a passive process that adapts to the cellular energy needs. On contrary, the cellular metabolism is dynamically regulated and plays a direct role in altering immunological reactions (Loftus & Finlay, 2016). The interdependency between cell metabolism and immunological response suggest that by changing the metabolism of cells it is possible to control their development and functions (Boothby and Rickert, 2017; Klein Geltink et al., 2018). Therefore, the findings on the immunometabolism might help to develop new therapeutic approaches.

To maintain homeostasis, all cells need access to sufficient and adequate nutrients. Under normal conditions in the presence of oxygen, resting immune cells use energy in the form of ATP, which is mostly produced via aerobic metabolism. As a result of the glycolysis occurring in the cytosol, glucose is converted to pyruvate with the net production of 2 ATP and 2 NADH per glucose molecule. In the next stage pyruvate is converted to acetyl-CoA and shuttled into the mitochondria where it is oxidized to carbon dioxide via the mitochondrial tricarboxylic acid (TCA) cycle resulting in the generation of reducing equivalents NADH and FADH₂. These reducing equivalents provide electrons for complexes I and II in the mitochondrial electron transport chain, resulting in proton transfer to the intermembrane space between inner and outer mitochondrial membranes, to build up the mitochondrial membrane potential. As a result of oxidative phosphorylation, oxygen is converted to water and the mitochondrial membrane potential is used by complex V to generate energy in the form of ATP (Gaber et al., 2017). In this homeostatic situation a minimum amount of lactate is produced to regenerate NAD⁺ in the cytoplasm and the majority of the glycolytic end product pyruvate is catabolized in the mitochondria.

Activated immune cells and most cancer cells need to increase their glucose uptake in order to generate metabolites for cell growth and proliferation regardless of the presence of oxygen or capacity limits of the TCA cycle, which also results in increased lactate production. This metabolic reprogramming results in a transition from oxidative phosphorylation to aerobic glycolysis, a phenomenon called the Warburg effect (Heiden et al., 2009).

The functions and differentiation of immune cells and cellular metabolism affect each other. The activation of immune cells is the basis for metabolic changes that affect the determination of the functions of immune cells, which allows immune cells to trigger immune responses (Buck et al., 2017). Inflammation and immune reactions significantly affect metabolic activity. Recent studies have revealed that changes in tissue metabolism are associated with high rates of lymphocyte proliferation and increased recruitment of inflammatory cells such as neutrophils and monocytes (Kominsky et al., 2010). Further, an acute or chronic immune response triggers a reaction of immune cells that generate effector cells producing cytokines or cytotoxic granules (Nieman et al., 2019). Immunological activation affects not only changes in tissue metabolism, but also changes in the immune cells themselves. Upon this activation immune cells have increased energy and biosynthetic requirements. Therefore, immune cells influence metabolic reprogramming to produce enough energy to be able to fulfill these requirements (Shehata et al., 2017).

Specific subpopulations of immune cells have different origins, targets, locations and functions. Accordingly, they use different metabolic pathways to generate intracellular energy and to produce metabolic intermediates, which are essential not only for cellular survival, growth, differentiation and proliferation but also instruct effector functions and gene expression (Buck et al., 2017). The linkage between metabolic and immune systems has been examined for individual cell types. These studies revealed that inflammatory M1 macrophages, rapidly proliferating effector T cells (such as T helper 1, T_H17 and cytotoxic CD8⁺ T cells), dendritic cells, NK cells and granulocytes rely upon glycolysis, while M2 macrophages, immunosuppressive T cells (T_{regs}) and CD8⁺ T memory cells mainly use oxidative phosphorylation (Loftus and Finlay, 2016; Makowski et al., 2020; O'Neill et al., 2016). Therefore, metabolic dysfunctions may lead to dysfunction of immune cells and thus

incorrect immune responses and inflammatory diseases. Furthermore, modulating the metabolism of immune cells may influence the treatment of inflammatory diseases (Assmann and Finlay, n.d.; Huang and Perl, 2018; Makowski et al., 2020; Pearce and Pearce, 2018). Compelling evidence was also obtained in animal studies. For instance, it has been shown that inhibition of glycolysis in animal models relieves symptoms of autoimmune diseases (Yin et al., 2015). The results of further experiments on animals open the possibilities of using metabolic inhibitors not only in the treatment of autoimmune diseases, but also in transplantation (Bettencourt and Powell, 2017) or in the production of T cells for improvement of cancer immunotherapy (Le Bourgeois et al., 2018). In conclusion, research on immunometabolism can provide promising results and open new targets and potential therapeutic possibilities for diseases in which the immune response plays a key role.

1.4.1 Neutrophils and their role in immunometabolism

Neutrophils are the most abundant innate immune cells in humans, representing 50% to 70% of the total amount of circulating leukocytes (Injarabian et al., 2019), but they are less common in mice (10% - 30%) (The Jackson Laboratory). Neutrophils together with eosinophils and basophils belong to the group of granulocytes, which are characterized by segmented cell nuclei. Due to their uniquely segmented nucleus they are often referred to as polymorphic leukocytes (PMNs) (Injarabian et al., 2019).

Neutrophils differentiate from hematopoietic stem cells in the bone marrow (Injarabian et al., 2019). They are the first line of the host's immune response to invasive pathogens through a variety of mechanisms such as chemotaxis, phagocytosis, intracellular degradation, release of reactive oxygen species (ROS), cytokine production and creation of extracellular neutrophil traps (NETs). They are also effector cells during inflammation caused by tissue damage. Recent years have also shown the growing importance of neutrophils in the modulation of adaptive immune response. Results gathered in the past years have revealed that neutrophils show phenotypic heterogeneity and functional diversity, which places them as important modulators not only of infection but also of adaptive immune responses and autoimmunity (Mortaz et al., 2018; Rosales, 2018).

Neutrophil metabolic status is not yet fully studied. Until recently, it had been thought that under physiological conditions, neutrophils rely mainly on glycolysis to obtain energy for survival and functioning, and that the mitochondrial function is limited to apoptosis (Maianski et al., 2004). However, in recent years new additional metabolic pathways such as the pentose phosphate pathway (PPP), Tricarboxylic acid (TCA) cycle, oxidative phosphorylation (OXPHOS), and a fatty acid oxidation (FAO) pathway which are involved in neutrophils effector functions including chemotaxis, generation of neutrophil extracellular traps (NETs) have been characterized to be active in neutrophils (Injarabian et al., 2019; Rice et al., 2018).

1.5 Metformin

Metformin (1,1-Dimethylbiguanide) has been the world's most widely used oral antidiabetic for almost 70 years and is taken by over 150 million people each year. Due to the effectiveness and affordability of the therapy, metformin is the preferred initial pharmacologic medication for the treatment of type 2 diabetes (American Diabetes Association, 2020). It is a synthetic guanidine derivative, extracted from *Galega officinalis*, a plant that was already used in medieval times for its anti-diabetic effect (Bailey and Day, 2004). Metformin has an antihyperglycemic effect mainly through the suppression of gluconeogenesis in the liver. It is also able to increase insulin sensitivity, resulting in increased absorption of glucose into skeletal muscle cells (An and He, 2016). Metformin reduces mortality and morbidity in type 2 diabetes patients (Luo et al., 2019). In addition to metabolically beneficial effects, metformin plays a role in various regulatory processes, such as cardiovascular and renal protection, and also exhibits antioxidant, antifibrotic and antiproliferative properties (Ursini et al., 2018). Moreover, metformin has been shown to reduce disease severity in models of autoimmune diseases, including systemic lupus erythematosus, multiple sclerosis and rheumatoid arthritis (Lee et al., 2017; Nath et al., 2009; Son et al., 2014). Nevertheless, despite this long-term clinical experience, the exact mechanism of metformin's action has not yet been fully clarified and is still discussed in the literature.

Preliminary data from studies conducted in our lab demonstrate that the development of skin inflammation in the passive model of EBA can be reduced by the administration of metformin (Figure 2).

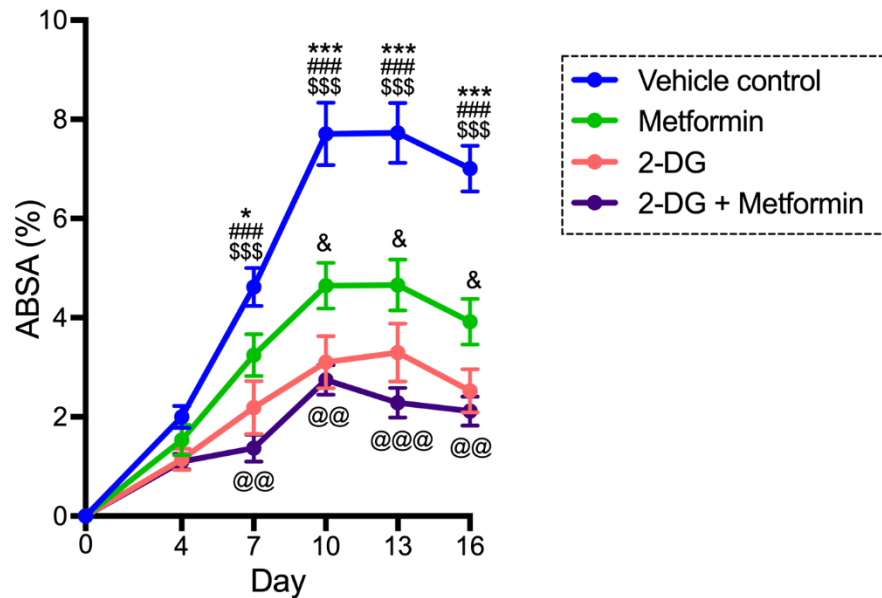


Figure 2. Metformin and 2-DG ameliorate BP-like EBA.

Severity of skin inflammation benchmarked as percentage of the total body surface area affected by skin lesions (ABSA). Results are presented as mean \pm SEM (n = 11-12 mice/group). Data were analyzed by two-way ANOVA with Holm-Sidak's multiple comparisons test. Statistical significances are indicated for the individual day as follows: *, $p < 0.05$; ***, $p < 0.001$ control vs. metformin group. ###, $p < 0.001$ control vs. 2-DG group. \$\$\$, $p < 0.001$ control vs. 2-DG/metformin group. &, $p < 0.05$ metformin vs. 2-DG group. @@, $p < 0.01$; @@@, $p < 0.001$ metformin vs. 2-DG/metformin group (Schilf et al., 2021).

1.5.1 Mechanisms of action

Emerging evidence demonstrates pleiotropic actions of metformin, the most prominent of which seems to be the effect on glucose metabolism. The exact underlying molecular mechanisms of metformin's action are complex and elusive. There are various pathways that are linked to the mechanisms of metformin, of which cellular energy sensor AMP-activated protein kinase (AMPK) pathway plays a vital role (Yan et al., 2020). Metformin inhibits the mitochondrial complex I (also known as NADH:ubiquinone oxidoreductase) of the respiratory chain, resulting in diminished electron transport and consequently reduced production of ATP, which increases AMP/ATP or ADP/ATP ratios (Owen et al., 2000). As a result, adenylate kinase convert ADP to AMP, further increasing the AMP/ATP ratio. AMP binds to the regulatory AMPK γ subunits, leading to the phosphorylation of the catalytic

AMPK α subunit at Thr-172 by liver kinase B1 (LKB1) and its indirect activation (Hardie, 2004).

Once activated, AMPK affects cellular metabolism through an increase of catabolism to stimulate ATP production and the inhibition of anabolism to minimize ATP consumption (Hardie et al., 2012). Recent evidence has shown that AMPK is not only involved in the lipids and carbohydrates metabolism but is also associated with other processes such as autophagy, mitochondrial biogenesis and disposal, cell polarity, cell growth and proliferation (Hardie, 2011). Moreover, the AMPK is an important immunomodulator through its role in inflammation and immunity (Jeon, 2016; O'Neill & Hardie, 2013; Wang et al., 2018). The effects of activated AMPK are summarized in Table 3.

Table 3. Effects of AMPK activation on cellular metabolism.

	Pathway	Mechanism of action	References
C A T A B O L	Glucose uptake	Phosphorylation of TXNIP and TBC1D1, which increases the plasma membrane localization of GLUT1 and GLUT4, respectively.	(Chavez et al., 2008; Wu et al., 2013)
	Glycolysis	Phosphorylation and activation of PFKFB2/PFKFB3, that produces fructose-2,6-bisphosphate, an allosteric activator of a rate-limiting enzyme PFK-1.	(Bando et al., 2005; Marsin et al., 2000)
	Glycogenolysis	Phosphorylation and activation of glycogen phosphorylase.	(Jeon, 2016)
	Lipolysis	Phosphorylation and activation of ATGL.	(Ahmadian et al., 2011)
	Fatty acid uptake	Translocation of the fatty acid transporter CD36 to the plasma membrane.	(Habets et al., 2009)
	Fatty acid oxidation	(i) Increased CPT-1 activity, an enzyme required for the transport of fatty acid into the mitochondria, and (ii) phosphorylation of ACC2 isoform of acetyl-CoA carboxylase, leading to the inhibited production of malonyl-CoA, a potent allosteric inhibitor of CPT-1.	(Hardie and Pan, 2002)
I C	Mitochondrial biogenesis	(i) Direct phosphorylation of PGC1 α and (ii) increased cellular NAD ⁺ levels, resulting in activation of PGC1 α by SIRT1.	(Cantó et al., 2009; Jäger et al., 2007)
	Autophagy	Direct and indirect activation of ULK1 by phosphorylation of ULK1 and inhibition of mTORC1, respectively.	(Egan et al., 2011; Russell et al., 2013)
A N A B O L I C	Gluconeogenesis	Inhibitory phosphorylation of CRTC2, HNF-4 α and class IIA histone deacetylases (HDACs), which promote the expression of gluconeogenic enzymes.	(Koo et al., 2005; Leclerc et al., 2001; Mihaylova et al., 2011)
	Glycogenesis	Inhibitory phosphorylation of glycogen synthase.	(Bultot et al., 2012)
	Fatty acid synthesis	Inhibitory phosphorylation of ACC1 and lipogenic transcription factor SREBP1c, which convert acetyl-CoA to malonyl-CoA and promote the expression of lipogenic enzymes including ACC1 and FA synthase, respectively.	(Hardie and Pan, 2002; Li et al., 2011)
	Cholesterol synthesis	Inhibitory phosphorylation of HMG-CoA reductase.	(Carling et al., 1989)
	Triacylglycerol and phospholipid synthesis	Inhibition of GPAT, although it is unclear whether GPAT is inhibited through direct phosphorylation or phosphorylation of an intermediate regulatory protein.	(Muoio et al., 1999)
	Protein synthesis	(i) Indirect inhibition of mTORC1 through the phosphorylation of TSC2 and raptor and (ii) phosphorylation of eEF2 kinase, a negative regulator of protein elongation.	(Gwinn et al., 2008; Inoki et al., 2003; Leprévier et al., 2013)
	rRNA synthesis	Inhibitory phosphorylation of TIF-IA, the RNA polymerase I-associated transcription factor.	(Hoppe et al., 2009)

While it seems that metformin acts mainly via the activation of AMPK, some actions have been found to be AMPK-independent, constituting a new interesting area of great importance for current research (Foretz et al., 2014; Miller and Birnbaum, 2010; Rena et al., 2017). These results highlight that metformin is involved in multiple pathways and despite its clinical use for decades, more research is required to truly understand the exact molecular mechanisms of metformin action.

1.6 Aim of the study

Epidermolysis bullosa acquisita (EBA) is a chronic, severe autoimmune skin blistering disease, for which treatment options are limited and unsatisfactory. Therefore, there is an urgent need to develop a new therapeutic approach. In the past decade, research attention has been directed toward metabolism-modulating drugs. Similarly, this study aimed to determine novel potential therapeutic targets by modulating neutrophil metabolism, which are crucial in the development of BP-like EBA.

Previous work from our group showed that the development of skin inflammation in the antibody-transfer induced EBA model was reduced by metformin and 2-deoxy-glucose, which are both known for their immunomodulatory functions. This study sought to assess the underlying mechanism of actions of these two drugs in the passive EBA mouse model and their effect on neutrophils activated by immune complexes, as IC-activated neutrophils are one of the major causes of tissue damage in pemphigoid diseases. Furthermore, to find other immunomodulators, the focus has been on compounds that affect neutrophil glycolysis, which is one of the major metabolic pathways in these cells.

Another purpose of this work was to examine whether the therapeutic effect of metformin in the antibody-transfer induced EBA model was to some extent due to activation of AMPK, which is considered to be a major mechanism of metformin action, and whether targeted AMPK activation is sufficient to result in a therapeutic effect, both *in vitro* and *in vivo*. To this end, the nucleoside 5-Aminoimidazole-4-carboxamide-1- β -D-ribofuranoside (AICAR) was used, a direct activator of AMPK.

2 MATERIALS AND METHODS

2.1 Materials

2.1.1 Mice

C57BL/6JRj wild type (WT) mice were obtained from Janvier Labs (Le Genest-Saint-Isle, France). The animals were fed drinking water and standard chow *ad libitum*. The animals were bred and housed in a 12-hour light-dark cycle at the animal facility of the University of Lübeck (Lübeck, Germany). All experimental protocols were approved by local authorities of the Animal Care and Use Committee of Schleswig-Holstein (Kiel, Germany) and performed in 8- to 14-week-old age- and sex-matched mice.

2.1.2 Laboratory equipment

Equipment	Source
Accu-jet pro pipette	BRAND GmbH, Wertheim, Germany
Analytical scale ABS/ABJ-BA-def- 1019	Kern & Sohn GmbH, Balingen, Germany
Bio-photometer plus 8.5 mm	Eppendorf AG, Hamburg, Germany
Centrifuge 5810R	Eppendorf AG, Hamburg, Germany
CFI Plan Apo λ 10x lense	Keyence Deutschland GmbH, Neu-Isenburg, Germany
CFI Plan Apo λ 20x lense	Keyence Deutschland GmbH, Neu-Isenburg, Germany
Freezer -20	Liebherr Hausgeräte GmbH, Ochsenhausen, Germany
Freezer -80	Thermo Fisher Scientific GmbH, Dreieich, Germany
HandyStep S dispenser	BRAND GmbH, Wertheim, Germany
Incubator Galaxy 170 S	New Brunswick
Keyence microscope BZ-9000E	Keyence Deutschland GmbH, Neu-Isenburg, Germany
Laminar hood	NuAire, Plymouth, Minnesota, USA
MACS MultiStand	Miltenyi Biotec, Bergisch Gladbach, Germany
MACSquant Analyzer 10	Miltenyi Biotec, Bergisch Gladbach, Germany
Magnetic hotplate stirrer VMS-C4	VWR International GmbH, Darmstadt, Germany
Mastercycler ep realplex	Eppendorf AG, Hamburg, Germany
Micro centrifuge Micro Star 17R	VWR International GmbH, Darmstadt, Germany

Mini-Shaker model Kühner	B. Braun Melsungen, Germany
NanoDrop 2000c spectrophotometer	Thermo Fisher Scientific, Waltham, MA, USA
Neubauer cell counting chamber	Laboroptik GmbH, Friedrichsdorf, Germany
pH meter HI208	HANNA instruments, Vöhringen, Germany
Pressure cooker	Fissler GmbH, Idar-Oberstein, Germany
QuadroMACS Separator	Miltenyi Biotec, Bergisch Gladbach, Germany
Refrigerator	Siemens, Munich, Germany
Tecan Infinite M200 PRO ELISA reader	Thermo Fisher Scientific GmbH, Dreieich, Germany
Thermomixer comfort	Eppendorf AG
Transferpette S (10 µl, 20 µl, 100 µl, 1000 µl, multi-channel 300 µl)	BRAND GmbH, Wertheim, Germany
Vortex	Vortex-Genie® 2-Scientific Industries Inc., Bohemia, New-York, USA
XF24 Extracellular Flux Analyzer	Agilent Technologies, Waldbronn, Germany

2.1.3 Disposable materials

Type of article	Source
26 gauge needle	BD Biosciences GmbH, Heidelberg, Germany
Cell strainer 40 µm	Becton Dickinson GmbH, Heidelberg, Germany
Corning® Transwell® polyester membrane cell culture inserts (6.5 mm Transwell with 3.0 µm pore polyester membrane insert)	Sigma-Aldrich, Darmstadt, Germany
Cover glass slides (24 x 60)	Paul Marienfeld GmbH, Lauda-Königshofen, Germany
Dako-pen	Dako Deutschland GmbH, Hamburg, Germany
ELISA high binding 96-well plate	Fisher Scientific GmbH, Schwerte, Germany
Falcon tubes (15 ml; 50 ml)	Sarstedt AG&Co., Nuembrecht, Germany
Feather disposable scalpel	Feather Safety Razor Co. LTD
High-binding 96-well chimney well black plates	Greiner Bio-One, Austria
LS positive selection columns	Miltenyi Biotec, Bergisch Gladbach, Germany
Ministart 0.2 µm	Sartorius Stedim Biotech GmbH, Göttingen, Germany

Parafilm	Th. Geyer GmbH & Co. KG, Renningen, Germany
PCR plate half skirt, 96 well, transparent, High-Profile, 200 µl	Sarstedt AG&Co., Nuembrecht, Germany
Pipette tips (10 µl; 100 µl; 1000 µl)	Sarstedt AG&Co., Nuembrecht, Germany
Reaction tubes (1.5 ml; 2 ml)	Sarstedt AG&Co., Nuembrecht, Germany
RNase-free PCR tubes (0.2 ml)	Fisher Scientific GmbH, Schwerte, Germany
Serological pipettes (5 ml; 10 ml; 25 ml)	Sarstedt AG&Co., Nuembrecht, Germany
SuperFrost/Plus-slide glasse	Gerhard Menzel, Glasbearbeitungswerk, GmbH&Co. KG, Germany
Syringe (1 ml, 5 ml; 20 ml)	Becton Dickinson GmbH, Heidelberg, Germany

2.1.4 Chemicals

Chemicals	Cat. no.	Source
2-Deoxy-D-glucose	MD05187	Biosynth Carbosynth, USA
2-Propanol	6752.1	Carl Roth GmbH & Co. KG, Karlsruhe, Germany
5-Aminoimidazole-4-carboxamide ribonucleotide (AICAR)	sc-200659B	Santa Cruz Biotech, Inc, USA
Antimycin A	A8674	Sigma-Aldrich, Darmstadt, Germany
Bepanthen Eye and Nose Ointment	01578681	Bayer AG, Germany
Carbonyl cyanide-p-trifluoromethoxyphenylhydrazone (FCCP)	15218	Cayman Chemicals, Ann Arbor, MI, USA
Chloroform	102432	Merck Millipore, USA
D-(+)-glucose	G 8270	Sigma-Aldrich, Darmstadt, Germany
Diethylpyrocarbonat (DEPC)-treated water	R0601	Thermo Fisher Scientific GmbH, Dreieich, Germany
EDTA solution 0.5 M pH 8	A3145.0500	AppliChem GmbH, Darmstadt, Germany
Ethanol 70%	T913.3	Carl Roth GmbH & Co. KG, Karlsruhe, Germany
Ethanol 96%	T171.4	Carl Roth GmbH & Co. KG, Karlsruhe, Germany
Fetal Bovine Serum	26400044	Thermo Fisher Scientific, Waltham, MA, USA
Galloflavin	14846	Cayman Chemicals, Ann Arbor, MI, USA

Heptelidic acid	14079	Cayman Chemicals, Ann Arbor, MI, USA
Human serum albumin	A1653	Sigma-Aldrich, Darmstadt, Germany
Hydrochloric acid (25%)	6331.1	Carl Roth GmbH & Co. KG, Karlsruhe, Germany
Ketamin hydrochloride	K2753	Sigma-Aldrich, Darmstadt, Germany
Leukotriene B ₄	CAY20110-25	Cayman Chemicals, Ann Arbor, MI, USA
L-Glutamine solution (200 mM)	G7513	Sigma-Aldrich, Darmstadt, Germany
Liberase TL Research Grade	5401020001	Roche, Mannheim, Germany
Luminol sodium salt	A4685	Sigma-Aldrich, Darmstadt, Germany
Metformin Hydrochloride	M2076	LKT Labs, USA
Moxifloxacin Hydrochloride	HY-66011	MedChemExpress LLC, NJ, USA
NaCl	9265.3	Carl Roth GmbH & Co. KG, Karlsruhe, Germany
Oligomycin A	75351	Sigma-Aldrich, Darmstadt, Germany
Pepsin	003009	Thermo Fisher Scientific GmbH, Dreieich, Germany
Polyoxyethylene sorbitan moonolaurate (Tween 20)	P1379	Sigma-Aldrich, Darmstadt, Germany
Recombinant Murine C5a	315-40	PeptoTech, Hamburg, Germany
Rotenone	R8875	Sigma-Aldrich, Darmstadt, Germany
Roti-Histofix (4% solution)	P087.2	Carl Roth GmbH & Co. KG, Karlsruhe, Germany
Sodium citrate dihydrate	W302600	Sigma-Aldrich, Darmstadt, Germany
Sodium pyruvate (100 mM)	11360070	Thermo Fisher Scientific GmbH, Dreieich, Germany
SYTOX™ Green Nucleic Acid Stain - 5 mM Solution in DMSO	S7020	Thermo Fisher Scientific, Waltham, MA, USA
TEPP-46	CAY13942-5	Cayman Chemicals, Ann Arbor, MI, USA
Tris (hydroxymethyl) aminomethane	37190.02	Serva electrophoresis GmbH, Heidelberg, Germany
Triton X-100	3051.2	Carl Roth GmbH & Co. KG, Karlsruhe, Germany

TRIzol™ Reagent	15596018	Thermo Fisher Scientific, Waltham, MA, USA
Trypan blue	T8154	Sigma-Aldrich, Darmstadt, Germany
Xylazine hydrochloride	X1251	Sigma-Aldrich, Darmstadt, Germany
Xylene	534056	Sigma-Aldrich, Darmstadt, Germany

2.1.5 Commercial buffers and solutions

Name	Cat. No.	Source
autoMACS Rinsing Solution	130-091-222	Miltenyi Biotec, Bergisch Gladbach, Germany
Dulbecco's Modified Eagle's Medium (DMEM)	D5030	Sigma-Aldrich, Darmstadt, Germany
Dulbecco's Phosphate-Buffered Saline (DPBS) pH 7.2 0.01 M	14190094	Thermo Fisher Scientific GmbH, Dreieich, Germany
Hanks' Balanced Salt Solution (HBSS)	14025100	Thermo Fisher Scientific GmbH, Dreieich, Germany
HEPES 1 M	L1613	Biochrom GmbH, Berlin, Germany
MACS BSA Stock Solution	130-091-376	Miltenyi Biotec, Bergisch Gladbach, Germany
Normal goat serum (NGS)	X0907	Dako Deutschland GmbH, Hamburg, Germany
PBS pH 7.2 0.1 M	70013-016	Invitrogen GmbH, Darmstadt, Germany
RPMI 1640 with L-glutamine	BE12-702F	Lonza Cologne GmbH, Köln, Germany
RPMI 1640 with L-glutamine w/o glucose w/o phenol red	C4116.0500	Genaxxon bioscience GmbH, Ulm, Germany
SYBR Select Master Mix	4472920	Thermo Fisher Scientific, Waltham, MA, USA

2.1.6 Antibodies

Antibody	Cat. no.	Application	Source
Alexa Fluor 488 anti-mouse CD206	141709	FC	BioLegend GmbH, Koblenz, Germany
Alexa Fluor® 594 AffiniPure Goat Anti-Rat IgG	112-585-167	IHC	Jackson ImmunoResearch, Suffolk, UK
APC- F4/80 Monoclonal Antibody (clone BM8)	17-4801-80	FC	eBioscience, Frankfurt, Germany

APC/Fire™ 750 anti-mouse/human CD11b	101261	FC	BioLegend GmbH, Koblenz, Germany
FcR Block Reagenz, Maus	130-092-575	FC	Miltenyi Biotec, Bergisch Gladbach, Germany
FITC anti-mouse CD206	141704	FC	BioLegend GmbH, Koblenz, Germany
FITC anti-mouse Ly-6G	127605	FC	BioLegend GmbH, Koblenz, Germany
Fixable Viability Dye eFluor 506	65-0866-14	FC	eBioscience, Frankfurt, Germany
FOXP3 Monoclonal Antibody	14-5773-82	IHC	Thermo Fisher Scientific GmbH, Dreieich, Germany
Normal rat IgG	C301	IHC	Emfret Analytics GmbH & Co. KG, Eibelstadt, Germany
PE rat anti-mouse Ly6G	551461	FC	BD Biosciences GmbH, Heidelberg, Germany
PerCP-Cy5.5 rat anti-mouse CD11b	550993	FC	BD Biosciences GmbH, Heidelberg, Germany
Polyclonal rabbit anti-human serum albumin IgG	A0433	<i>in vitro</i> ROS assay	Sigma-Aldrich, Darmstadt, Germany
Rat anti-mouse Ly6G	127602	IHC	BioLegend GmbH, Koblenz, Germany
Fluorescence dyes	Cat. no.	Application	Source
CountBright™ Absolute Counting Beads	C36950	FC	Thermo Fisher Scientific GmbH, Dreieich, Germany
DAPI fluoromount G	0100-20	IHC	BIOZOL Diagnostica Vertrieb GmbH, Munich, Germany

2.1.7 Primers used for RT-qPCR

All primers were purchased from biomers.net (biomers.net GmbH, Ulm, Germany).

Gene name	Forward primer (5'→3')	Reverse primer (5'→3')	Gene ID	Size (bp)
<i>Ccl2</i>	GGCTCAGCCAGATGCAGTTA	GGTGATCCTCTGTAGCTCTCC	20296	100
<i>Cxcl2</i>	CCAACCACCAGGCTACAGG	GCGTCACACTCAAGCTCTG	20310	108
<i>Glut1</i>	CATCCTTATTGCCAGGTGTTT	GAAGATGACACTGAGCAGCAGA	20525	82
<i>Glut3</i>	TTCTGGTCGGAATGCTCTTC	AATGTCCTCGAAAGTCCTGC	20527	143
<i>Glut4</i>	CATTGTCGGCATGGGTTTCC	GCAGGAGGACGGCAAATAGA	20528	77
<i>Il-10</i>	GCTGTCATCGATTCTCCCC	ACACCTTGGTCTTGGAGCTTAT	16153	88
<i>Il-1β</i>	GAAATGCCACCTTTTGACAGTG	TGGATGCTCTCATCAGGACAG	16176	116
<i>Oct1</i>	TGGCCGCATCTACCCAATAG	TCCCATACGGCCAAGACAAG	20517	124

<i>Oct2</i>	CATTGGTGGCATCGTCACAC	AGCAATAGCACAAAGTCCCCC	20518	117
<i>Oct3</i>	TATAGTGGCAGGGGTGTCGT	GTCACACAAGCCTGAGCAGA	20519	193
<i>Psm4</i>	ACACTGGCCAATGACTGTGAG	TTGCCTTTGGGTTGGACAGT	19185	92
<i>Tgf-β1</i>	CTGCTGACCCCCACTGATAC	AGCCCTGTATTCCGTCTCCT	21803	94
<i>Tnf-α</i>	CCCTCACAATCAGATCATCTTCT	GCTACGACGTGGGCTACAG	21926	61

2.1.8 Kits and others

Name	Cat. no.	Source
Neutrophil Isolation Kit, mouse	130-097-658	Miltenyi Biotec, Bergisch Gladbach, Germany
LTB4 parameter assay	KGE006B	R&D Systems GmbH, Wiesbaden-Nordenstadt, Germany
Seahorse XF24 FluxPak	100850-001	Agilent Technologies, Waldbronn, Germany
RNeasy Micro Kit	74004	QIAGEN GmbH, Hilden, Germany
RevertAid First Strand cDNA Synthesis Kit	K1622	Thermo Fisher Scientific, Waltham, MA, USA
Annexin V-FITC Detection Kit	PK-CA577-K101-100	PromoCell, Heidelberg, Germany

2.1.9 Self-made buffers and solutions

Name	Chemical composition
10 x PBS (0.1 M)	450.0 gr NaCl 87.0 gr Na ₂ HPO ₄ * 2H ₂ O 10.17 gr NaH ₂ PO ₄ * H ₂ O Dissolved in 5L DDW
1 x PBS pH 7.2 (0.01 M)	Dilute 1:10 PBSx10 Adjusted pH to 7.2
1 x PBST	100 ml 10 x PBS 1 ml Tween Dissolved in 900 ml DDW
50 mM bicarbonate buffer, pH 9.6	0.7575 g Na ₂ CO ₃ 1.5 g NaHCO ₃ Dissolved in 0.5 L DDW. Adjusted pH to 9.6
0.01 M Tris-buffered saline (TBS) 20 mM Tris + 0.5 M NaCl pH 7.6	2.42 g Tris 29.22 g NaCl Dissolved in 1L DDW. Adjusted pH to 7.6
10 mM Sodium citrate buffer + 0.05% Tween 20	Dissolved 2.9 g of sodium citrate dehydrate in 1L DDW. Added 0.5 ml of Tween 20. Adjusted pH to 6.0
MACS Buffer	475 ml autoMACS Rinsing Solution 25 ml MACS BSA Stock Solution

Seahorse assay medium	DMEM L-glutamine (final conc: 2 mM) D-(+)-glucose (final conc: 10 mM) Sodium Pyruvate (final conc: 1 mM)
Chemiluminescence (CL) Medium	47.75 ml RPMI-1640 w/o phenol red 0.5 ml FCS 0.5 ml glucose 1.25 ml HEPES

2.2 Methods

2.2.1 Generation of affinity purified rabbit anti-murine COL7C IgG

In order to induce antibody transfer-induced EBA in mice, it is necessary to first generate the rabbit anti-murine COL7C IgG, which cross-react with murine skin, causing the symptoms of the disease in mice. The production of autoantibodies using New Zealand White rabbits consists of three main steps and was previously described (Sitaru et al., 2005). Firstly, the generated three peptides of the murine type VII collagen NC1 domain were provided by the Department of Dermatology, Lübeck. Next, these peptides were used by Eurogen- tec GmbH to immunize New Zealand White rabbits. Obtained immune sera were purified to isolate total IgG fraction using recombinant protein G resin affinity column chromatography. Lastly, specific rabbit anti-murine COL7C IgG was produced using affinity column chromatography. For this study, the total and the specific anti-mCOL7C IgG were kindly provided by the Department of Dermatology, Lübeck (AG Sadik). The antibodies were stored at -20 °C until further use.

2.2.2 Induction of antibody transfer EBA mouse model

Experimental antibody transfer BP-like EBA mouse model was induced, as previously described (Schilf et al., 2021). Briefly, age and sex matched C57BL/6JR WT mice received three subcutaneous (s.c.) injections of 50 µg (in 100 µl) of rabbit anti-mCOL7C IgG in total, into the neck, left foreleg, and right hindleg on days 0, 2, and 4 of the experiment, respectively. The experiment was running for 16 days. During this time, the mice were weighed and examined for general condition and cutaneous lesions, specifically erythema, blisters, erosions, crusts, or alopecia, every three days starting from day 4 of the experiment. To perform a clinical examination, mice were anaesthetized intraperitoneally

(i.p.) with 10 µl/gr body weight of ketamine (100 mg/ml) and xylazine (15 mg/ml) mixture. During the anesthesia, ophthalmic ointment (Bepanthen) was applied to the corneas to prevent them from drying out, and awakening was supervised until full recovery. For treatment, 250 mg/kg AICAR (Santa Cruz Biotech, Inc) was injected i.p. daily throughout the entire experiment, starting from day 0 of the experiment. The corresponding vehicle, saline, administered to the control group was injected i.p. At the end of the experiment on day 16, the mice were euthanized, and skin biopsies, ears, blood, serum, lymph nodes, livers and spleens were harvested for further investigation. Two independent experiments were conducted.

2.2.3 Evaluation of disease severity in antibody transfer EBA mouse model

To assess the disease severity of skin inflammation in the experimental antibody transfer EBA mouse model, the percentage of the total body surface affected by erythema, crusts, alopecia and erosions was regularly determined (day 4, 7, 10, 13 and 16 of the experiment). The affected body surface area (ABSA) was measured by allocating individual percentile to a specific body part based on its relative size in the body (Table 4). In addition, the area under curve (AUC) that reflects the total disease severity throughout the experiment, was calculated using GraphPad Prism 8.4.3.

Table 4. Scoring table used to determine the disease severity in antibody-transfer EBA (ery: erythema; cru: crusts; alo: alopecia; ero: erosions).

Body parts	Type of lesion	Fraction from the total body area (%)	ABSA (%)
Left ear	ery, cru, alo, ero	2.5	
Right ear	ery, cru, alo, ero	2.5	
Left eye	ery, cru, alo, ero	0.5	
Right eye	ery, cru, alo, ero	0.5	
Snout	ery, cru, alo, ero	2.5	
Oral mucosa	ery, cru, alo, ero	2.5	
Head & neck	ery, cru, alo, ero	9.0	
Left foreleg	ery, cru, alo, ero	5.0	
Left hindleg	ery, cru, alo, ero	5.0	
Right foreleg	ery, cru, alo, ero	10.0	
Right hindleg	ery, cru, alo, ero	10.0	
Tail	ery, cru, alo, ero	10.0	
Trunk	ery, cru, alo, ero	40.0	
Total score		100	

2.2.4 Flow cytometry analysis of skin samples

In this study, the flow cytometry technology is used to identify immune cell types present in the perilesional skin of EBA mouse model. For this purpose, perilesional skin was taken from the back of the mice, which were sacrificed on day 16 of the experiment. Before starting the fluorescence-activated cell sorting (FACS) staining, the skin samples were prepared as followed: the skin samples were added directly to tubes containing 1 ml RPMI medium, L-glutamine and 10% fetal calf serum (FCS) supplemented with 180 µg Liberase TL Research Grade (72 µl from 2.5 mg/ml stock). Using scissors, the skin samples were cut into small parts and tubes were incubated at 37 °C on shaker for 90 min. Using 70 µm filter and the stump of a 5 ml syringe, the skin samples were mashed till single cell suspensions were obtained. The filters were washed with 5 ml MACS buffer, the tubes were centrifuged for 5 min at 400 g at 4 °C and the supernatants were removed. The suspensions were washed with 5 ml MACS buffer, centrifuged for 5 min at 400 g at 4 °C, the supernatants

were removed, and pellets were resuspended in 100 µl MACS buffer containing 1:10 FcR Block and 1:100 viability dye. After 15 min of incubation at RT protected from light, the cells were incubated with mixtures of the following antibodies (all diluted 1:100 in PBS unless otherwise noted): (i) PE-conjugated anti-mouse Ly6G, (ii) APC-conjugated anti-mouse F4/80, (iii) PerCP-Cy5.5-anti-mouse CD11b, (IV) FITC-conjugated anti-mouse CD206. The samples were incubated for 30 min at RT protected from light. Flow cytometry was conducted on a MACSquant Analyzer 10 (Miltenyi Biotec, Bergisch Gladbach, Germany) and analyzed with FlowJo software V10.

2.2.5 Isolation of murine bone marrow

All cells were derived from C57BL/6Jrj WT mice. The isolation of cells from the bone marrow was performed following previous protocol with minor modifications (Swamydas and Lionakis, 2013). Briefly, mice were anesthetized via intraperitoneal injection of mixture of ketamine (100 µg/g) and Xylazin (15 µg/g) and sacrificed by cervical dislocation. To isolate bone marrow from the hind legs (femora and tibiae), the mouse abdomen area and skin of the hind legs were sterilized with 70% ethanol. Subsequently, the skin was removed exposing the musculature and the muscles of femur and tibia which were also detached. Using sharp sterile scissors, the hind leg was cut off above the acetabulum. The femur and tibia were separated at the knee joint using scissors. Following that, tibiae and femora were transferred into sterile 5 ml MACS buffer Solution. All following processes were conducted under a sterilized class II cell culture hood. With a sterile scalpel, the adhering tissues were removed from the bones. The medullary cavities were flushed by injecting MACS buffer using a 26-gauge needle. The bone marrow suspension was suspended by pipetting and filtered through a 40 µm cell strainer. The suspension was centrifuged for 5 min at 400 g at 4 °C. After removing the supernatant, the cell pellet was resuspended in 1 ml MACS buffer. The cell number was determined using Neubauer chamber.

2.2.6 Isolation of neutrophils using MACS

To isolate the murine neutrophils of bone marrow, immunomagnetic cell separation technique was performed using Neutrophil Isolation Kit (Miltenyi, Bergisch Gladbach, Germany) according to the manufacturer's instructions with minor modifications. In brief,

after determining the number of cells in the bone marrow using a Neubauer chamber, the cells suspension was centrifuged for 5 min at 400 g at 4 °C. The supernatant was removed, and the cell pellet was resuspended in 200 µl of MACS buffer per 5×10^7 total cells. Subsequently, 50 µl per 5×10^7 total cells of Neutrophil Biotin-Antibody Cocktail was added and well mixed. After 10 min of incubation on ice, the cells were washed by adding 5-10 ml of MACS Buffer and centrifuged for 5 min at 400 g at 4 °C. Next, the supernatant was aspirated, and the cell pellet was resuspended in 400 µl of MACS buffer per 5×10^7 total cells. 100 µl per 5×10^7 total cells of Anti-Biotin Microbeads was added, followed by 15 min incubation on ice. The cells were washed by adding 5-10 ml of MACS buffer and centrifuged (5 min, 400 g, 4 °C). After aspirating the supernatant, the cell pellet was resuspended in 500 µl MACS buffer up to 5×10^8 total cells. After placing the LS columns on the magnet and 50 ml Falcon tubes underneath, the LS columns were rinsed with 3 ml of MACS Buffer per column. The cell suspension was applied, followed by three washing cycles – 3 ml MACS buffer per column. The negative flow through was collected and centrifuged (5 min, 400 g, 4 °C). After discarding the supernatant, the cell pellet was resuspended in 1 ml MACS buffer and the number of purified neutrophils was determined using the Neubauer chamber. In our laboratory, isolation of neutrophils from murine bone marrow using MACS routinely obtains preparations with >95% purity (Figure 3).

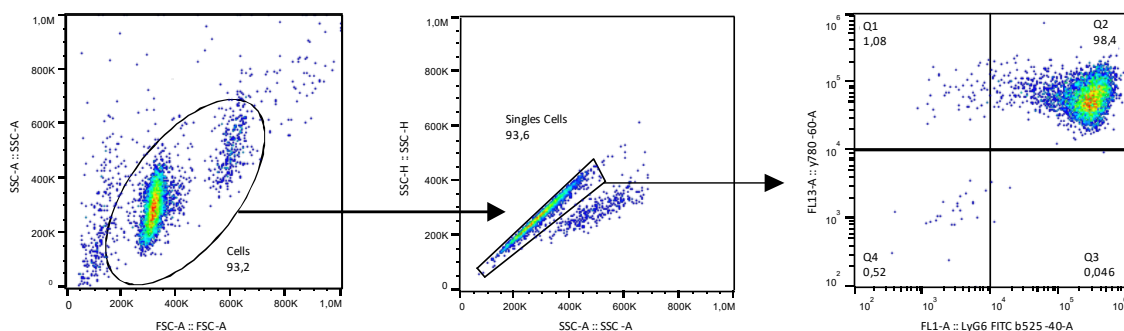


Figure 3. Representative murine bone marrow-derived neutrophils purity after isolation using MACS.

Neutrophils were isolated from C57BL/6 bone marrow cells by using the Neutrophil Isolation Kit, an LS Column, and a QuadroMACS Separator. The cells were fluorescently stained with Anti-CD11b-APC/vio750 and Anti-Ly-6G-FITC and analyzed by flow cytometry using the MACSQuant Analyzer. After the separation, cell suspensions were typically >95% pure neutrophils. Ten thousand events were acquired in each analysis.

2.2.7 ROS Release assay upon stimulation with fixed immune complexes

Isolated murine neutrophils were stimulated with artificial generated immune complexes (ICs). Fixed ICs were formed, as previously described with minor modifications (Chou et al., 2010). Briefly, high-binding 96-well ELISA plate (Corning, Corning, NY, USA) was coated with 100 μ l per well of 10 mg/ml human serum albumin (HSA) in 50 mM carbonate/bicarbonate buffer (pH 9.6), diluted 1:500. After 3 hours of incubation at 37°C, wells were washed thrice with 0.01 M PBS (pH 7.2). Consequently, the wells were blocked with 100 μ l/well of 10% FCS in PBS and incubated for 1 hour at RT. Afterwards, the wells were washed thrice with PBS and incubated overnight at 4 °C with rabbit polyclonal anti-HSA IgG at a 1:400 dilution in PBS or with PBS alone as a negative control.

Neutrophils were isolated as described (2.2.6), resuspended in RPMI-1640 containing 1% FCS, 1 g/L D-(+)-Glucose and 25 mM HEPES to a density of 2×10^6 cells/ml. Thereafter, tested substances were prepared as a 2x solutions and diluted 1:1 with the cells, followed by the pre-incubation at 37°C for various time points. 50 μ l of 0.2 mM luminol was added to the solutions. Following three washing cycles of the wells with PBS, 200 μ l of the cell suspension was added into each well of the high-binding 96-well ELISA plate.

The chemiluminescence reaction was monitored for 2 hours at 37°C using Tecan Infinite M200 PRO ELISA reader (Thermo Fisher Scientific, Waltham, MA, USA). Afterwards, the area under the curve was calculated and used for comparison. After completing the 2 hours chemiluminescence reaction, the samples were spun down, and the supernatant was collected and stored at -20°C for ELISA measurements.

2.2.8 LTB₄ competitive enzyme immunoassay

LTB₄ was quantified using the LTB₄ parameter assay kit (R&D Systems, Wiesbaden, Germany) according to the manufacturer's instructions. In brief, 50 μ l of the cell-free supernatants of neutrophils after stimulation with ICs for 2 hours was added to the wells, followed by adding 50 μ l of the primary antibody solution. After 1 hour of incubation at RT on a microplate shaker at 300 rpm, 50 μ l of LTB₄ conjugated was added to each well and incubated for 3 hours at RT on the shaker. The wells were washed four times with 400 μ l of wash buffer. 200 μ l of substrate solution was added and incubated for 30 min at RT in a

place protected from light. After adding 100 μ l of stop solution, the measurements were performed at 450 nm with a reference wavelength of 540 nm using the Infinite M200 PRO ELISA reader. A four-parameter logistic (4-PL) curve was generated and the concentrations of LTB₄ corresponding to the mean absorbance from the standard curve were calculated.

2.2.9 Metabolic analysis of murine neutrophils

For the analysis of cell metabolism *in vitro*, the cellular acidification rate (ECAR) [mpH/min] and oxygen consumption rate (OCR) [pmol/min] were examined using the XF24 Extracellular Flux Analyzer (Agilent Technologies, Waldbronn, Germany). The ECAR measures the change over time of the media pH, is mainly affected by secretion of the glycolysis end product lactate and is considered an indirect measure of glycolysis activity in cells. While the measurement of OCR enables the assessment of mitochondria activity over time and their role in cell physiology.

The day before the measurement, the XF Sensor Cartridge was filled with 1 ml per well of Seahorse XF Calibrant Solution and placed in 37 °C without additional CO₂ supply. Murine BM-derived neutrophils were resuspended in Seahorse assay medium (DMEM without Phenol Red supplemented with L-glutamine (final concentration: 2 mM), glucose (final concentration: 10 mM), Sodium Pyruvate (final concentration: 1 mM); pH 7.4; 37 °C). 1.0x10⁶ neutrophils per well (100 μ l) were plated on an XF24 plate, coated as previously described, and centrifuged until the speed has reached 40 x g. The plate was incubated for 30 minutes in a CO₂-free incubator at 37 °C. Thereafter, 425 μ l per well of assay medium (37 °C) was added, followed by the 30 min of incubation in a CO₂-free incubator at 37 °C. Injection ports A to D were filled with 75 μ l assay medium containing oligomycin (final concentration: 1 μ M), FCCP (final concentration: 1 μ M), antimycin A + rotenone (final concentration: 1 μ M each) and 2-deoxy-D-glucose (final concentration: 100 mM) respectively. If indicated, cells were pre-incubated for 30 min at 37 °C with 10 mM metformin, 1 mM AICAR and/or stimulated with ICs.

The XF Assay run as followed:

Calibrate

Equilibrate

Base line readings (Loop 5 times):

5 min Loop Start - 3 min Mix – 2 min Wait – 3 min Measure – Loop End

Inject port A (Oligomycin) (Loop 3 times):

3 min Loop Start – 3 min Mix – 2 min Wait – 3 min Measure – Loop End

Inject Port B (FCCP) (Loop 3 times):

3 min Loop Start – 3 min Mix – 2 min Wait – 3 min Measure – Loop End

Inject Port C (Antimycin A + Rotenone) (Loop 3 times):

3 min Loop Start – 3 min Mix – 2 min Wait – 3 min Measure – Loop End

Inject Port D (2-DG) (Loop 3 times):

3 min Loop Start – 3 min Mix – 2 min Wait – 3 min Measure – Loop End

End program

2.2.10 Sytox Green

Extracellular NETs formation was measured using Sytox Green (Thermo Fisher Scientific, Waltham, MA, USA), a cell-impermeable DNA binding dye. Fixed ICs were formed as previously described (2.2.7) with minor modifications. The high-binding 96-well chimney well black plates (Greiner Bio-One, Austria) were coated with 100 μ l per well of 10 mg/ml human serum albumin (HSA) in 50 mM carbonate/bicarbonate buffer (pH 9.6), diluted 1:100. The rabbit polyclonal anti-HSA IgG was diluted 1:80.

Freshly isolated mice neutrophils (2.2.6) were resuspended in HBSS medium at density of 2×10^6 cells/ml. Tested substances were prepared as a 2x solutions and diluted 1:1 with the cells. After 30 min of pre-incubation at 37°C and 5% CO₂, 5 μ M of Sytox Green was added. Subsequently, Sytox Green fluorescence was monitored for 5 hours by Infinite M200 PRO ELISA reader (Thermo Fisher Scientific, Waltham, MA, USA) at 37 °C at an excitation wavelength of 492 nm and an emission wavelength of 530 nm. Afterwards, the area under the curve was calculated and used for comparison.

2.2.11 Immunohistochemistry

Immunohistochemistry (IHC) stainings were performed to detect and present the specific composition of the cellular infiltrate of the perilesional skin in the BP-like EBA mouse model. After harvesting the skin at the end of experiment on day 16, the skin biopsies were fixed in 4% Histofix solution, paraffin embedded, cut to 6- μ m sections, and stored at -20 °C until further use.

Before starting a designated staining protocol, the slides were deparaffinized and rehydrated at RT by immersing them through the following solutions:

- Xylene, two washes 3 minutes each
- 96% Ethanol, two washes 3 minutes each
- 70% Ethanol, one wash 3 minutes
- 50% Ethanol, one wash 3 minutes
- Distilled water, two washes 3 minutes each
- PBS (pH 7.2), two washes 3 minutes each

2.2.11.1 Detection of Ly6G using IHC

For the Ly6G staining antigen retrieval, the sections were treated with pepsin for 10 min at RT, washed thrice with 0.01 M TBS (pH 7.6) for 5 min, and blocked for 1 hour with 5% normal goat serum (NGS) in 0.01 M TBS. Consequently, the rat anti-mouse Ly6G antibody (1:100 in 5% NGS in TBS) or the normal rat IgG antibody (1:100 in 5% NGS in TBS) for isotype control were added for overnight incubation at 4 °C. Subsequently, the slides were washed thrice with 0.01 M TBS for 5 min and incubated with Alexa Fluor® 594 goat anti-rat antibody (1:500 in 0.01 M TBS) for 1 hour at RT. Following triple washing with 0.01 TBS for 5 min, the slides were mounted with DAPI fluoromount G and left overnight at RT on a flat surface protected from light. Ly6G+ cells were counted in three independent high-power fields (HPF) at 200x magnification for each sample and averaged, using the Keyence Microscope BZ-9000E series.

2.2.11.2 Detection of FoxP3 using IHC

For the FoxP3 staining antigen retrieval was performed in Sodium citrate buffer (10 mM Sodium citrate, 0.05% Tween 20, pH 6.0) using a pressure cooker at 100 °C for 10 min, followed by triple washing with 0.01 M PBST (pH 7.2) for 5 min. Afterwards, the slides were treated with 1% Triton X-100 in PBS for 30 min at RT, washed thrice with 0.01 M PBST, and blocked for 1 hour with 5% NGS in PBST at RT before the addition of rat anti FoxP3 antibody (1:50 in 5% NGS in PBST) or total rat IgG antibody (1:50 in 5% NGS in PBST) for overnight incubation at 4 °C. Then, the slides were washed thrice with 0.01 M PBST for 5 min and incubated with Alexa Fluor® 594 goat anti-rat antibody (1:500 in 0.01 M PBST) for 1 hour at RT. Following three washing cycles with 0.01 M PBST for 5 min, the slides were mounted with DAPI fluoromount G and left overnight at RT on a flat surface protected from light. FoxP3+ cells were counted manually in three independent high-power fields (HPF) at 200x magnification for each sample and averaged, using the Keyence Microscope BZ-9000E series.

2.2.12 RNA isolation from skin samples

Total RNA was isolated from cryosections of skin biopsies using TRIzol® Reagent (Thermo Fisher Scientific, Waltham, MA, USA) according to the manufacturer's instructions with minor modifications. In detail, frozen skin biopsies were crushed to a fine powder in liquid nitrogen. Later, 1 ml of TRIzol Reagent was added to 50 to 100 mg of pulverized frozen tissue. Then, 0.2 ml of chloroform was added to each sample, which were subsequently vigorously vortexed for 15 s and incubated for 3 min at RT. Following centrifugation at 10,000 g for 15 min at 4 °C, the colorless upper aqueous phases containing the RNA were transferred into a fresh 1.5 ml tubes. Afterwards, 0.5 ml of isopropyl alcohol was added, incubated for 10 min at RT and centrifuged at 10,000 g for 15 min at 4 °C. The supernatants were removed completely, and the RNA pellets were washed with 1 ml of 75% ethanol. The samples were vortexed and centrifuged at 5,000 g for 5 min at 4 °C. The washing procedure was repeated once, and ethanol was removed. The samples were air dried for 5-10 min until ethanol was completely evaporated and subsequently, the RNA pellets were dissolved in 15 µl DEPC-treated water. The RNA concentrations were measured by Nanodrop 2000c spectrophotometer (Thermo Fisher Scientific, Waltham, MA, USA).

2.2.13 RNA isolation from cells

The total RNA was isolated from cells using RNeasy Micro Kit (Qiagen, Germany). The neutrophils were isolated as described in 2.2.6. Afterwards, cells were spun down for 5 min at 400 g at 4 °C and the supernatant was removed. Neutrophils were resuspended in 350 µl Buffer RLT and vortexed. 350 µl of 70% ethanol was added to the lysate and mixed well by pipetting. After transferring the sample into the RNeasy MinElute spin column, the centrifugation for 15 s at 8000 g followed. The flow-through was discarded, and 350 µl of Buffer RW1 was added to the RNeasy MinElute spin column. Afterwards, the sample was centrifuged for 15 s at 8000 g and the RNeasy MinElute spin column was placed in a new 2 ml collection tube. 500 µl of Buffer RPE was added to the spin column and centrifuged for 15 s at 8000 g. The flow-through was discarded, 500 µl of 80% ethanol was added to the RNeasy MinElute spin column and centrifuged for 2 min at 8000 g. The flow-through and collection tube were discarded, and RNeasy MinElute spin column was placed in a new 2 ml collection tube. The centrifugation for 2 min at 10000 g followed and the RNeasy MinElute spin column was placed in a new 1.5 ml collection tube. Thereafter, 14 µl of RNase-free water was added directly to the center of the spin column membrane and the samples was centrifuged for 1 min at 10000 g. The RNA concentrations were measured by Nanodrop 2000c spectrophotometer (Thermo Fisher Scientific, Waltham, MA, USA).

2.2.14 cDNA synthesis

Reverse transcription of the isolated RNA to cDNA was performed using the RevertAid First Strand cDNA Synthesis Kit (Thermo Fisher Scientific, Waltham, MA, USA) according to the manufacturer's instructions with minor modifications. Briefly, to a sterile, nuclease-free 200 µl tube on ice 1 µl of oligo (dT)₁₈ primer was used for 500 ng of total RNA and next nuclease-free water was added to give a total volume of 12 µl. Thereafter, 8 µl of master mix containing the following reagent was added:

- 4 µl 5X Reaction Buffer
- 1 µl RiboLock RNase Inhibitor
- 2 µl 10 mM dNTP Mix
- 1 µl RevertAid Transcriptase

The solution was gently mixed and centrifuged briefly. Subsequently, the reaction mixture and mRNA were incubated for 60 min at 42 °C and terminated by heating at 70 °C for 5 min in S1000™ Thermal Cycler (Eppendorf AG, Hamburg, Germany). Samples were stored at -20°C until further use or prepared for RT-qPCR.

2.2.15 Real time quantitative PCR (RT-qPCR)

To quantify and compare the mRNA levels of selected genes, the produced cDNA (2.2.14) was used for RT-qPCR. All primers (2.1.7) were purchased from biomers.net (biomers.net GmbH, Ulm, Germany) at concentration of 100 µM. The reactions were conducted in a 96-well PCR plate using the SYBR Select Master Mix (Thermo Fisher Scientific, Waltham, MA, USA). 10 µl of the reaction mix was prepared for an individual well as followed:

- 4 µl of cDNA
- 5 µl of SYBR Select Master Mix (2X)
- 0.5 µl of 5 µM forward primer
- 0.5 µl of 5 µM reverse primer

All RT-qPCR reactions were performed in duplicates on the Eppendorf Mastercycler ep Realplex (Eppendorf, Hamburg, Germany) with 50 °C for 2 min, 95 °C for 2 min, followed by 40 cycles each of 95 °C for 15 s, and 60 °C for 1 min each. The results were analysed using $2^{-\Delta\Delta CT}$ method. The expression level of the gene of interest was normalized to the expression of *Psm4* gene. Moreover, all used primers are designed to either span an exon-exon junction or are designed that a primer pair is separated by an intron sequence of at least >2000bp, prohibiting amplification of genomic DNA during the PCR cycle conditions.

2.2.16 Migration Assay

Freshly isolated neutrophils from murine bone marrow (2.2.6), were resuspended to a density of 5×10^6 neutrophils in chemiluminescence medium (CL medium). The absolute number of cells was adjusted using 10 µl of CountBright™ Absolute Counting Beads (Thermo Fisher Scientific GmbH, Dreieich, Germany) and assayed via flow cytometry. Firstly, a nonbinding 24-well plate (6.5 mm transwell with 3.0 µm pore polycarbonate membrane insert; Sigma-Aldrich, Darmstadt, Germany) was incubated with CL medium for

1 h at 37 °C (700 µl of CL medium was added directly into the plate and 100 µl was added into transwell inserts). Neutrophils were incubated with 1 mM AICAR or CL medium for 30 min at 37 °C and 5% CO₂. For chemokinesis, to the AICAR-treated and control cells, chemoattractants C5a and LTB₄ were added to obtain concentration of 100 nM and 10 nM, respectively. The CL medium was discarded from the plate and 1 ml of CL medium was added to the bottom wells, additionally for chemotaxis and chemokinesis C5a and LTB₄ were added to obtain concentration of 100 nM and 10 nM, respectively. 25 x 10⁴ cells in 200 µl were placed into the transwell inserts and the plate was incubated for 2 h at 37 °C and 5% CO₂. After the incubation time, to the 495 µl of suspension taken from the bottom well, 5 µl of Counting Beads was added. The number of migrated neutrophils was determined using flow cytometry MACSquant Analyzer 10 (Miltenyi Biotec, Bergisch Gladbach, Germany). The data were presented as a percentage of migrated neutrophils.

2.2.17 Cytotoxicity Assay

To examine whether the drugs used in this study had apoptotic or necrotic effect on the neutrophils, a two-color flow cytometry was performed using Annexin V-FITC Detection Kit (PromoCell, Heidelberg, Germany). Apoptosis, known as programmed cell death, was detected using Annexin V, which binds to phosphatidylserine, cytoplasmic-facing aminophospholipid that turns outwards in an early phase of apoptosis. Propidium iodide, on the other hand, binds to nucleic acids of necrotic cells with compromised membrane (Crowley et al., 2016).

Briefly, 1 x 10⁵ cells were incubated for 3 hours at 37 °C with or without drugs of interest (10 mM metformin, 4 mM 2-DG, 1 mM AICAR, 30 µM heptelidic acid, 1 mM/0.5 mM/0.3 mM/0.1 mM moxifloxacin). To prepare positive control (dead cells), cells were heated for 15 min at 89 °C. Afterwards, cells were spun down for 5 min at 400 g at 4 °C and the supernatants were removed. Single stained cells were resuspended in 99 µl 1X binding buffer and 1 µl of Annexin V-FITC/PI. Double stained cells were resuspended in 100 µl mastermix containing 98 µl 1x binding buffer, 1 µl Annexin V and 1 µl PI per sample. The unstained control was resuspended in 100 µl 1X binding buffer. The samples were vortexed thoroughly and incubated for 5 min at RT in the dark. After that, the samples were placed on ice until they were measured. 1 x 10⁴ cells per sample were acquired on MACSquant

Analyzer 10 (Miltenyi Biotec, Bergisch Gladbach, Germany) and analyzed with FlowJo software V10. The cytotoxic effect was determined as percentage of apoptotic and necrotic cells of the viable control cells.

The results of the cytotoxicity assays revealed that none of the substances used induced apoptotic or necrotic cell death (Figure 4).

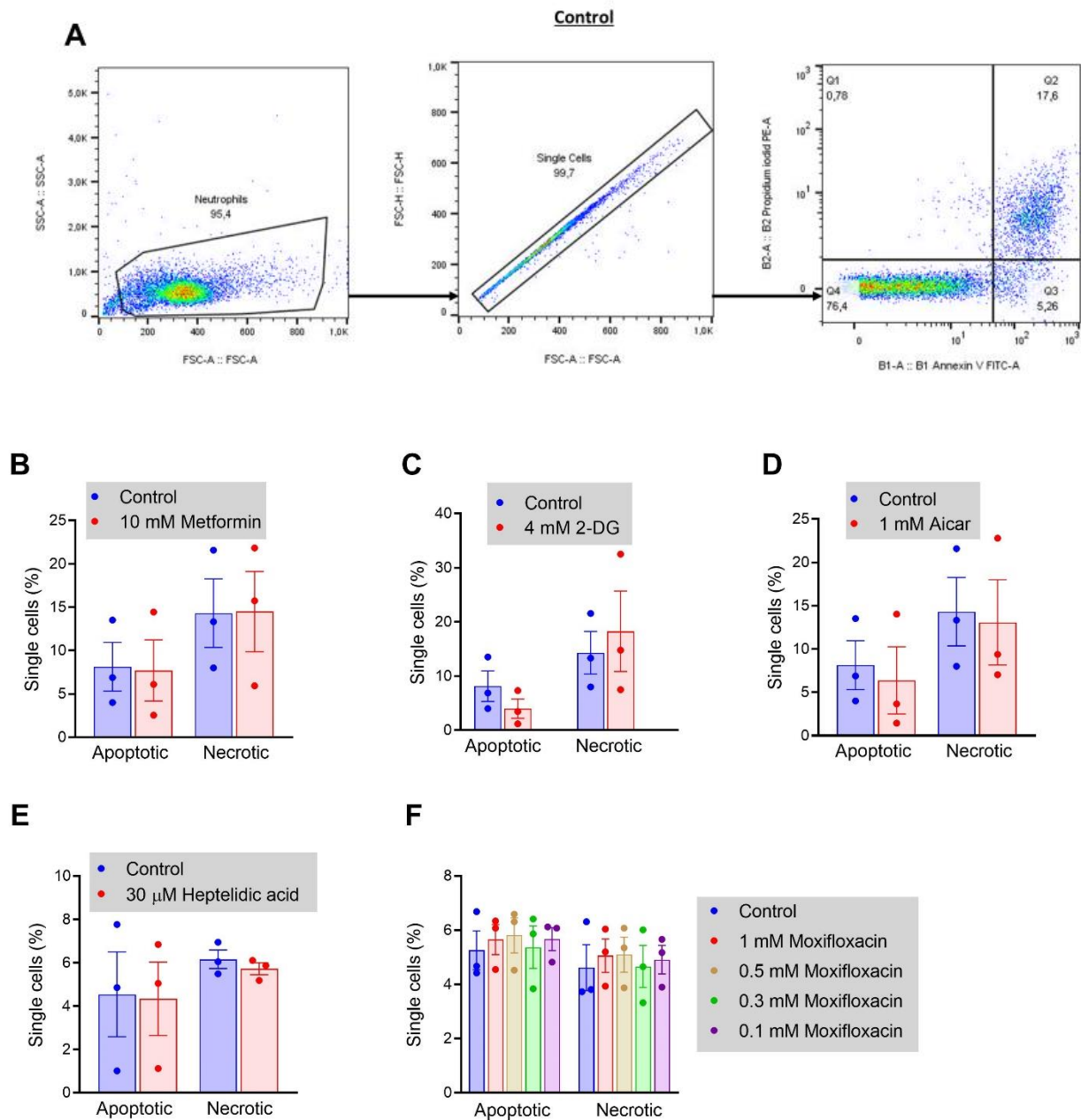


Figure 4. Drugs used in *in vitro* experiments are not cytotoxic.

Freshly isolated murine BM neutrophils were incubated for 3 hours at 37 °C with/without drugs of interest. Next, apoptosis and necrosis in the cell populations were determined by staining with anti-Annexin V (FITC) and propidium iodide (PI), respectively. The cytotoxic effect is presented as percentage of the viability of control cells. **(A)** Representative flow cytometry data of gating strategy for analysis of neutrophils to identify apoptotic and necrotic cells. Percentage of apoptotic and necrotic neutrophils after 3 h of incubation with **(B)** 10 mM metformin, **(C)** 4 mM 2-DG, **(D)** 1 mM AICAR, **(E)** 30 μM Heptelidic acid, **(F)** 1 mM/0.5 mM/0.3 mM/0.1 mM moxifloxacin. Data are presented as mean ± SEM, n = 3 and each dot represents an independent experiment.

2.2.18 Statistical analysis

Statistical analysis was performed using GraphPad Prism 8.4.3 (GraphPad, San Diego, CA, USA). Groups were compared by one- or two-way ANOVA with Holm-Sidak's multiple comparisons test, Kruskal-Wallis with Dunn's multiple comparison, and Tukey's multiple comparisons test, as indicated. A two-tailed Mann-Whitney U test was used to determine statistical difference between two groups of not normally distributed data. A p-value of <0.05 was considered statistically significant. If not otherwise indicated, mean \pm standard error of the mean (SEM) is presented.

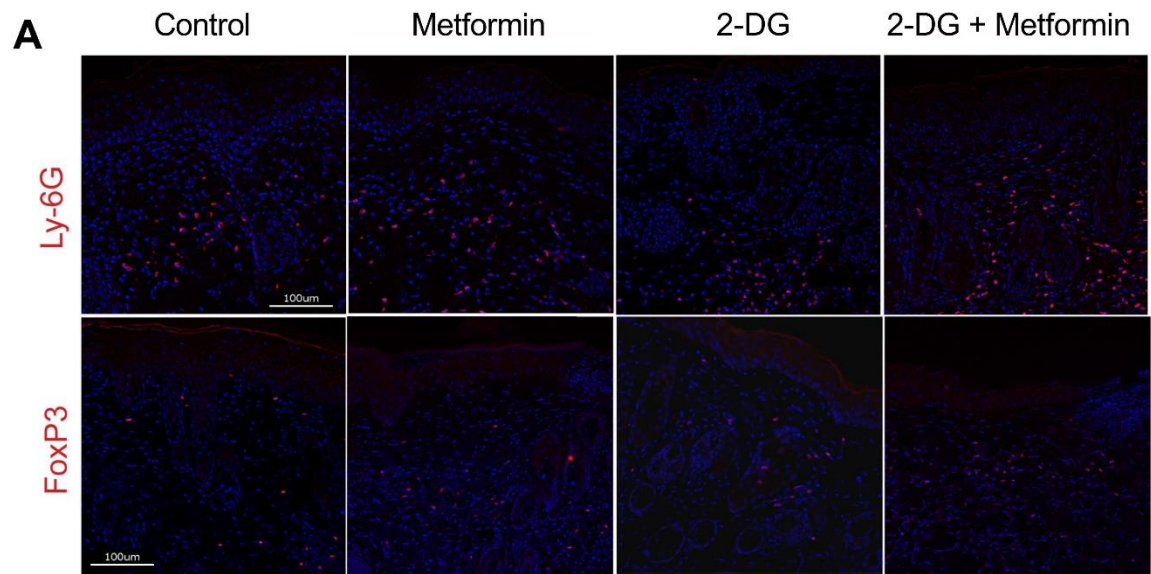
3 RESULTS

3.1 Mechanisms of metformin and 2-DG action in the BP-like EBA mouse model

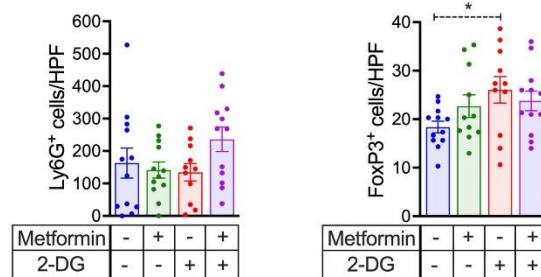
Preliminary data from our lab showed that metformin and 2-deoxy-glucose (2-DG) ameliorate the disease symptoms in the antibody transfer model of BP-like EBA (Figure 2). Studies on BP-like EBA have shown that neutrophils and T_{regs} are involved in the effector phase of EBA pathogenesis (Bieber et al., 2017), therefore the cellular composition of the dermal infiltrate of perilesional skin harvested at the end of the experiment on day 16 was analyzed. By staining for the cell markers Ly6G and FoxP3, we were able to assess the density of neutrophils and T_{regs} infiltration in the skin, respectively. IHC analysis revealed no difference in the density of Ly-6G⁺ cells between the groups (Figure 5B). However, the non-significant trend towards an increase of FoxP3⁺ T_{regs} cells under treatment with metformin alone and the combination of 2-DG with metformin was observed and reached statistical significance for the comparison between the vehicle and the 2-DG treatment group (Figure 5B) (2-DG: 26.05 ± 2.73 vs. Control: 18.39 ± 1.2 ; adj. p-value = 0.0404; Metformin: 22.7 ± 2.32 vs. Control: 18.39 ± 1.2 ; adj. p-value = 0.1553; 2-DG + Metformin: 23.78 ± 2.02 vs. Control: 18.39 ± 1.2 ; adj. p-value = 0.1375).

In order to further characterize the differences in skin inflammation under given treatment, the expression levels of specific genes in perilesional skin obtained on day 16 was investigated (Figure 5C). The mRNA levels of the anti-inflammatory cytokine IL-10 increased under the treatment with metformin alone as well as in combination of metformin with 2-DG, while the non-significant trend towards an increase of TGF- β 1 level was observed under the treatment with metformin alone and reached statistical significance for the combination of 2-DG with metformin, compared with controls (IL-10: Metformin: $0.9 \times 10^{-2} \pm 0.2 \times 10^{-2}$ vs. Control: $0.2 \times 10^{-2} \pm 0.04 \times 10^{-2}$; adj. p-value = 0.0413; 2-DG + Metformin: $1.2 \times 10^{-2} \pm 0.5 \times 10^{-2}$ vs. Control: $0.2 \times 10^{-2} \pm 0.04 \times 10^{-2}$; adj. p-value = 0.0455; TGF- β 1: Metformin: 0.47 ± 0.17 vs. Control: 0.18 ± 0.08 ; adj. p-value = 0.4601; 2-DG + Metformin: 0.8 ± 0.25 vs. Control: 0.18 ± 0.08 ; adj. p-value = 0.0371). In addition, the monotherapy with metformin tended to increase the mRNA levels of TNF- α , IL-1 β and CXCL2, albeit not statistically significant. The treatment with 2-DG alone showed a non-significant tendency

of increased TNF- α and IL-1 β levels. Likewise, the combination of metformin with 2-DG tended towards increased CXCL2 levels, although not statistically significant.



B



C

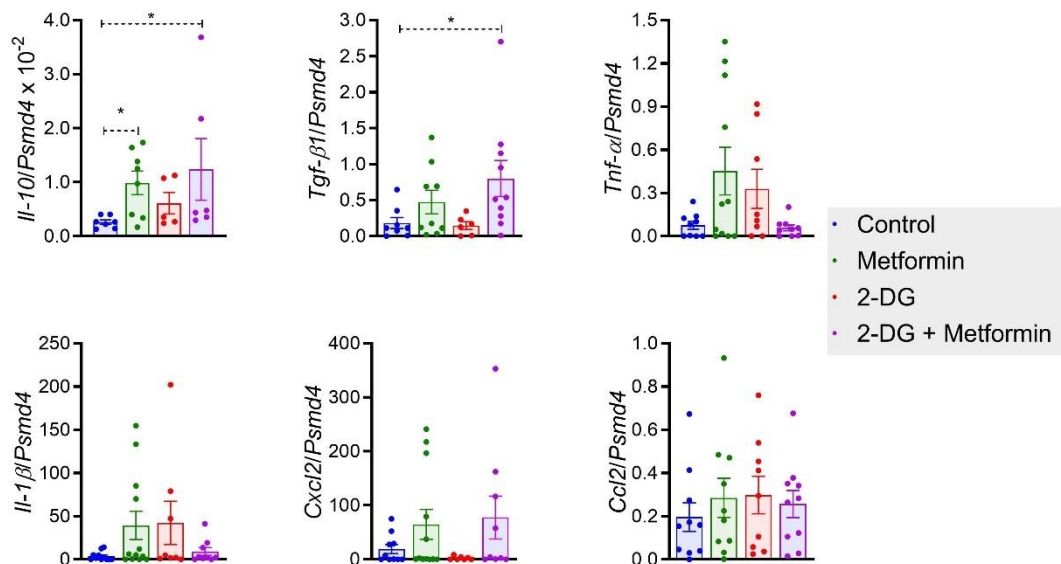


Figure 5. Cellular infiltration of the perilesional skin and expression of the genes involved in the skin inflammation.

(A) Representative IHC staining for Ly6G and FoxP3 of perilesional skin harvested on day 16 in the BP-like EBA model. (B) The quantification of the density of cells, positive for the Ly6G and FoxP3 markers; n = 11-12 mice per group. (C) mRNA expression levels of select genes in perilesional skin harvested on day 16; n = 6-12 mice per each group. All results are presented as mean ± SEM. Results were compared by Kruskal-Wallis and Dunn's multiple comparison test. *, p < 0.05 for the comparisons indicated. Scale bars represent 100 μm.

3.2 Gene expression of metformin and glucose receptors in murine neutrophils

Neutrophils play a pivotal role in the pathogenesis of the BP-like EBA model and may be a key target for the effects observed in the *in vivo* experiments. To further investigate the potential effects of metformin (and 2-DG) on neutrophil function, initial experiments sought to identify whether the two substances may be effectively taken up by the cells via commonly accepted transporters.

The most important transporters through which metformin enters the cells are organic cation transporters (OCTs), members of the SLC22 transporter family. The first one discovered and so far best examined is OCT1 (Wang et al., 2002). However, it has been demonstrated that also OCT2 (Kimura et al., 2005) and OCT3 (Chen et al., 2015) are involved in the metformin transport. Therefore, by using RT-qPCR the expression of these transporters in murine BM-derived neutrophils was assessed. The mRNA levels of OCT1-3 were detectable in neutrophils, however the expression levels were low and several times lower than those found in the liver and kidneys (Figure 6A).

In addition, it is concluded that the main source of energy in neutrophils is glycolysis, which begins by importing glucose into the cell through GLUT transporters, a member of the SLC2A family of membrane transporters. Under normal physiological conditions, GLUT1, GLUT3, and GLUT4 have a high affinity for glucose, allowing transport of glucose into the cells (Macheda et al., 2005). Given that the main source of energy in neutrophils is glycolysis, the expression of GLUT1, 3, and 4 was investigated using RT-qPCR. The results demonstrated moderate expression of GLUT1, high expression of GLUT3 and low expression of GLUT4, compared to liver and kidney in murine neutrophils (Figure 6B).

The data presented here suggest low expression of OCT1 and OCT3 receptors capable of metformin uptake and predominant expression of GLUT1 and GLUT3 with low expression of GLUT4, capable of glucose and 2-DG uptake.

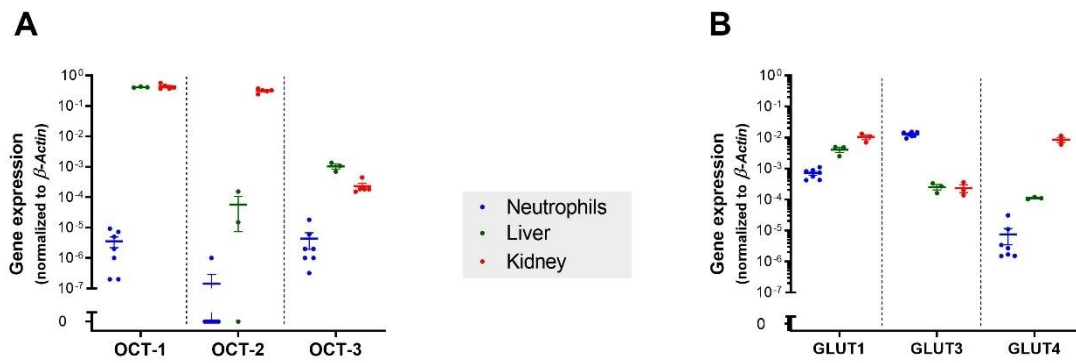


Figure 6. mRNA expression of select genes in murine neutrophils, liver, and kidney tissue.

Gene expression of (A) OCT1, OCT2, OCT3 and (B) GLUT1, GLUT3, GLUT4 in murine neutrophils, liver, and kidney tissue. 3 independent experiments are presented as mean \pm SEM. N = 3-7 and each dot represents one mouse.

3.3 Metabolic activity of neutrophils in response to ICs and metformin

In the light of the gene expression results indicating that neutrophils are capable of metformin uptake, the next steps were to investigate how much metformin affected cellular functions in neutrophils.

Immune complex-induced neutrophil activation is considered to be one of the major reasons for tissue damage in pemphigoid diseases, like BP-like EBA (Sadik et al., 2018). On that account, it has been investigated how *ex vivo* stimulation with ICs affects the murine neutrophils glycolysis, one of the key metabolic pathways in neutrophils (Kumar and Dikshit, 2019), and OXPHOS. By adding oligomycin, an ATP synthase inhibitor, the ATP/ADP ratio decreases, which stimulates glycolysis (TeSlaa and Teitell, 2014). On the other hand, as mitochondrial ATP production decreases, so does the cellular respiration. The addition of FCCP, an uncoupler of mitochondrial membrane potential, leads to maximal activity of the respiratory chain by transporting protons across the mitochondrial inner membrane and depolarization of the mitochondrial membrane potential (Divakaruni et al., 2014). The injection of antimycin A and rotenone, the inhibitors of complex III and I of the electron transport chain, respectively, results in complete inhibition of mitochondrial respiration (Divakaruni et al., 2014). Whereas 2-DG, a glucose derivative and inhibitor of glycolysis, is phosphorylated by hexokinase to 2-deoxyglucose-phosphate (2-DG-P), which cannot be used in further steps of glycolysis and accumulates in the cell. 2-DG-P inhibits hexokinase in a noncompetitive, and phosphoglucose isomerase in a competitive manner. (Seo et al., 2014).

3.3.1 The effect of immune complexes and metformin on the glycolytic activity of murine bone marrow-derived neutrophils

As it has been shown that glycolysis is vital for energy production in neutrophils, the extracellular flux analysis (ECAR) with the Seahorse XF24 analyzer was employed. The findings demonstrate that stimulation of neutrophils with ICs caused a significant increase of the basal glycolysis rate (Control: 4.22 ± 1.58 vs. IC: 16.52 ± 0.62 ; adj. p-value = 0.043; Figure 7B), whereas no significant changes could be identified in maximal glycolysis, glycolytic capacity, and non-glycolytic acidification rates. At the same time, metformin (10 mM) appears to have slightly elevated basal glycolysis but did not significantly alter glycolytic metabolism overall. Correspondingly, 10 mM metformin tended to stimulate basal glycolysis in IC-stimulated neutrophils, although not statistically significant (Figure 7).

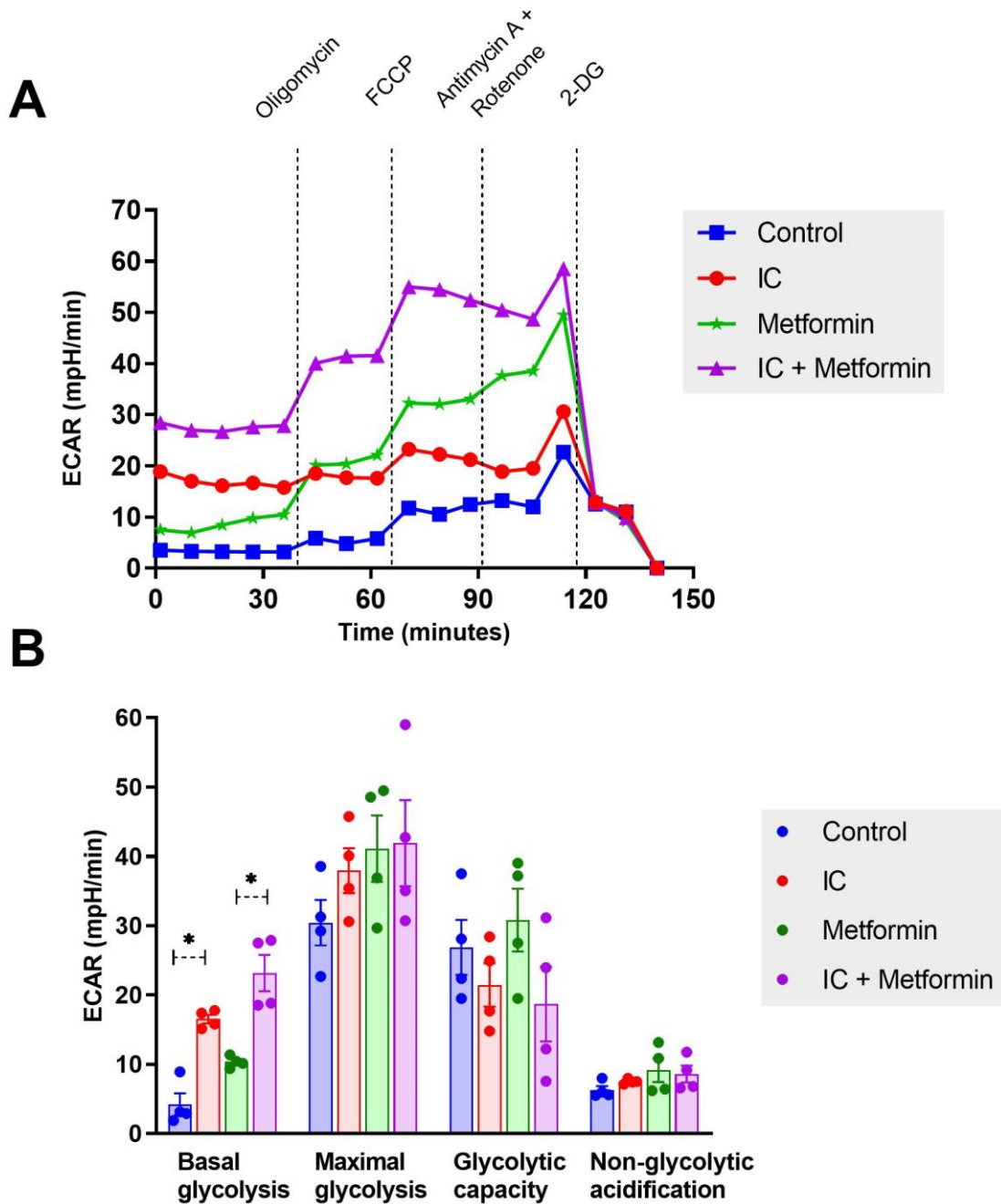


Figure 7. Stimulation of neutrophils with ICs enhances aerobic glycolysis, whereas metformin does not affect it.

Neutrophil metabolic activity in response to ICs and metformin treatment was profiled by Seahorse XF24 analyzer. **(A)** Representative experiment measuring ECAR over time in murine neutrophils with and without stimulation by ICs and treatment with metformin (10 mM). **(B)** ECAR of murine neutrophils with and without treatment with metformin (10 mM) and ICs. The difference between Control and IC + Metformin of the basal glycolysis rate was statistically significant however for reasons of clarity is not shown on the graph. Results are presented as mean \pm SEM. N = 4 and each dot represents an independent experiment. Results were analyzed by two-way ANOVA with Holm-Sidak's multiple comparison test. *, $p < 0.05$ for the comparisons indicated.

3.3.2 The effect of immune complexes and metformin on the mitochondrial respiration of murine bone marrow-derived neutrophils

Besides glycolysis, mitochondrial respiration of murine BM-derived neutrophils was analyzed.

As expected, the treatment with metformin, which is classically described as an inhibitor of mitochondrial complex I, has reduced OXPHOS (Figure 8). In more detail, treatment with metformin led to a significant decrease in basal respiration, ATP production and maximal respiration, consistent with inhibition of the complex I of the OXPHOS system (basal respiration: Control: 55.81 ± 7.7 vs. Metformin: 14.38 ± 1.89 ; adj. p-value = 0.0252; ATP production: IC: 51.15 ± 5.96 vs. IC + Metformin: 12.56 ± 2.8 ; adj. p-value = 0.0410; max. respiration: Control: 102.98 ± 12.55 vs. Metformin: 39.71 ± 10.58 ; adj. p-value <0.001). On the other hand, the stimulation with immobilized ICs did not affect the murine neutrophils OXPHOS parameters (Figure 8B).

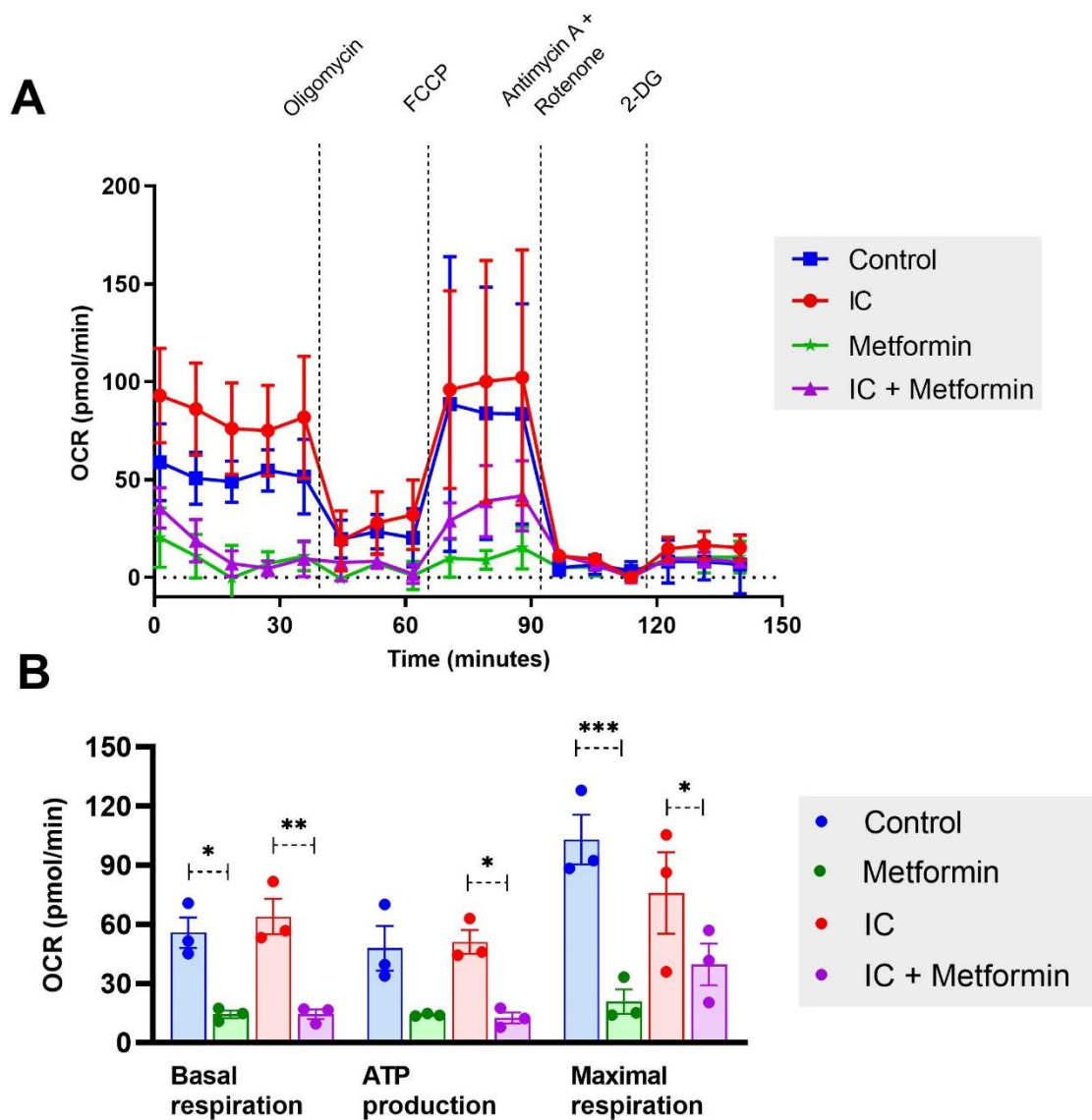


Figure 8. Metformin reduces mitochondrial respiration in murine BM-derived neutrophils.

Neutrophil metabolic activity in response to ICs and metformin treatment was profiled by Seahorse XF24 analyzer. **(A)** Representative experiment measuring OCR over time in murine neutrophils with and without stimulation by ICs and treatment with metformin (10 mM). **(B)** OCR of murine neutrophils with and without treatment with metformin (10 mM) and ICs. The difference between Control and IC + Metformin of the basal respiration and maximal respiration rates was statistically significant however for reasons of clarity is not shown on the graph. Results are presented as mean \pm SEM. N = 3 and each dot represents an independent experiment. Results were analyzed by two-way ANOVA with Holm-Sidak's multiple comparison test. *, $p < 0.05$; **, $p < 0.01$; ***, $p < 0.001$ for the comparisons indicated.

3.4 The effect of metformin, 2-DG and oligomycin on the IC-triggered release of ROS and LTB₄ from murine neutrophils

As ROS and LTB₄ both have previously been described to be detrimental to the progression of EBA, the role of metformin and 2-DG with respect to the release of these two agents has been investigated. Stimulation of neutrophils with ICs significantly induced the release of ROS and LTB₄ (Figure 9). However, incubation of PMNs with 4 mM 2-DG almost completely abolished ROS and LTB₄ release. In line with this finding, incubation of PMNs with 10 mM metformin significantly inhibited both ROS and LTB₄ release (Metformin: for ROS: $2.35 \times 10^7 \pm 0.25 \times 10^7$ vs. $4.35 \times 10^7 \pm 0.5 \times 10^7$; adj. p-value = 0.0012; for LTB₄: 57.12 ± 28.31 vs. 812.9 ± 170.0 ; adj. p-value = 0.0007; 2-DG: for ROS: $0.55 \times 10^7 \pm 0.38 \times 10^6$ vs. $4.35 \times 10^7 \pm 0.5 \times 10^7$; adj. p-value < 0.0001; for LTB₄: 142.0 ± 77.87 vs. 812.9 ± 170.0 ; adj. p-value = 0.0016; Figure 9A). While the effect of 0.5 mM metformin on ROS and LTB₄ release in IC-stimulated neutrophils versus vehicle-treated IC-stimulated neutrophils was not significant (for ROS: $3.31 \times 10^7 \pm 0.7 \times 10^7$ vs. $4.35 \times 10^7 \pm 0.5 \times 10^7$; adj. p-value = 0.3755; for LTB₄: 1202.0 ± 200.7 vs. 1309 ± 182.4 ; adj. p-value = 0.6462; Figure 9B).

To evaluate whether the effect observed in metformin-treated neutrophils is linked to inhibition of mitochondrial metabolic activity and energy production, a more specific inhibitor of OXPHOS was tested. For this purpose, oligomycin, an ATP synthase inhibitor, was used. Interestingly, oligomycin significantly inhibited the IC-triggered ROS release in a dose-dependent manner beginning at a concentration as low as 1 μM (1 μM: $2.1 \times 10^7 \pm 0.18 \times 10^7$ vs. $3.13 \times 10^7 \pm 0.34 \times 10^7$; adj. p-value = 0.0024; 10 μM: $1.1 \times 10^7 \pm 0.41 \times 10^7$ vs. $3.13 \times 10^7 \pm 0.34 \times 10^7$; adj. p-value < 0.0001; Figure 9C). On the other hand, the inhibition of LTB₄ release was more resistant to oligomycin and was significant only upon treatment with higher concentrations of oligomycin (10 μM: 109.7 ± 63.65 vs. 827.3 ± 319.2 ; adj. p-value = 0.0245; Figure 9C), indicating selective differences of these two neutrophil responses in their susceptibility to mitochondrial modulation.

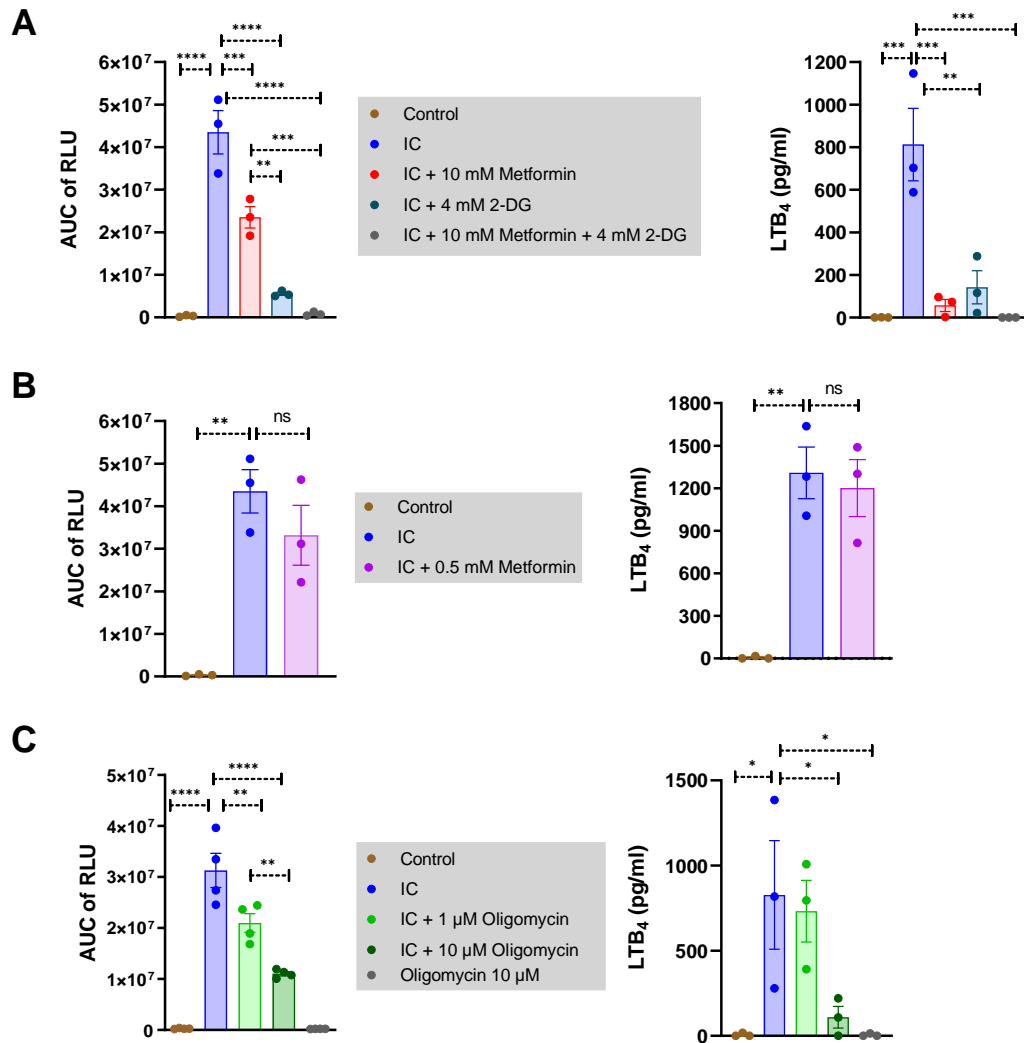


Figure 9. Metformin, 2-DG and oligomycin inhibit the release of ROS and LTB₄ from murine BM-derived neutrophils.

Neutrophils were treated with metformin/2-DG/oligomycin for 30 min and next stimulated with ICs. ROS release was measured as emitted light and shown in RLU. Thereafter, LTB₄ was detected in cell-free supernatants collected after ROS release measurement. **(A)** ROS and LTB₄ release from neutrophils upon stimulation with ICs under treatment with 10 mM metformin and/or 4 mM 2-DG. **(B)** ROS and LTB₄ release from neutrophils upon stimulation with ICs under treatment with 0.5 mM metformin **(C)** ROS and LTB₄ release from neutrophils upon stimulation with ICs under treatment with 1 μM or 10 μM oligomycin. All results are presented as mean ± SEM. N = 3-4 and each dot represents an independent experiment. Results were analyzed by one-way ANOVA and Holm-Sidak's multiple comparisons test. ns: not significant; *, p < 0.05; **, p < 0.01; ***, p < 0.001; ****, p < 0.0001 for the comparisons indicated. The experiments were carried out together with T. Bremer.

3.5 Pharmacological targeting of aerobic glycolysis

As the data presenting the inhibitory effect of 2-DG on the release of ROS and LTB₄ indicated that glycolysis is essential for the neutrophil response to IC stimulation (chapter 3.4), the additional inhibitors blocking varying steps in the glycolysis pathway, such as heptelidic acid (HA), galloflavin (GF) and TEPP-46, have been investigated (Figure 10).

To this end, freshly isolated murine BM-derived neutrophils were incubated for 15 min with 100 μM TEPP-46 or 30 min with heptelidic acid (3 μM, 10 μM, 15 μM, 20 μM, 30 μM) or 50 μM galloflavin. Next, neutrophils were stimulated with ICs and ROS released was measured. Thereafter, LTB₄ was detected in cell-free supernatants collected after ROS release measurements.

Heptelidic acid (koningic acid), a selective inhibitor of glyceraldehyde 3-phosphate dehydrogenase (GAPDH) (Liberti et al., 2017), dose-dependently reduced the release of ROS and LTB₄ (Figure 10B). In detail, heptelidic acid nullified the release of both ROS and LTB₄ at 30 μM and significantly reduced the release of ROS and LTB₄ at concentrations of 15 μM and 20 μM. Additionally inhibition of ROS release upon 10 μM treatment was also statistically significant (for ROS: 10 μM: $1.1 \times 10^7 \pm 0.47 \times 10^7$ vs. IC: $2.4 \times 10^7 \pm 0.21 \times 10^7$; adj. p-value = 0.0006; 15 μM: $0.44 \times 10^7 \pm 0.22 \times 10^7$ vs. IC: $2.4 \times 10^7 \pm 0.21 \times 10^7$; adj. p-value < 0.0001; 20 μM: $0.14 \times 10^7 \pm 0.08 \times 10^7$ vs. IC: $2.4 \times 10^7 \pm 0.21 \times 10^7$; adj. p-value < 0.0001; 30 μM: $0.35 \times 10^6 \pm 0.08 \times 10^6$ vs. IC: $2.4 \times 10^7 \pm 0.21 \times 10^7$; adj. p-value < 0.0001; for LTB₄: 15 μM: 86.14 ± 86.14 vs. IC: 316.9 ± 26.05 ; adj. p-value = 0.0117; 20 μM: 15.20 ± 15.20 vs. IC: 316.9 ± 26.05 ; adj. p-value = 0.0020; 30 μM: 0.0 vs. IC: 218.3 ± 27.06 ; adj. p-value < 0.0019; Figure 10B).

TEPP-46, is described to be an allosteric activator of pyruvate kinase M2 (PKM2) tetramerization, blocking its nuclear translocation, and as a result inhibiting the glycolysis (Angiari et al., 2020). 100 μM TEPP-46 significantly inhibited the release of ROS and LTB₄ from IC-stimulated neutrophils (for ROS: 100 μM TEPP-46: $1.4 \times 10^7 \pm 0.09 \times 10^7$ vs. IC: $2.07 \times 10^7 \pm 0.17 \times 10^7$; adj. p-value = 0.0012; for LTB₄: 100 μM TEPP-46 28.77 ± 6.92 vs. IC: 472.4 ± 42.66 ; adj. p-value < 0.0001; Figure 10C).

Galloflavin, a substance that inhibits A and B form of lactate dehydrogenase (Manerba et al., 2012), showed inhibition of ROS release. 50 μ M galloflavin significantly inhibited the release of ROS from IC-stimulated neutrophils (50 μ M galloflavin: $0.23 \times 10^7 \pm 0.03 \times 10^7$ vs. IC: $1.83 \times 10^7 \pm 0.33 \times 10^7$; adj. p-value = 0.0002; Figure 10D). However, the release of LTB₄ tended to increase upon the treatment with 50 μ M galloflavin, albeit not statistically significant (50 μ M galloflavin: 449.1 ± 79.77 vs. IC: 294.8 ± 82.38 ; adj. p-value = 0.1506; Figure 10D).

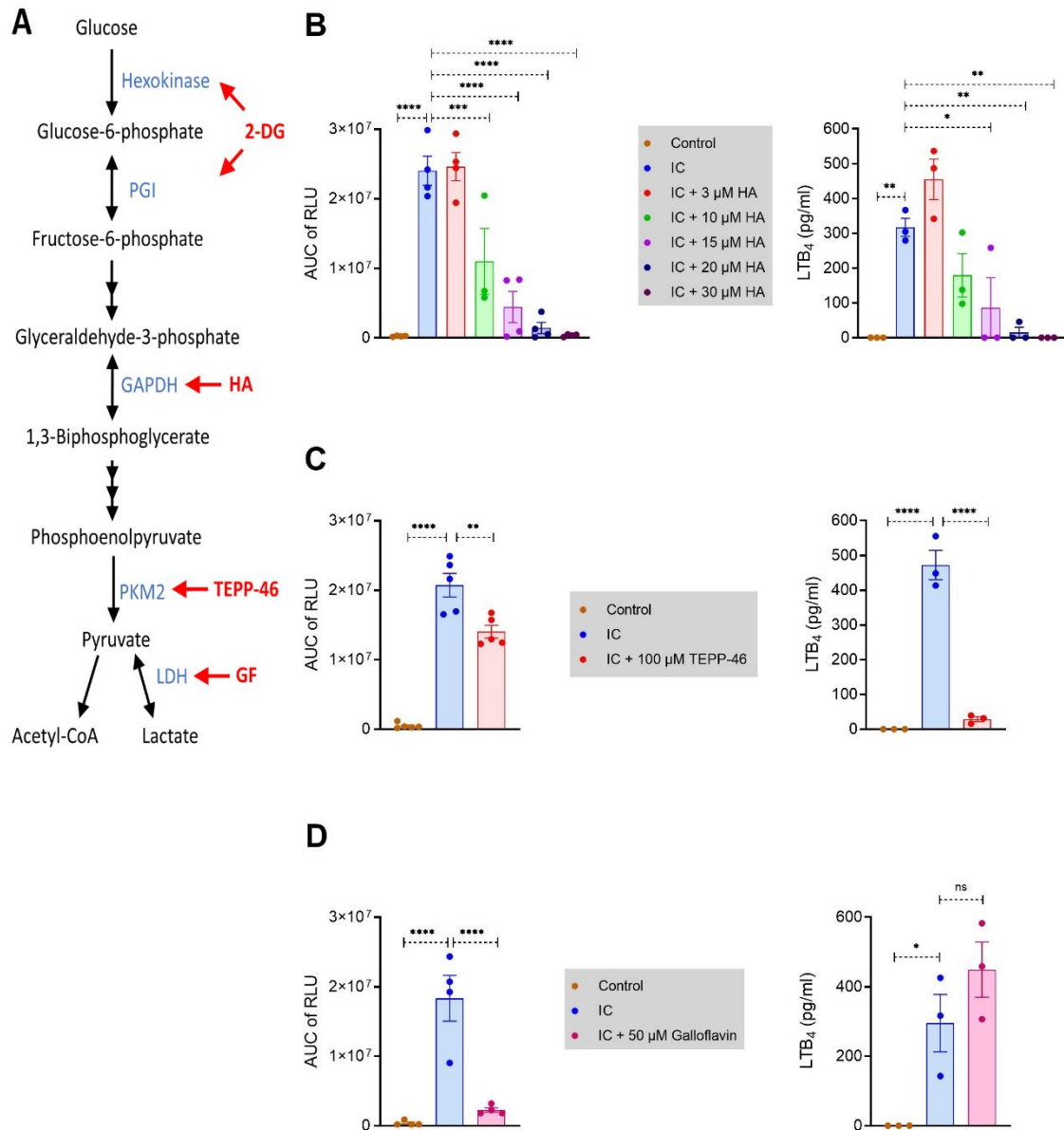


Figure 10. Aerobic glycolysis contributes to the response of neutrophils to immune complexes.

Murine BM-derived neutrophils were treated with heptelidic acid, TEPP-46 or galloflavin, and next stimulated with ICs. ROS release was measured as emitted light and shown in RLU. Thereafter, LTB₄ was detected in cell-free supernatants collected after ROS release measurement. **(A)** Schematic representation of the glycolytic pathway; GAPDH: glyceraldehyde-3-phosphate dehydrogenase; HK: hexokinase; PGI: phosphoglucose isomerase; PKM2: pyruvate kinase M2; LDH: lactate dehydrogenase. **(B)** ROS and LTB₄ release from neutrophils upon stimulation with ICs and under treatment with heptelidic acid (3 μM, 10 μM, 15 μM, 20 μM, 30 μM). **(C)** ROS and LTB₄ release from neutrophils upon stimulation with ICs and under treatment with 100 μM TEPP-46. **(D)** ROS and LTB₄ release from neutrophils upon stimulation with ICs and under treatment with 50 μM galloflavin. All results are presented as mean ± SEM. N = 3-5 and each dot represents an independent experiment. Results were analyzed by one-way ANOVA and Holm-Sidak's multiple comparisons test. *, p < 0.05; **, p < 0.01; ***, p < 0.001; ****, p < 0.0001 for the comparisons indicated.

3.6 The inhibitory effect of moxifloxacin on the IC-triggered release of ROS and LTB₄ from murine neutrophils

Metformin is known to be mainly transported into the cell via OCTs transporters. The data presented above (Paragraph 3.2) suggest low expression of OCT1 and OCT3 receptors capable of metformin uptake. Based on that, the next step was to investigate whether the inhibitory effect of metformin on the ROS release would be diminished by reducing the transport of metformin into the cells. For this purpose, moxifloxacin, a potent inhibitor of OCT-mediated transport of metformin (Brake et al., 2016), was tested.

In this study, 30 min pre-incubation of freshly isolated neutrophils with moxifloxacin (0.1 mM, 0.3 mM, 0.5 mM, and 1 mM) was followed by 30 min of incubation with 10 mM metformin. Subsequently, the cells were stimulated with ICs and ROS released was measured.

From the two experiments performed, it could be deduced that moxifloxacin does not reverse the inhibitory effect of metformin on ROS release (Figure 11A), therefore, no further experiments were carried out in this combination. However, it was intriguing that the moxifloxacin alone also inhibited the release of ROS. Therefore, the investigation of IC-triggered ROS release upon moxifloxacin treatment was further examined, as was the release of LTB₄ in cell-free supernatants collected after ROS release measurements. Figure 11B demonstrates, that both ROS and LTB₄ release were inhibited in a dose-dependent manner upon moxifloxacin treatment. In detail, the IC-triggered release of ROS was significantly inhibited upon 0.3 mM, 0.5 mM, and 1 mM moxifloxacin, whereas at 0.1 mM concentration no statistically significant inhibition was detectable (0.3 mM: $0.65 \times 10^7 \pm 0.13 \times 10^7$ vs. IC: $1.56 \times 10^7 \pm 0.25 \times 10^7$; adj. p-value = 0.0007; 0.5 mM: $0.38 \times 10^7 \pm 0.1 \times 10^7$ vs. IC: $1.56 \times 10^7 \pm 0.25 \times 10^7$; adj. p-value <0.0001; 1 mM: $0.29 \times 10^7 \pm 0.05 \times 10^7$ vs. IC: $1.56 \times 10^7 \pm 0.25 \times 10^7$; adj. p-value <0.0001; 0.1 mM: $1.04 \times 10^7 \pm 0.15 \times 10^7$ vs. IC: $1.56 \times 10^7 \pm 0.25 \times 10^7$; adj. p-value = 0.0697; Figure 11B). The LTB₄ release was dose-dependently inhibited upon every moxifloxacin concentration used (0.1 mM: 124.6 ± 19.34 vs. IC: 218.3 ± 27.06 ; adj. p-value = 0.0013; 0.3 mM: 76.39 ± 10.16 vs. IC: 218.3 ± 27.06 ; adj. p-value <0.0001; 0.5 mM: 22.66 ± 6.95 vs. IC: 218.3 ± 27.06 ; adj. p-value <0.0001; 1 mM: 4.9 ± 4.9 vs. IC: 218.3 ± 27.06 ; adj. p-value <0.0001; Figure 11B).

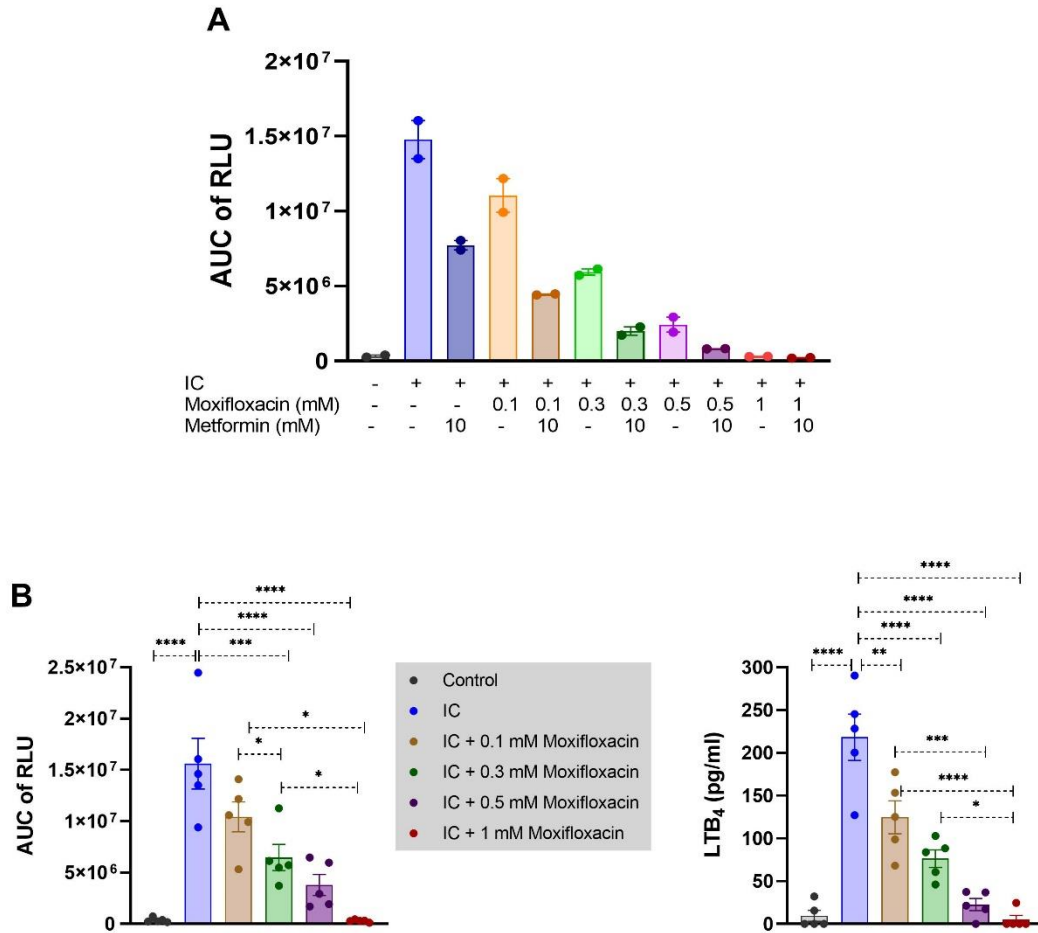


Figure 11. Moxifloxacin inhibits ROS and LTB₄ release in a dose-dependent manner from murine BM-derived neutrophils.

First, murine BM-derive neutrophils were pre-incubated for 30 min with various concentrations (0.1 mM, 0.3 mM, 0.5 mM, and 1 mM) of moxifloxacin. Then, the neutrophils were treated with 10 mM metformin, and next stimulated with ICs. ROS release was measured as emitted light via reaction with luminol and shown here as RLU. Thereafter, LTB₄ was detected in cell-free supernatants collected after ROS release measurement. **(A)** ROS release from neutrophils upon stimulation with ICs and under treatment with moxifloxacin (0.1 mM, 0.3 mM, 0.5 mM, and 1 mM) and/or 10 mM metformin. **(B)**. ROS release from neutrophils upon stimulation with ICs and under treatment with moxifloxacin (0.1 mM, 0.3 mM, 0.5 mM, and 1 mM). All results are presented as mean \pm SEM. N = 2 for **(A)** and N = 5 for **(B)**. Each dot represents an independent experiment. Results were analyzed by one-way ANOVA and Holm-Sidak's multiple comparisons test. *, p < 0.05; **, p < 0.01; ***, p < 0.001; ****, p < 0.0001 for the comparisons indicated.

3.7 Neutrophil metabolic activity in response to ICs and AICAR

The mechanisms underlying metformin action are complex, but the main mechanism of its action is believed to be the activation of AMPK. Therefore, it has been investigated whether the activation of AMPK alone is sufficient to induce a similar therapeutic effect, both *in vitro* and *in vivo*. For this purpose, the nucleoside 5-Aminoimidazole-4-carboxamide-1- β -D-ribofuranoside (AICAR) was used, a direct activator of AMPK, which enters the cell and is phosphorylated to the nucleotide 5-amino-4-imidazolecarboxamide riboside 5'-monophosphate (ZMP) and binds the γ subunit in place of AMP, resulting in AMPK activation. ZMP mimics AMP effects on the AMPK system, such as direct allosteric activation and promotion of phosphorylation by AMPK kinase (Corton et al., 1995).

The first step was to determine whether AICAR directly affects neutrophils, which are significantly involved in the effector phase of EBA pathogenesis. To this end, the influence of AICAR and/or ICs on neutrophil metabolism was studied.

To determine whether AICAR and/or ICs directly regulate neutrophil metabolism, oxygen consumption rate (OCR) and extracellular acidification rate (ECAR) of live BM-derived neutrophils were measured.

Treatment with 1 mM AICAR and/or stimulation with ICs impacted aerobic glycolysis of murine BM-derived neutrophils (Figure 12A). In detail, stimulation of neutrophils with ICs caused a significant increase of the basal glycolysis rate (Control: 4.22 ± 1.58 ; IC: 16.52 ± 0.62 ; adj. p-value = 0.002), whereas no significant change could be noticed in maximal glycolysis, glycolytic capacity, and non-glycolytic acidification rates. At the same time, treatment with AICAR significantly reduced a glycolytic capacity rate (Control: 26.87 ± 3.97 ; AICAR: 15.42 ± 2.77 ; adj. p-value = 0.0035), while no significant change was noted in maximal glycolysis rate. Interestingly, basal glycolysis and non-glycolytic acidification rates tended to increase under AICAR treatment, albeit not statistically significant (basal glycolysis: Control: 4.22 ± 1.58 ; AICAR: 11.54 ± 1.81 ; adj. p-value = 0.081; non-glycolytic acidification: Control: 6.27 ± 0.58 ; AICAR: 14.58 ± 1.14 ; adj. p-value = 0.077).

Treatment with 1 mM AICAR affected mitochondrial respiration in murine BM-derived neutrophils, whereas stimulation with ICs did not alter it (Figure 12B). More detailed, treatment with AICAR significantly reduced maximal respiration rate (Control: 102.98 ± 12.55 ; AICAR: 29.49 ± 4.17 ; adj. p-value = <0.0001), whereas basal respiration and ATP production showed a decreased tendency under the treatment, but not significant (basal respiration: Control: 55.81 ± 7.7 ; AICAR: 27.93 ± 3.25 ; adj. p-value = 0.151; ATP production: Control: 47.9 ± 11.26 ; AICAR: 20.4 ± 2.92 ; adj. p-value = 0.1227).

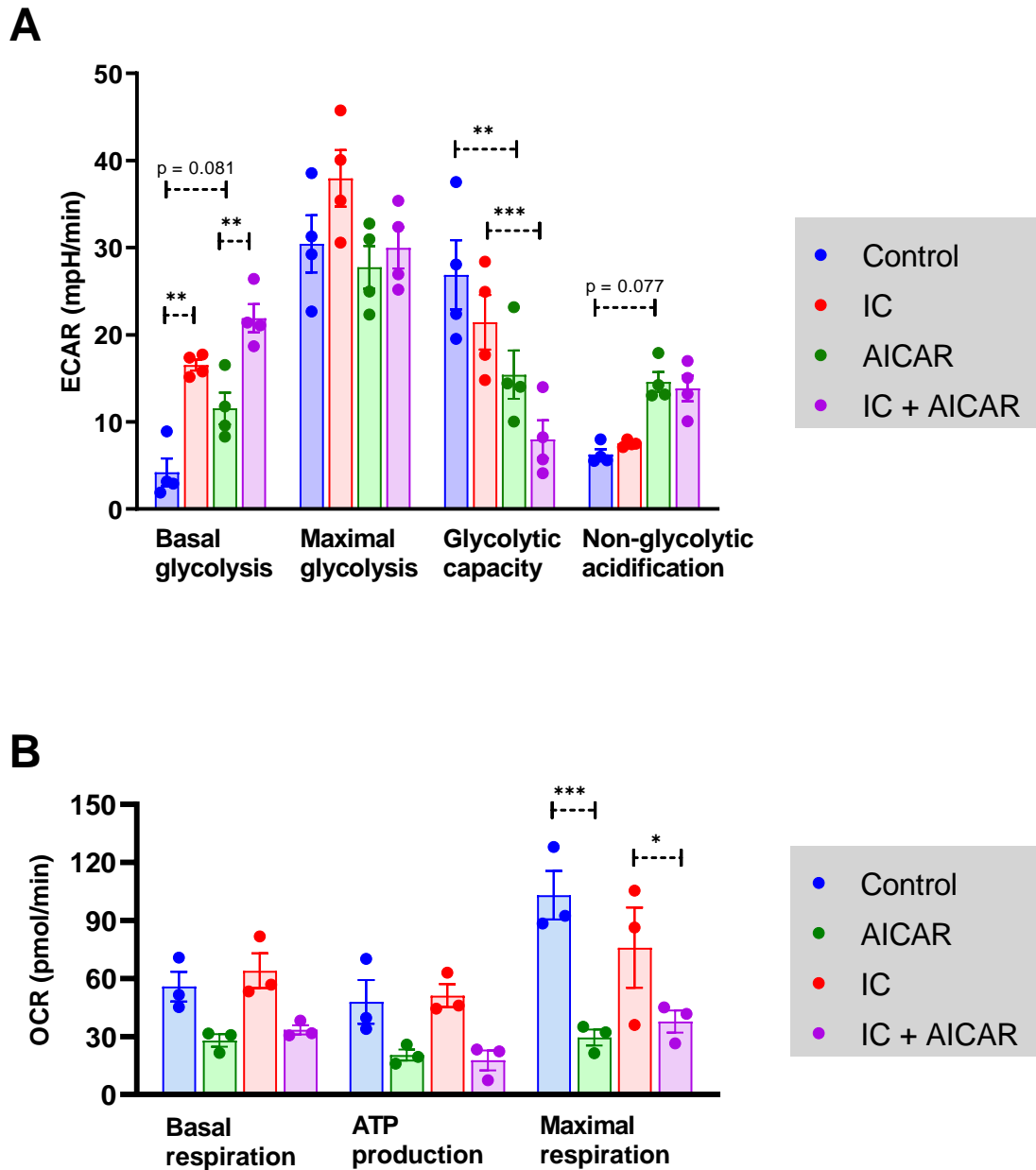


Figure 12. AICAR affects murine BM-derived neutrophil metabolism.

Neutrophil metabolic activity in response to ICs and AICAR treatment was profiled by Seahorse XF24 analyzer. **(A)** ECAR of murine neutrophils with and without treatment with AICAR (1 mM) and ICs. **(B)** OCR of murine neutrophils with and without treatment with AICAR (1 mM) and ICs. The difference between Control and IC + AICAR of the basal glycolysis, glycolytic capacity and maximal respiration rates was statistically significant however for reasons of clarity is not shown on the graph. Results are presented as mean \pm SEM. N = 4 for **(A)**; N = 3 for **(B)**. Each dot represents an independent experiment. Results were analyzed by two-way ANOVA with Holm-Sidak's multiple comparison test. *, $p < 0.05$; **, $p < 0.01$; ***, $p < 0.001$ for the comparisons indicated.

3.8 The effect of AICAR on the IC-triggered release of ROS and LTB₄ from murine neutrophils

After investigating that AICAR treatment affects neutrophil metabolism, the next step was to examine how AICAR influences the major neutrophil functions, which is the regulation of immune response. To this end, the effect of AICAR on the IC-triggered release of ROS and LTB₄ (Figure 13), which play an essential role in the development of skin inflammation in the antibody transfer EBA, was assessed.

In the conducted experiments, BM-derived neutrophils were first pre-incubated with AICAR for 2.5 h or 0.5 h and then stimulated with ICs. The comparison of variables was obtained by using one-way ANOVA and Tukey's multiple comparisons test. The performed experiments have shown that neutrophil stimulation with ICs caused significant release of ROS from neutrophils, regardless of the pre-incubation period (for 2.5 h: Control: $0.03 \times 10^7 \pm 0.007 \times 10^7$ vs. IC: $1.41 \times 10^7 \pm 0.24 \times 10^7$; adj. p-value = <0.0001; for 0.5 h: Control: $0.06 \times 10^7 \pm 0.02 \times 10^7$ vs. IC: $1.4 \times 10^7 \pm 0.31 \times 10^7$; adj. p-value = 0.001;) (Figure 13 A and C). In contrast, after 0.5 h pre-incubation period, the release of LTB₄ from IC-activated neutrophils, was visibly increased, but did not reach statistical significance. However, the release of LTB₄ upon ICs stimulation was significantly increased only after 2.5 h pre-incubation (for 2.5 h: Control: 30.91 ± 22.22 vs. IC: 330.3 ± 72.46 ; adj. p-value = 0.025; for 0.5 h: Control: 7.83 ± 7.83 vs. IC: 422.1 ± 123.8 ; adj. p-value = 0.054) (Figure 13 B and D). Treatment with 1 mM AICAR significantly inhibited ROS release in both incubation times, additionally 0.3 mM concentration had a significant inhibitory effect in 2.5 h pre-incubation time, compared to IC-stimulated neutrophils (for 2.5 h: IC + 1 mM AICAR: $0.23 \times 10^7 \pm 0.02 \times 10^7$ vs. IC: $1.41 \times 10^7 \pm 0.24 \times 10^7$; adj. p-value = 0.0004; for 0.5 h: IC + 1 mM AICAR: $0.45 \times 10^7 \pm 0.09 \times 10^7$ vs. IC: $1.4 \times 10^7 \pm 0.31 \times 10^7$; adj. p-value = 0.0377; IC + 0.3 mM AICAR: $0.41 \times 10^7 \pm 0.06 \times 10^7$ vs. IC: $1.41 \times 10^7 \pm 0.24 \times 10^7$; adj. p-value = 0.004) (Figure 13 A and C). Moreover, treatment with 1 mM and 0.3 mM AICAR significantly inhibited LTB₄ release after 2.5 h pre-incubation compared to vehicle-treated neutrophils, upon IC-stimulation, whereas after 0.5 h the inhibition showed tendency towards reduced LTB₄ release, albeit not statistically significant (for 2.5 h: IC + 1 mM AICAR: 53.09 ± 24.72 vs. IC: 330.3 ± 72.46 ; adj. p-value = 0.0445; IC + 0.3 mM AICAR: 52.89 ± 36.67 vs. IC: 330.3 ± 72.46 ; adj. p-value = 0.0443; for 0.5 h: IC + 1

mM AICAR: 127.4 ± 49.97 vs. IC: 422.1 ± 123.8 ; adj. p-value = 0.397; IC + 0.3 mM AICAR: 106.3 ± 45.84 vs. IC: 422.1 ± 123.8 ; adj. p-value = 0.317) (Figure 13 B and D).

Moreover, Figure 13E shows that the reduction of ROS release is dose- and time-dependent. The release of ROS decreases with increasing AICAR dose and the effect appears to be enhanced with increasing duration of incubation.

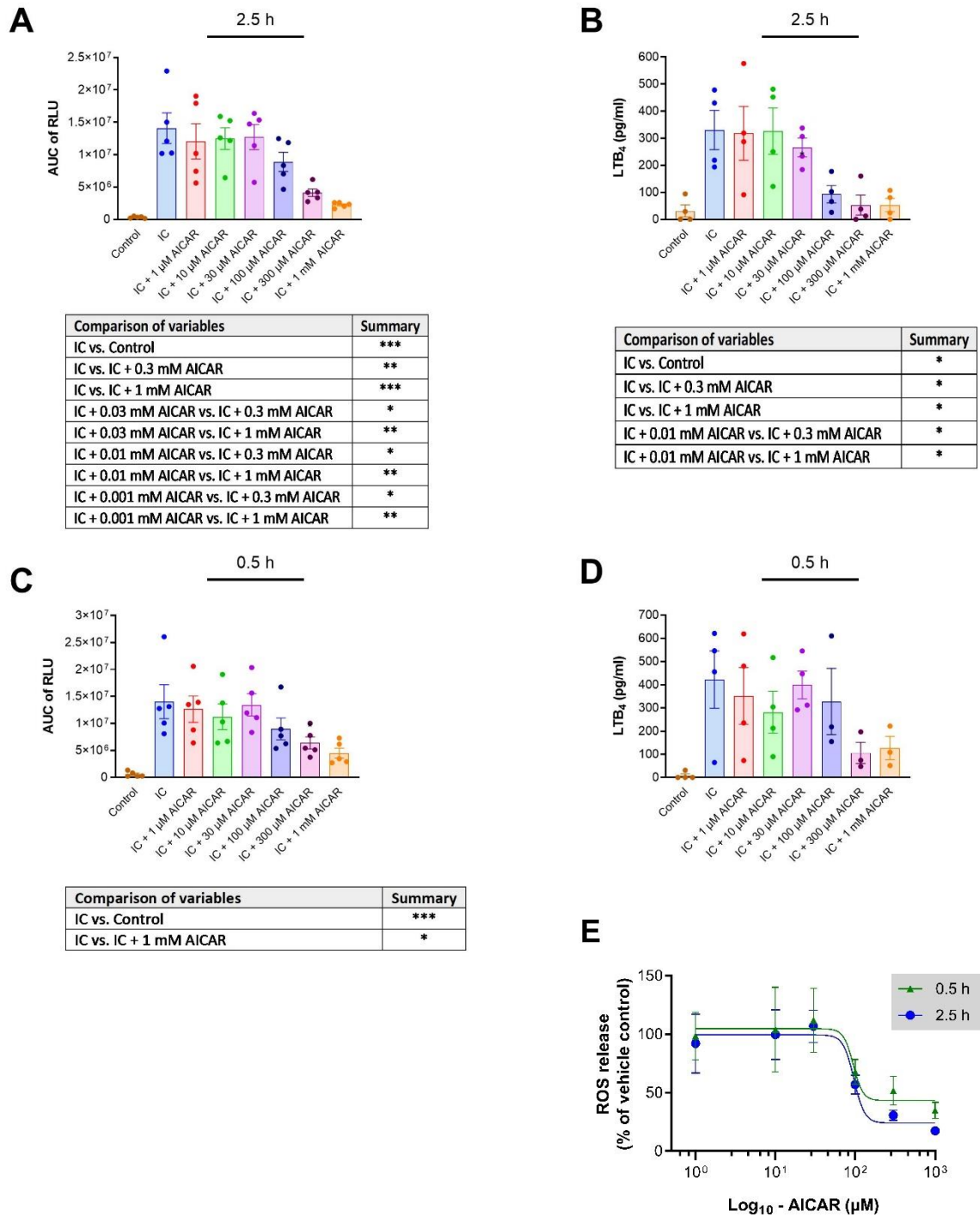


Figure 13. AICAR inhibits the release of ROS and LTB₄ from murine BM-derived neutrophils.

Neutrophils were treated with AICAR for 2.5 h or 0.5 h and next stimulated with ICs. ROS release was measured as emitted light and shown in RLU. Thereafter, LTB₄ was detected in cell-free supernatants collected after ROS release measurement. **(A), (B)** ROS and LTB₄ release from neutrophils upon stimulation with ICs and under treatment with AICAR for 2.5 h. **(C), (D)** ROS and LTB₄ release from neutrophils upon stimulation with ICs and under treatment with AICAR for 0.5 h. **(E)**, Dose-response relationship of the effect of AICAR on ROS release. All results are presented as mean ± SEM. N = 3-4 and each dot represents an independent experiment. Results were analyzed by one-way ANOVA and Tukey's multiple comparisons test; *, p < 0.05; **, p < 0.01; ***, p < 0.001 for the comparisons indicated.

3.9 The effect of AICAR on NETs

After demonstrating that AICAR inhibits ROS release from neutrophils, the next step was to investigate whether AICAR can also affect extracellular net formation, as it has been shown that the production of ROS by NADPH oxidase is required to form NETs (Jorch and Kubes, 2017).

In the following experiments, murine BM-derived neutrophils were first pre-incubated with various concentrations of AICAR, followed by measurement of formation of NETs using Sytox Green, a cell-impermeable DNA binding dye (Figure 14). Upon stimulation with ICs, neutrophils displayed significant increase in NETs formation (IC: 10946 ± 497.9 ; Control: 6001 ± 602.8 , adj. p-value = 0.0096). AICAR treatment significantly inhibited NETs formation at all concentrations (10 μ M, 150 μ M, 300 μ M and 1 mM) compared to vehicle-treated IC-stimulated neutrophils (IC: 10946 ± 497.9 ; IC + 10 μ M: 7748 ± 1946 , adj. p-value = 0.0353; IC + 150 μ M: 6164 ± 774.3 , adj. p-value = 0.0096; IC + 300 μ M: 5594 ± 391.8 , adj. p-value = 0.0074; IC + 1 mM: 4601 ± 550.1 , adj. p-value = 0.0025).

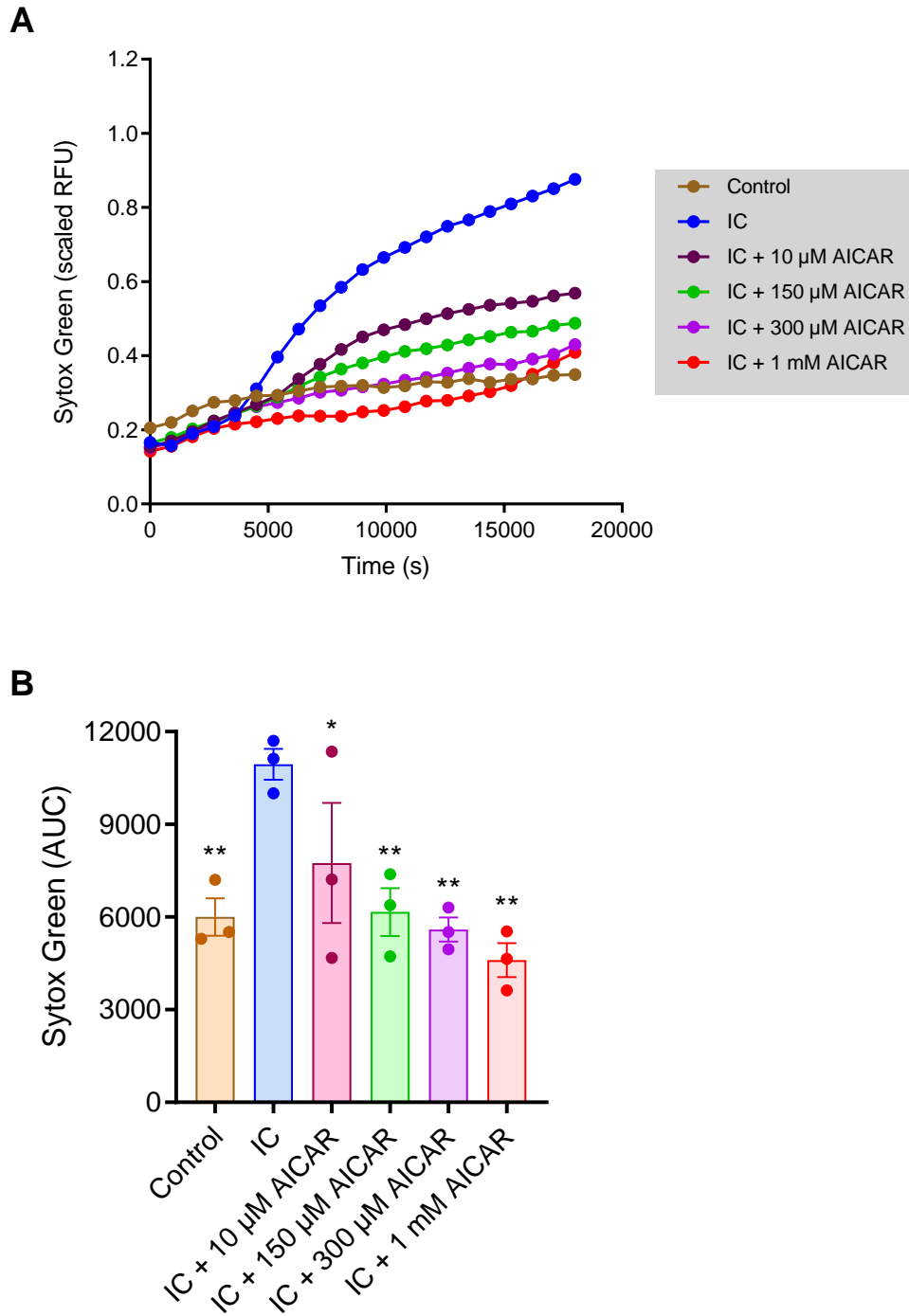


Figure 14. AICAR inhibits murine NETs formation.

Murine BM-derived neutrophils were pre-incubated with various concentrations of AICAR for 30 min. Extracellular NETs formation was measured using Sytox Green, a cell-impermeable DNA binding dye for 5 h at 37 °C. **(A)** Representative DNA release overtime shown as relative fluorescent units (RFU) measured by SYTOX Green. **(B)** Total extracellular DNA calculated as area under curve (AUC) normalized to IC-stimulated neutrophils. Results are presented as mean \pm SEM. N = 3 and each dot represents an independent experiment. Results were analyzed by one-way ANOVA with Holm-Sidak's multiple comparison test. ***, $p < 0.001$, ****, $p < 0.0001$ for the comparisons indicated.

3.10 Stimulus dependent inhibition on neutrophil migration by AICAR

In the effector phase of BP-like EBA, the influx of immune cells, including neutrophils, takes place. This recruitment is controlled by chemoattractants, a biochemically diverse group which includes, among others, complement component C5a and lipid mediator LTB₄. As it has been demonstrated that C5a and LTB₄ are crucial for the development of the murine BP-like EBA mouse model (Sadik et al., 2018; Sezin et al., 2017), the role of AICAR on chemotaxis of PMNs has been investigated.

In the conducted migration assay, the neutrophils were first incubated for 30 min with 1 mM AICAR, followed by determination of chemotaxis (directed migration) and chemokinesis (random cell movement) using the permeable membrane (Figure 15). Treatment with 1 mM AICAR inhibited C5a-mediated migration, more specifically, the directed migration-chemotaxis was significantly inhibited, compared to vehicle treated neutrophils (3.77 ± 1.81 vs. 39.13 ± 10.64 ; adj. p-value = 0.0004). While LTB₄-mediated migration was not affected by AICAR treatment.

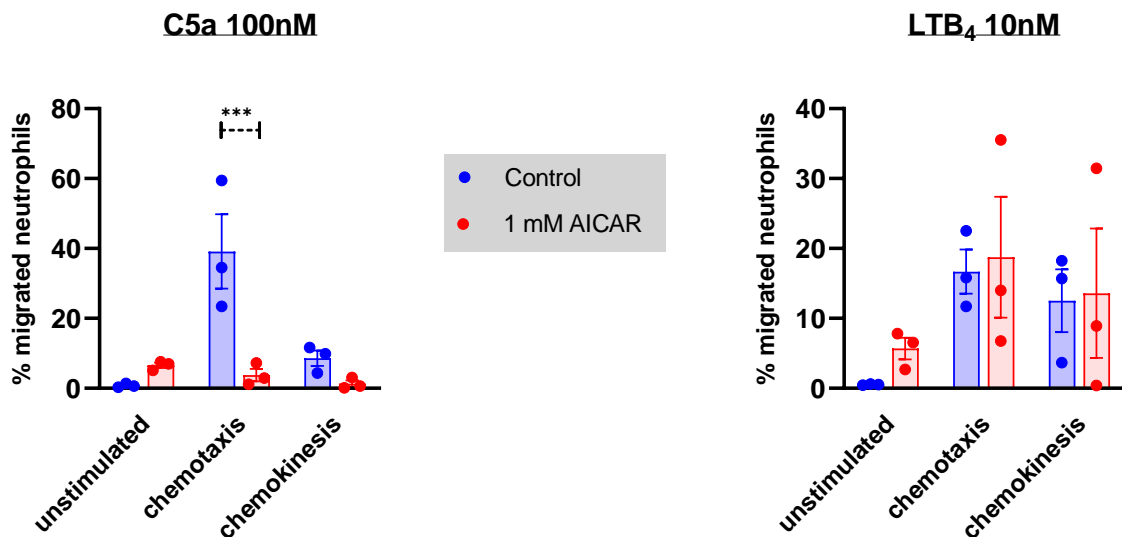


Figure 15. AICAR inhibits C5a-mediated, but does not alter LTB₄-mediated, migration of murine BM-derived neutrophils.

The effect of 1 mM AICAR on chemotaxis and chemokinesis of BM-derived neutrophils in response to C5a and LTB₄. All results are presented as mean \pm SEM of migrated cells (percentage). N = 3 and each dot represents an independent experiment. Results were analyzed by two-way ANOVA and Holm-Sidak's multiple comparisons test. ***, p < 0.001 for the comparisons indicated.

3.11 The effect of AICAR in the antibody transfer model of BP-like EBA

Following *in vitro* experiments, which demonstrated that AICAR not only influences the response of neutrophils but also their metabolism, the effect of AICAR in the BP-like EBA mouse model has been tested. Therefore, it has been investigated whether the activation of AMPK alone is sufficient to induce a therapeutic effect in BP-like EBA mouse model.

In order to examine the therapeutic potential of direct AMPK inhibition in the effector phase of EBA, the autoantibody-transfer-induced EBA model was induced in C57Bl6/J WT mice by subcutaneous injection of 50 µg of rabbit anti-mCOL7C IgG into the neck, left foreleg, and right hindleg on days 0, 2, and 4 of the experiment, respectively. Mice were treated daily with AICAR (250 mg/kg/day, i.p.), starting on day 0 of the experiment. Summarizing the data of two independent EBA experiments, the treatment with 250 mg/kg/day AICAR had at most mild but no significant effect on the disease manifestation in experimental EBA comparing the groups across all time points by two-way ANOVA and Holm-Sidak's multiple comparisons test (Figure 16). Skin lesions including erythema, crusts, alopecia, and erosions were observed in both the AICAR treated and the vehicle group (Figure 16C). Figure 16A demonstrates clinical severity of skin inflammation benchmarked as percentage of the total body surface area affected by skin lesions (ABSA). Starting from day 4 after the initial rabbit anti-mCOL7C IgG injection, both groups demonstrated symptoms of the disease (clinical score day 4; vehicle group: $\bar{X} = 2.9 \pm 0.4$; AICAR treated group: $\bar{X} = 2.7 \pm 0.5$ % of ABSA; $p = 0.97$). Although treatment with AICAR showed tendency towards reduced disease expression compared to untreated mice (clinical score day 10; vehicle group: $\bar{X} = 10.4 \pm 0.79$; AICAR treated group: $\bar{X} = 8.8 \pm 0.98$ % of ABSA; adj. p-value = 0.48; Figure 16A), it was not statistically significant. On day 13, the disease severity declined in both groups as the resolution phase set in (clinical score day 13; vehicle group: $\bar{X} = 8.68 \pm 0.86$; AICAR treated group: $\bar{X} = 7.5 \pm 0.85$ % of ABSA; adj. p-value = 0.72; Figure 16A). On the last day of the experiment, day 16, the difference in the disease severity increased, but it was still not significant (clinical score day 16; vehicle group: $\bar{X} = 6.7 \pm 0.65$; AICAR treated group: $\bar{X} = 4.8 \pm 0.84$ % of ABSA; adj. p-value = 0.36; Figure 16A). The total disease score was defined as the area under the curve (AUC) and it was not statistically significant (vehicle group: AUC = 98.11 ± 8.85 ; AICAR treated group: AUC = 82.67 ± 10.78 ; p-value = 0.42; Figure 16B).

Neutrophils are critically involved in the pathogenesis of BP-like EBA. In addition to neutrophils, other cell types, such as macrophages also contribute to the development of skin lesions in EBA. In an attempt to examine whether AICAR treatment had an impact on the composition of inflammatory cells in the dermal infiltrate, the percentage of neutrophils and macrophages was assessed by staining perilesional skin obtained at the end of the experiment on day 16 for the cell markers Ly6G and F4/80, respectively (Figure 16 D and E).

As recent studies indicate that the polarization of neutrophils and macrophages into alternatively activated N2 and M2, respectively, has been demonstrated to play anti-proliferative role by promoting secretion of anti-inflammatory mediators (Cuartero et al., 2013; Rao et al., 2014), it was further investigated whether AICAR treatment mediates N2 neutrophil and M2 macrophages activation, by staining perilesional skin harvested at the end of the experiment on day 16 with the macrophage mannose marker, CD206.

The findings demonstrate that treatment with AICAR tended to reduce the neutrophil and macrophage infiltration in the perilesional skin, albeit not statistically significant (percentage of Ly6G⁺; vehicle group: 15.63 ± 5.9 ; AICAR treated group: 9.85 ± 2.5 ; p-value = 0.97; Figure 16D; percentage of F4/80⁺; vehicle group: 3.35 ± 0.8 ; AICAR treated group: 2.3 ± 0.8 ; p-value = 0.25; Figure 16E). The data showed no statistically significant increase of N2 neutrophils under AICAR treatment, likewise there was no statistical difference in M2 macrophages (percentage of CD206⁺ of Ly6G⁺; vehicle group: 11.3 ± 1.2 ; AICAR treated group: 18.31 ± 3.8 ; p-value = 0.25; Figure 16D; percentage of CD206⁺ of F4/80⁺; vehicle group: 87.49 ± 1.6 ; AICAR treated group: 83.0 ± 4.0 ; p-value = 0.38; Figure 16E).

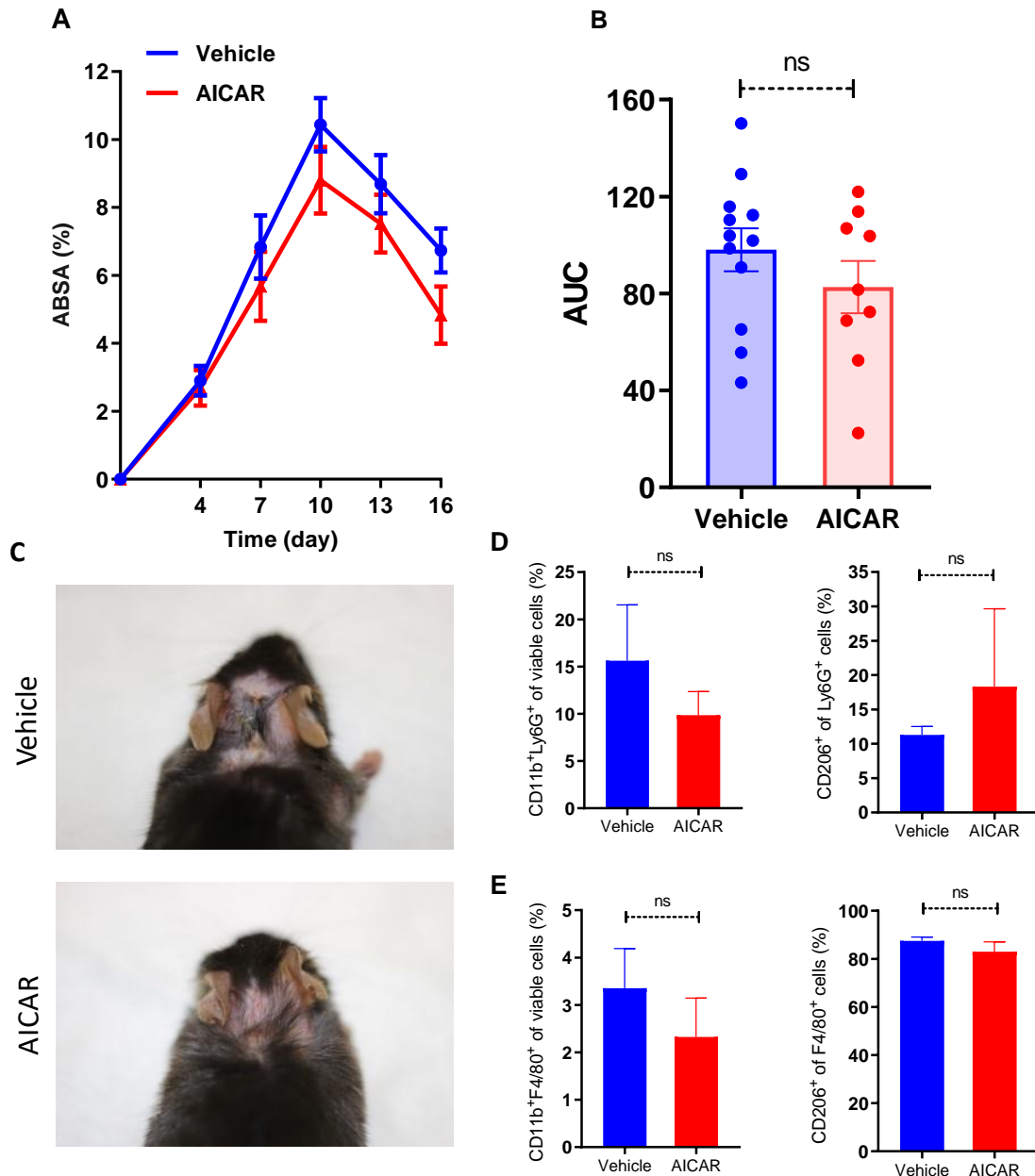


Figure 16. AICAR treatment does not ameliorate disease in the antibody transfer model of BP-like EBA.

To examine the therapeutic potential of AMPK activator, AICAR, in EBA, firstly an antibody-transfer EBA model was induced in C57Bl6/J WT mice by subcutaneous injection of 50 μ g of rabbit anti-mCOL7C IgG into the neck, left foreleg, and right hindleg on days 0, 2, and 4 of the experiment, respectively. Mice ($n = 9$) were treated daily with AICAR (250 mg/kg/day, i.p.) and the corresponding vehicle control group ($n = 12$) was treated i.p. with saline instead, starting on day 0 of the experiment. **(A)** Clinical severity of skin inflammation benchmarked as percentage of the total body surface area affected by skin lesions (ABSA). **(B)** Area under the curve (AUC) of the affected surface body area is shown. **(C)** Representative clinical pictures on day 10 of the experiment are shown; erythema, erosions, crusts and alopecia, characteristic features for EBA are seen in the skin. **(D)** The percentage of CD11b⁺Ly6G⁺ cells and CD206⁺ of Ly6G⁺ cells in perilesional skin harvested on day 16, evaluated by flow cytometry. **(E)** The percentage of CD11b⁺F4/80⁺ cells and CD206⁺ of F4/80⁺ cells in perilesional skin harvested on day 16, evaluated by flow cytometry. Results were pooled from 2 independent experiments and are presented as mean \pm SEM ($n = 9$ -12 mice/group) with dots representing individual mouse. Data presented in **A** were analyzed using 2-way ANOVA and Holm-Sidak's multiple comparisons test, whereas data in **B**, **D**, and **E** were analyzed using a two-tailed Mann-Whitney U test. ns: not significant, *, $p < 0.05$ for the comparisons indicated.

4 DISCUSSION

BP-like EBA is an autoimmune blistering disease characterized by IgG autoantibodies directed against type VII collagen, causing the formation of mucocutaneous blisters. It is a rare, chronic disease for which there is still only a limited treatment available. The current therapy is non-specific, and mainly based on corticosteroids and immunosuppressive drugs. This combination very often does not lead to remission of the disease and does not protect from relapses (Engineer and Ahmed, 2001). The treatment of EBA is also associated with development of multiple side effects, therefore requiring new therapeutic approaches to be identified. In recent years, novel therapeutic options, which mainly target the effector phase of EBA have been developed (Kasperkiewicz et al., 2016; Koga et al., 2019). Particularly noteworthy are the novel therapy strategies that have been established by targeting immunometabolism, which through changes in the intracellular metabolism of the immune cells modulates their functions and thereby the immune response (O'Neill et al., 2016). Although, some of the immunomodulators have been successfully tested in animal models of autoimmune or immune-inflammatory diseases (such as psoriasis, systemic lupus erythematosus, multiple sclerosis) or cancer (Pålsson-McDermott and O'Neill, 2020; Singh et al., 2015), there is still little known about their possible application in autoimmune skin blistering diseases. Accordingly, this study sought to determine new potential therapeutic targets in BP-like EBA, based on cellular metabolism.

4.1 Neutrophil glucose metabolism as a target in BP-like EBA

The combination of results analyzed from the *in vivo* experiment performed in our laboratory and the *in vitro* experiments carried out in this dissertation, revealed that OXPHOS inhibitor, metformin, and glycolysis inhibitors such as 2-DG or heptelidic acid, could be a promising alternative to the conventional treatment strategies for BP-like EBA.

The first step was to assess the effect of metformin and 2-DG treatment on skin inflammation on the cellular and molecular level in the antibody transfer model of BP-like EBA. FoxP3⁺ regulatory T cells (T_{regs}) are a heterogeneous subset of specialized CD4⁺T cells that derive from the thymus (natural T_{regs}) or the periphery (induced T_{regs}) (Li et al., 2015). T_{regs} play a key role in modulating autoimmunity and inflammatory processes. In addition

to their suppressive properties, they are able to adapt to the environment, enhancing their functions (Wing and Sakaguchi, 2012). Furthermore, T_{regs} produce significant levels of transforming growth factor- β (TGF- β) and interleukin-10 (IL-10). Notably, TGF- β can also stimulate the production of IL-10 by T_{regs} (Saraiva and O'Garra, 2010). IL-10 and TGF- β are multifunctional cytokines, with one of the most prominent functions being the induction of humoral immune responses. More importantly, apart from being produced by T_{regs} , they promote the development of T_{regs} and boost their suppressive functions (Kerperien et al., 2018).

Even though the mechanisms of action of metformin and 2-DG are radically different, with metformin exhibiting multiple mechanisms of action and 2-DG inhibiting the first two glycolysis enzymes: hexokinase and phosphoglucose isomerase, an increase of FoxP3⁺ T_{regs} cells under the treatment with metformin was observed, although not statistically significant. The increased FoxP3⁺ T_{regs} cell count was statistically significant for the comparison between the vehicle and the 2-DG treatment group (Figure 5B), which is consistent with the previous findings (Liu et al., 2018; Sun et al., 2016). Moreover, the cytokine IL-10 level was increased under the treatment with metformin alone as well as in combination with 2-DG, while a non-significant trend towards an increase TGF- β 1 level was observed under the treatment with metformin alone and reached statistical significance for the combination treatment of 2-DG with metformin (Figure 5C). The increased levels of IL-10 and TGF- β 1 under treatment with metformin was previously described to be effective in experimental autoimmune encephalomyelitis (Sun et al., 2016). It has been previously shown, that T_{regs} and IL-10 contribute to the amelioration of the symptoms in the EBA mouse model (Bieber et al., 2017b; Kulkarni et al., 2016). Interestingly, although there was at most a noticeable trend for increased mRNA levels of TNF- α , IL-1 β and CXCL2 (Figure 5C), metformin did not significantly alter the presence of pro-inflammatory cytokines in the skin. This finding is not consistent with previous studies, in which metformin reduced the level of pro-inflammatory cytokines (Tsuji et al., 2020; Ursini et al., 2018). A possible explanation may be that in the EBA mouse model, the production of pro-inflammatory cytokines is stronger than the action of metformin.

All things considered, the results presented in Figure 5 imply the possibility that treatment with metformin and/or 2-DG either affects the induction of T_{regs} , or the anti-inflammatory

cytokines, IL-10 and TGF- β 1 to some degree, and that the cooperation between them, could contribute to the reduced skin inflammation in the EBA mouse model, by suppressing pathological immune responses.

Moreover, IHC analysis of the perilesional skin revealed no alteration in the density of neutrophils infiltration under treatment (Figure 5B), which is in line with previous studies (Sezin et al., 2019), where despite a significant improvement of the skin inflammation, no difference in the count of neutrophils was detected upon treatment. A possible explanation might be that for the histopathological examination a biopsy of the perilesional skin is collected. The recruitment of neutrophils into the skin and their activation is necessary to create lesions in the EBA (Sezin et al., 2017), thus their accumulation there is to be expected, even during the course of treatment. It would therefore be beneficial to study the time kinetics of the exact development of the inflammation with respect to neutrophil influx, in the EBA model.

Sezin et al. presented by depletion of neutrophils, that neutrophils are imperative for the development of skin inflammation in the effector phase of BP-like EBA. Upon recruitment into the skin, neutrophils are activated by binding to the immune complexes created by IgG autoantibodies and NC1 domain of the collagen VII via Fc γ receptors. Kasperkiewicz et al. demonstrated that mice lacking the FcR common γ -chain were completely protected from EBA. Thus, neutrophil activation and Fc γ receptors signaling are crucial for the formation of tissue injury in experimental EBA. This was the main reason why in the conducted *in vitro* experiments, neutrophils, and their response to ICs stimulation under the effect of various substances of interest, were examined.

Neutrophil metabolism is almost completely independent of OXPHOS (Kramer et al., 2014). Few functional mitochondria in neutrophils exhibit very low Krebs cycle and OXPHOS activity (Loftus and Finlay, 2016), which indicate that neutrophils do not use mitochondria to produce energy. The functions of mitochondria in neutrophils are still elusive. It was considered that mitochondrial functions in neutrophils are limited to apoptosis signaling (Maiani et al., 2004), recently however, mitochondria have gained an importance in neutrophil effector functions such as chemotaxis, oxidative burst, and NETs formation (Kumar and Dikshit, 2019). However, as a result of inhibition of the glycolytic pathway,

neutrophils are able to reprogram their metabolism to OXPHOS in order to preserve cellular survival and immune suppression (Rice et al., 2018).

Despite the fact that metabolic changes in IC-activated neutrophils have not been previously reported, they might soon be anticipated. In a similar example, macrophages play a role in immunological responses and contribute to the development of skin lesions in EBA (Hirose et al., 2016), an intracellular metabolic shift is immanent in the polarization and fulfilling functions by activated macrophages (Zhu et al., 2015). Interestingly, in the conducted experiments, the stimulation of neutrophils with ICs did not affect OXPHOS (Figure 8), suggesting that oxidative phosphorylation is not essential for neutrophils to induce a response to ICs stimulation. This fact has further enhanced the importance of glycolysis in neutrophils. As expected, metformin, an inhibitor of mitochondrial complex I (Owen et al., 2000), reduced OXPHOS and ATP production (Figure 8). Moreover, metformin inhibited the release of ROS and almost completely nullified the LTB₄ release from IC-activated neutrophils (Figure 9A). The main source of ROS in neutrophils is oxidative burst mediated by NADPH oxidase (NOX2) (Nguyen et al., 2017), hence it is possible, that metformin decreases the release of ROS through the NOX2 inhibition. On a related note, Nguyen et al. describes that metformin suppresses ROS production in human colon cancer cells due to inhibition of NOX2. Another possible source of ROS is electron leakage from complexes I and III in mitochondria (Morgan and Liu, 2011). Wong et al. demonstrated that superoxides can be produced by both forward and reverse electron fluxes, depending on different substrates as fuel molecules. In contrast, metformin inhibits the ROS generation driven by reverse electron transport, although it does not stimulate the forward flux ROS release, as anticipated (Batandier et al., 2006), which could also contribute to the therapeutic effect of metformin. Additionally, Batandier et al. showed that the inhibition of electron transfer by metformin was limited, offering a possible explanation as to why the ROS release was partially inhibited by metformin, as part of the electrons are still able to leak from complexes I and III, thus producing ROS. However, given that ROS in neutrophils is produced mainly by NOX2, the inhibition of ROS production in the mitochondria probably did not contribute in a significant way to the effect induced by metformin. With respect to LTB₄ inhibition by metformin, the underlying principle is unknown. A possible explanation might be an influence of AMPK activation by metformin. AMPK is responsible for maintaining intracellular energy balance by activating processes

that produce energy in the form of ATP and inhibiting processes that consume ATP. The production of LTB₄ by neutrophils is an anabolic process, so it is possible that this process is inhibited in order to save energy. Moreover, Sun et al. showed that AMPK activation inhibited the leukotriene B₄ receptor type 1 (BLT1), which attenuated LPS-induced cardiac dysfunction *in vivo*, probably through the inhibition of NF-κ B signaling and mitochondrial impairment. However, because neutrophils have few functional mitochondria, this mechanism could contribute vaguely, if any, to the inhibition of LTB₄ secretion from IC-stimulated neutrophils.

Furthermore, a lower dose of metformin (0.5 mM) did not blunt the neutrophil response to ICs activation (Figure 9B). Taking into account the results presented by Schilf et al., where 0.5 mM metformin did not affect OXPHOS, one comes to the conclusion that the effect induced by 10 mM metformin on neutrophils is related to the inhibition OXPHOS, as 10 mM metformin inhibits both.

However, the *in vitro* experiments conducted for the purpose of this dissertation have shown that only supra-pharmacological dose of metformin influences neutrophils metabolism and their response. A therapeutic dose of metformin in animals in hepatic portal vein is < 80 μM, and after hepatic uptake the concentration in systemic plasma is reduced to 10-40 μM (Wilcock and Bailey, 1994). It is worth mentioning that although the concentration used is much higher than the maximal therapeutic concentration, it was still not cytotoxic to the cells (Figure 4B). Metformin enters the cells through organic cation transporters (OCTs), mainly OCT1 and OCT3 (Wang et al., 2002). After determining the mRNA expression of these transporters, it became apparent that the expression levels of these transporters in neutrophils are very low (Figure 6A). This therefore suggests that neutrophils are partially insensitive to metformin, which might explain why supra-pharmacological doses are required to achieve sufficient *in vitro* intracellular concentration, and thereby induce pharmacological effects. This also indicates that metformin is a weak OXPHOS inhibitor.

In the light of the metformin results, it has also been investigated how oligomycin, an OXPHOS inhibitor more specific than metformin, affects the immune response of neutrophils (Figure 9C). Oligomycin inhibits ATP synthase by blocking the F₀ subunit, preventing the phosphorylation of ADP to ATP, and thus the energy production (Shchepina

et al., 2002). Figure 9C presents, that oligomycin inhibited both ROS and LTB₄ release from IC-stimulated neutrophils. However, it seems unlikely that the effect of oligomycin was caused by the lack of energy in the form of ATP. It should be taken into account that OXPHOS and glycolysis are coupled together (ZHENG, 2012). In the case of OXPHOS inhibition by oligomycin, the cell increases the glycolysis rate to generate energy (Figure 7A Figure 8A). In addition, in the conducted experiments, the medium used contained glucose, which provided fuel for glycolysis and energy production. Alternatively, oligomycin changes the mitochondrial membrane potential (Rego et al., 2001). Hence, the effect of oligomycin on ICs activated neutrophils might have resulted from inhibition of OXPHOS, which in turn led to a change in mitochondrial membrane potential. These results would also suggest that intact mitochondrial membrane potential is required for neutrophil response.

Taken together, that the main function of both metformin and oligomycin is to inhibit OXPHOS and the fact that they inhibit the neutrophil response to ICs stimulation, despite the lack of a change in OXPHOS of ICs-activated neutrophils, is of great interest. This fact highlights the need to further investigate the non-metabolic role of mitochondria in activated neutrophil response, given that they do not play a role in energy metabolism (Kramer et al., 2014).

Neutrophils rely mainly on glycolysis to cover their energy demands (Stienstra et al., 2017). For this process, glucose is indispensable, which enters the cells through a plasma membrane via GLUT transporters. A predominant expression of GLUT1 and GLUT3 with low expression of GLUT4 (Figure 6B) suggests that neutrophils are capable of glucose and 2-DG uptake, which is consistent with data previously described (Macheda et al., 2005; Maher et al., 2005).

The studies presented in this dissertation show that neutrophil stimulation with ICs causes an increase in glycolysis (Figure 7/Figure 12A). Even though it has been described that metformin stimulates glycolysis (Andrzejewski et al., 2014; Griss et al., 2015), the data from this study does not confirm this statement. However, this could be explained by the fact that in the presented publications, breast and lung cancer cells were pre-incubated with metformin for a minimum of 24 hours, glycolysis was upregulated in order to compensate for the decrease in ATP production by the mitochondria. Likewise, Figure 8B presents that

metformin reduced ATP production, yet did not have a significant effect on glycolysis (Figure 7B), which could be explained by perhaps a shorter pre-incubation period. Considering that only 25% of BM-derived neutrophils survive 24 h incubation in cell culture (Boxio et al., 2004), it would be physiologically inadequate to investigate *in vitro*.

Furthermore, 2-DG, a glucose derivate and known inhibitor of glycolysis (Seo et al., 2014), halted the increased glycolytic flux in IC-stimulated neutrophils, by stopping the glycolysis (Figure 7A). The hypothesis, that the inhibition of glycolysis by 2-DG contributes to the reduction of skin inflammation, is additionally supported by the *in vitro* findings of the effect of 2-DG on ROS and LTB₄ release, two factors that are the central triggers of the formation of skin inflammation in the BP-like EBA model (Sadik et al., 2018). The release of NADPH oxidase-derived ROS causes DEJ separation consequent to the formation of blisters in the antibody-mediated EBA model (Chiriac et al., 2007). On the other hand, the chemoattractant LTB₄ recruits the neutrophils to the DEJ (Sezin et al., 2017) and regulates multiple cellular functions such as chemotaxis, adhesion, transmigration, and production of ROS (Woo et al., 2002). As anticipated, 2-DG inhibited the IC-triggered release of ROS and LTB₄ from neutrophils (Figure 9A). Presented results with therapeutic effect of 2-DG achieved by inhibiting glycolysis and neutrophils response to IC stimulation, confirm the assumption that glycolysis is an indispensable pathway in neutrophils and implement that aerobic glycolysis is a promising potential therapeutic target in BP-like EBA.

To support this notion, other glycolysis inhibitors such as heptelidic acid, TEPP-46 and galloflavin have been investigated. Although each of these factors is a known inhibitor of glycolysis, they act at different steps of glycolysis pathway (Fig. 10A). Heptelidic acid, also known as koningic acid, is a selective inhibitor of GAPDH, and thereby inhibit the conversion of glyceraldehyde-3-phosphate to 1,3-bisphosphoglycerate (Liberti et al., 2017). TEPP-46, an allosteric activator that activates PKM2 tetramerization, blocks its nuclear translocation, and as a result inhibits the formation of pyruvate from phosphoenolpyruvate (Angiari et al., 2020). Whereas galloflavin, a LDH inhibitor, inhibits the pyruvate transformation to lactate (Manerba et al., 2012). Studies conducted in this thesis demonstrate that treatment with heptelidic acid and TEPP-46 inhibited both ROS and LTB₄ release from IC-stimulated neutrophils (Figure 10B+C). Intriguingly, the treatment with galloflavin inhibited only ROS release, while suggesting a not statistically significant trend of elevated LTB₄ release (Figure

10D). To the best of my knowledge, there have been no demonstrated cases of LDH inhibition causing an increase of LTB₄ release and the mechanism is yet-to-be unraveled. Under aerobic conditions, pyruvate is produced by glycolysis, which enters the Krebs cycle after conversion to acetyl-CoA, whereas under anaerobic conditions, pyruvate is converted into lactate and secreted from the cell (Awasthi et al., 2019). However, lactate can be generated in the presence of oxygen, a phenomenon called the Warburg effect, which occurs mainly in cancer cells and in many activated (pro-inflammatory) immune cell populations (Heiden et al., 2009; Kornberg, 2020). Interestingly, although lactate is considered to be a metabolic "waste" generated mainly under pathological conditions such as shock, sepsis or ischemia (Andersen et al., 2013), recent novel studies demonstrated that lactate can also modulate immune-inflammatory response (Haas et al., 2015) and induce NETosis in bovine neutrophils (Alarcón et al., 2017), which would indicate that lactate is not only a byproduct, but instead plays a functional role in neutrophil biology. Moreover, Carestia et al. showed, that LTB₄ is a potent inducer of NETs formation. Therefore, it would be highly interesting if increased release of LTB₄ would be a compensation mechanism for reduced NETs formation by IC-activated neutrophils, due to the inhibition of LDH. Another possible explanation is provided by Han et al. They demonstrated, that by inhibiting LDH, which is the last step of glycolysis, the glucose uptake and ATP production decreased, resulting in increase of PDH protein expression and production of pyruvate. Consequently, the Krebs cycle activity enhanced and subsequently OXPHOS was increased (Han et al., 2015). This in turn, could result in increased production of fatty acids, essential for the generation of LTB₄. Another possibility is, that excess of generated pyruvate might be degraded by alternative mechanisms that do not counteract the LTB₄ release. On the other hand, galloflavin is a relatively newly discovered drug and the inhibition of LDH is the only biochemical effect described, thus it is possible that there are other pathways that compensate for the reduced lactate level, which would be interesting for future research to explore.

Notably, inhibiting different steps of the glycolysis have been a therapeutic target for cancer and autoimmune diseases, including the drugs presented in this study. Liberti et al. showed that heptelidic acid, by specific inhibition of GAPDH, a rate-limiting enzyme during the Warburg Effect, reduced glycolytic flux in the cells with high aerobic glycolysis. In addition, other GAPDH inhibitor, dimethyl fumarate (DF), an immunomodulatory drug used

for the treatment of multiple sclerosis and psoriasis, downregulated aerobic glycolysis both *in vitro* and *in vivo* (Kornberg et al., 2018). More interestingly, Wannick et al. suggested that DF ameliorated disease symptoms in the EBA mouse model through the reduced infiltration of neutrophils and monocytes in the skin by activating hydroxycarboxylic acid receptor 2 (HCA₂). The results demonstrated in this dissertation provide a possible mechanism of the DF therapeutic effect via the inhibition of glycolysis. It has been investigated, that treatment with TEPP-46 weakened pancreatic cancer cells metabolic activity, and in combination with LDHA inhibitor, cell proliferation was significantly reduced (Mohammad et al., 2019). This data proves, that the combination of compounds affecting different glycolysis steps has a synergistic therapeutic effect. Next, TEPP-46 through induction of PKM2 tetramerization and glycolysis inhibition, hindered the development of Th17 and Th1 cells *in vitro* and alleviated experimental autoimmune encephalomyelitis *in vivo* (Angiari et al., 2020). Interestingly, the pro-inflammatory Th1 and Th17 cells have been reported to be involved in the pathogenesis of autoimmune disorders, including psoriasis (Zaba et al., 2009). Therefore, treatment with TEPP-46 could be a new promising therapeutic option in BP-like EBA mouse model. Finally, it has been reported, that galloflavin suppressed the growth of human endometrial and breast cancer cells by inhibiting the final step of glycolysis (Farabegoli et al., 2012; Han et al., 2015). Moreover, the galloflavin monotherapy inhibited proliferation of pancreatic ductal adenocarcinoma cells, but in combination with metformin the anti-cancerous effect increased (Wendt et al., 2020).

Collectively, the combination of OXPHOS and glycolysis inhibitors may result in an increased therapeutic effect and provide a new multimodal approach in the treatment of not only EBA but all pemphigoid diseases (PDs). It is worth mentioning that metformin, and glycolysis inhibitors, 2-DG and dimethyl fumarate, are well tolerated by humans (Burness and Deeks, 2014; Singh et al., 2005). Moreover, the current strategy of PDs treatment has many side effects. Metformin, on the other hand, is the most commonly used drug with few side effects and interestingly, it counteracts the effects of glucocorticoids (Seelig et al., 2017), which are used in PDs therapy, making metformin a promising agent for PDs treatment.

An unexpected result of the studies in this thesis was that the treatment with moxifloxacin, a potent inhibitor of OCT-mediated transport of metformin (Brake et al., 2016), did not

reverse the inhibitory effect of metformin on the ROS release (Figure 11A), and intriguingly, inhibited both ROS and LTB₄ release in a dose-dependent manner from IC-stimulated neutrophils (Figure 11B). Moxifloxacin is a fluoroquinolone antibiotic approved for use in the treatment of pneumonia, tuberculosis and uncomplicated skin infections, among other afflictions (Keating and Scott, 2004). To this date it is not fully understood how fluoroquinolones influence inflammation. However, it has been shown that another quinolone, 2-Phenyl-4-quinolone (YT-1) led to the inhibition of respiratory burst in rat neutrophils through the inhibition of phosphodiesterase and thus accumulation cAMP (Wang et al., 1998). In addition, moxifloxacin reduced levels of inflammatory cytokines such as IL-1 β and IL-17A, and infiltrate of TNF- α -expressing cells, in mice lungs during bacterial pneumonia. (Beisswenger et al., 2014). Considering the fact that moxifloxacin is already an approved drug for the treatment of other diseases, and its inhibitory effect on the release of ROS and LTB₄ from IC-activated neutrophils presented in these studies, its effect in BP-like EBA mouse model should be investigated.

4.2 The role of activated AMPK in the EBA

Another purpose of this study was to examine a potential therapeutic role of AMPK activation in the passive model of EBA. In recent years it has been shown that this enzyme, besides being a crucial cellular energy sensor, is an important immunomodulator by regulating immune mediated inflammation (Huang et al., 2018; Jeon, 2016; Nath et al., 2005; Wang et al., 2018). Supported by the efficacy of metformin treatment in a passive EBA model (Fig.2), it has been hypothesized in this dissertation, that a similar therapeutic effect could be achieved by targeting pharmacological activation of AMPK. For this purpose, the nucleoside 5-Aminoimidazole-4-carboxamide-1- β -D-ribofuranoside (AICAR) was used. AICAR has been successfully tested in some animal disease models including acute lung injury, diabetic retinopathy, lung inflammation, inflammatory bowel disease and multiple sclerosis (Bai et al., 2010; Hoogendijk et al., 2013; Kubota et al., 2011; Nath et al., 2005; Zhao et al., 2008). Should AICAR treatment in EBA mouse model be successful, AICAR and other AMPK activators may offer a promising novel therapeutic approach in the EBA treatment. Their advantage over metformin would be higher specificity and thus better control and less potential side effects.

As the effector phase of EBA is mostly neutrophil-driven, the performed *in vitro* experiments were primarily focused on neutrophils. AICAR, which by mimicking AMP activates AMPK, is used in preclinical *in vitro* and *in vivo* experiments. In the present study, treatment with AICAR tended to increase glycolysis, albeit not statistically significant (Fig. 12A), which would be consistent with the described effects of AMPK activation, that anabolic processes are switched off and catabolic processes, including increased glucose uptake and glycolysis are switched on (Kemp et al., 2003). Although glycolysis produces less energy per glucose molecule than OXPHOS, a trend toward a metabolic shift towards the aerobic glycolysis could be observed (Fig. 12). This phenomenon is called a Warburg effect, which occurs not only in cancer cells, but also in other pro-inflammatory immune cell populations (Kornberg, 2020). This could be explained by the fact that neutrophils rely mainly on glycolysis due to the small number of functional mitochondria, causing the glycolytic pathway to be favored. In addition, it has been described that AICAR promotes glycolytic pathway by increasing of expression of glycolytic enzyme genes, such as LDHA, ALDOA, PCK2, GLUT4 (Grigorash et al., 2018). Interestingly, a decrease in glycolysis has been shown upon AICAR treatment in HEK293 (human embryonic kidney 293) and rat hepatocytes cells (Vincent et al., 2015; Vincent et al., 1992), suggesting that AICAR affects metabolism in cell line specific manner. Moreover, AICAR increased non-glycolytic acidification almost significantly (Fig. 12A). TCA cycle and glycogenolysis are the main sources of protons for non-glycolytic acidification (Winer & Wu, 2014). Since the TCA cycle plays a minor role in neutrophil energy production, it is likely that the observed trend towards an increase of non-glycolytic acidification (Fig. 12A) is caused by protons derived from glycogen breakdown by AMPK-activated glycogen phosphorylase (Jeon, 2016). This result could support the idea that by activating AMPK, AICAR triggers catabolic processes for obtaining energy.

Consistent with previous findings (Guigas et al., 2007; Spangenburg et al., 2013), OXPHOS tended to decrease under AICAR treatment, albeit not statistically significant (Fig. 12B). It is to be noted that AICAR treatment can enhance mitochondrial biogenesis in rat skeletal muscles (Suwa et al., 2015) and human fibroblasts (Golubitzky et al., 2011). However, in these experiments the treatment with AICAR continued for 14 or 3 days, respectively, which could mean that chronic AICAR treatment shifts metabolism toward OXPHOS, or that the effect induced by AICAR depends on the specific cell type. Nevertheless, given the

results presented by Jose et al., in which it was demonstrated that depending on the cell line, OXPHOS biogenesis can be activated or reduced, the latter is more likely. Notably, Spangenburg et al. demonstrated that lower dose of AICAR (0.1 mM) did not cause a decrease of OCR in cultured C2C12 myotubes, while higher doses (0.25 – 2.0 mM) inhibited mitochondrial function, even though AICAR increased AMPK phosphorylation independent of concentration. Thus, it is possible that higher AICAR concentrations result in non-specific effects. Indeed, Guigas et al. presented, that accumulation of ZMP caused by 1 mM AICAR treatment inhibited complex I of the respiratory chain in intact hepatocyte mitochondria. Taken together it is highly possible, that in *in vitro* experiments conducted in this dissertation, the metabolic changes in neutrophils caused by 1 mM AICAR treatment could be not only specific for neutrophils but could be also triggered by the used concentration of AICAR.

As ROS and LTB₄ both have previously been characterized to be crucial for the development of skin inflammation in EBA (Chiriac et al., 2007; Sezin et al., 2017), in the presented study it has been investigated how AICAR influences the release of these two agents. In Figure 13 it has been demonstrated that treatment with AICAR inhibited the release of both ROS and LTB₄. It has been previously described that AICAR alters the release of ROS in a cell type-specific manner (Jose et al., 2011). However, given that ROS in neutrophils is produced mainly by NOX2, it is likely that reduced production of ROS resulted via AICAR-induced AMPK activation inhibiting NOX2. This hypothesis is supported by the results presented by Alba et al., where it has been shown that activated AMPK in human neutrophils decreased the levels of ROS, specifically of O₂*⁻ and H₂O₂. Moreover, they demonstrated that treatment with AICAR decreased p47^{phox} serine phosphorylation levels. The p47^{phox} is the cytosolic component of NOX2, whose phosphorylation and translocation to the cell membrane is essential for the activation of NOX2 (El-Benna et al., 2008). Another interesting explanation could be the one suggested by Ceolotto et al. In their studies it has been indicated that rosiglitazone, through AMPK activation inhibited NADPH activity probably through protein kinase C (PKC) inhibition, thus inhibiting the production of ROS in endothelial cells. The functional role of inhibiting NOX2 via activated AMPK could be to preserve energy by reducing the ATP-consuming reactions, such as the production of ROS. Moreover, activated neutrophils secreted LTB₄ (Figure 13 B+D), as previously established (Afonso et al., 2012), while treatment with AICAR inhibited the secretion of LTB₄ from IC-

activated neutrophils (Figure 13 B+D). With respect to LTB₄ inhibition by AICAR it could be speculated that AMPK activation inhibited LTB₄ production by activated neutrophils in order to conserve energy. Collectively, the exact underlying mechanisms of action of AICAR on ROS and LTB₄ release from IC-stimulated neutrophils is not fully elucidated and further research is needed.

The mechanisms of inhibition of NOX2 by activated AMPK described above probably also contributed to the inhibition of NETs formation in a dose dependent manner by IC-activated neutrophils (Figure 14). This would be consistent with the findings of Menegazzo et al., where treatment with metformin, of which AMPK activation is the major mechanism of action, inhibited NETosis *in vitro* and reduced NETosis biomarkers *in vivo* by inhibiting the PKC-NADPH oxidase pathway. Upon activation of NADPH oxidase, ROS is released, which in turn activates the release of proteins and chromatin that together form NETs (Jorch and Kubes, 2017). In the presented results NETosis was not completely inhibited (Figure 14). This may be related to the fact that NETosis can also occur in NOX2-independent pathways such as calcium influx and mitochondrial ROS production (Douda et al., 2015), which are probably not inhibited by AMPK activation. Furthermore, NETs formation by neutrophils has been discovered relatively recently and a unified model of NET formation is still not established. Interestingly, recent evidence suggests that NETs formation is not limited to infectious diseases alone but might occur in other diseases such as systemic lupus erythematosus (SLE), rheumatoid arthritis (RA), diabetes, atherosclerosis, vasculitis, thrombosis, cancer, wound healing and trauma (Jorch and Kubes, 2017), therefore, it would be extremely intriguing to study the effect of NETosis inhibition in a BP-like EBA model.

It has been hypothesized that AICAR could suppress the development of BP-like EBA by inhibiting neutrophil migration. To this end, the focus has been on the potential inhibition by AICAR of C5a- and LTB₄-induced neutrophil chemotaxis. Both C5a and LTB₄ play indispensable roles in the formation of BP-like EBA (Sadik et al., 2018; Sezin et al., 2017). AICAR inhibited C5a-mediated chemotaxis (Figure 15). Anaphylatoxin C5a, the primary chemoattractant, initiates a neutrophil-mediated autoimmune inflammation of the skin through the recruitment of neutrophils, which in turn induces the recruitment of LTB₄ (Sadik et al., 2018). Although AICAR did not inhibit neutrophil migration toward LTB₄ directly (Figure 15), it could attenuate it indirectly through decreased LTB₄ release from IC-

activated neutrophils, as shown previously (Figure 13). Importantly, no loss of viability in neutrophils exposed to 1 mM AICAR concentration was noted (Figure 4D). It is unclear why AICAR inhibited migration in a stimulus dependent manner. It is possible, that AICAR could down-regulate the C5a receptors, which prevented the neutrophils from migrating. Reduction of receptor expression by activated AMPK has been described by Nakamaru et al., where AICAR treatment down-regulated the insulin receptor expression in HepG2 cells *in vitro*. Another possibility might be that pre-incubation with AICAR blocked some C5a/C5aR activating pathway. In this respect, further investigation is needed to elucidate cell type and migration pattern in the mechanism of AICAR action.

Despite the evident *in vitro* effects of AICAR on murine neutrophils, AICAR treatment did not significantly ameliorate the disease manifestation in the *in vivo* EBA mouse model (Figure 16). Interestingly though, the treatment with AICAR was associated with a non-significant tendency towards lower numbers of neutrophils and macrophages in the dermal infiltrate (Figure 16 D+E). Neutrophils and macrophages are both involved in the blister formation in BP-like EBA (Misa Hirose et al., 2016; Sezin et al., 2017). The not statistically significant trend toward reduced neutrophil count in the infiltrate could correlate with the presented result in Figure 15, showing that AICAR inhibited C5a-mediated neutrophil migration. In addition, a slight increase, although not statistically significant, in N2 neutrophils, which have been described to have antiproliferative functions (Cuartero et al., 2013), was observed upon AICAR treatment (Figure 16D). In line with these findings, it is possible that the decrease of pro-inflammatory neutrophils and macrophages, the increase of anti-inflammatory N2 neutrophils, and blunted neutrophils response to ICs (inhibition of ROS and LTB₄ release, as well as reduced NETs formation) contributed to the non-significant subtle amelioration of BP-like EBA symptoms. Although, it should be noted that *in vivo* (latin for "within the living") experiments are conducted in a more complex integrated system than *in vitro*, so there may be many possibilities for explaining the lack of *in vitro-in vivo* correlation. The *in vitro* experiments were performed using isolated neutrophils and such conditions might not reflect the physiological environment during an active immune response of the living organism. For instance, the pharmacokinetics and pharmacodynamics of *in vitro* tested drugs may differ from *in vivo* results, influencing efficacy due to the many ongoing metabolic processes in the body, which could interact with, or even counteract, the substance of interest. Therefore, it is possible that, to obtain

similar results in *in vivo* experiments to those performed *in vitro*, one would need to increase the concentration of AICAR or change its route of administration, to achieve similar intracellular activity in neutrophils. More importantly, the mouse model used for the present study - antibody transfer-induced EBA, is a passive model recreating only the effector phase of EBA. This model is convenient, as the symptoms are visible only after a few days, making it easy to study therapeutic effects of the drug of choice (Bieber et al., 2017). However, this model does not reproduce the immune response to COL7. Therefore, it would be tempting to study the effect of AICAR on EBA induction in an active model. Additionally, it would enable not only to investigate the outcome of AICAR on mechanisms involved in disease formation, but also to assess long-term therapeutic effects.

4.3 Summary

The results of this work show preliminary evidence for a potential new way for the treatment autoimmune skin blistering diseases like EBA, or alternatively supplement the conventional treatments. It has been demonstrated that by inhibiting neutrophil metabolism, the disease symptoms could be ameliorated. Metformin, an OXPHOS inhibitor, exhibits various pharmacological effects and its *in vivo* effect is likely to be a combination of these factors, such as the protective effects of T_{regs} and anti-inflammatory cytokines, IL-10 and TGF- β , and the inhibition of pro-inflammatory effects including the release of ROS and LTB₄ from IC-activated neutrophils. The specific OXPHOS inhibitor, oligomycin, in a similar fashion inhibited the release of ROS and LTB₄ from neutrophils. It has also been presented that OCTs, the transporters responsible for metformin entry into the cells, are not highly expressed on neutrophils. Thus, offering a possible explanation why supra-pharmacological doses were needed to produce a therapeutic effect *in vitro*. Furthermore, tested glycolysis inhibitors such as 2-DG, heptelidic acid, galloflavin and TEPP-46 inhibited the response of ICs activated neutrophils by inhibiting ROS and LTB₄ secretion. In addition to these inhibitors, it was surprising to note that moxifloxacin, a fluoroquinolone antibiotic, inhibited ROS and LTB₄ release as well.

In addition to *in vitro* studies, the effect of AMPK activation using AICAR in the EBA model was examined. While administration of AICAR blunted response of IC-activated neutrophils *in vitro*, there was only a subtle, but not significant, amelioration observed after *in vivo*

administration of AICAR. *In vitro* experiments showed that AICAR influenced neutrophil metabolism through a tendency toward stimulation of glycolysis and inhibition of OXPHOS, and since the opposite effect of AICAR on other cell metabolism has also been described, it could be concluded that AICAR influences metabolism in a cell line specific manner. Moreover, it has been demonstrated that AICAR increased non-glycolytic acidification almost significantly, supporting the idea that catabolic processes are activated by AICAR in order to obtain energy. Blunted response to the IC-activated neutrophils was shown to inhibit not only the secretion of ROS and LTB₄, but also the formation of NETs. Furthermore, the trend towards a reduced neutrophil and macrophages count, and elevated number of N2 neutrophils, was detected in the skin in the EBA model. The reduced number of neutrophils could be due to inhibition of C5a-mediated migration of neutrophils, as shown in *in vitro* experiments. Taken together, the presented inhibitory effect of AICAR on IC-activated neutrophils in *in vitro* experiments, might have contributed to the slight improvement of symptoms in the EBA mouse model.

Regarding *in vivo* results from mice treated with AICAR, it could be inferred that the therapeutic effect generated by treatment with metformin during the course of passive EBA model (Fig. 2) is not only induced by the main mechanism of action of metformin, i.e. activation of AMPK, but by possible involvement of other AMPK-independent mechanisms.

Additionally, the strategy of AMPK activation to regulate the immune response continues to be noteworthy. However, further studies are needed to completely elucidate the exact mechanisms of AICAR action as well as its cell-type specific effects.

Collectively, this work highlights that modulating immunometabolism of neutrophils might be a promising therapeutic strategy in the treatment of BP-like EBA.

5 REFERENCES

- Adachi, A., Komine, M., Suzuki, M., Murata, S., Hirano, T., Ishii, N., Hashimoto, T., Ohtsuki, M., 2016. Oral colchicine monotherapy for epidermolysis bullosa acquisita: Mechanism of action and efficacy. *J. Dermatol.* 43, 1389–1391. <https://doi.org/10.1111/1346-8138.13395>
- Afonso, P.V., Janka-Junttila, M., Lee, Y.J., McCann, C.P., Oliver, C.M., Aamer, K.A., Losert, W., Cicerone, M.T., Parent, C.A., 2012. LTB4 IS A SIGNAL RELAY MOLECULE DURING NEUTROPHIL CHEMOTAXIS. *Dev. Cell* 22, 1079–1091. <https://doi.org/10.1016/j.devcel.2012.02.003>
- Ahmadian, M., Abbott, M.J., Tang, T., Hudak, C.S.S., Kim, Y., Bruss, M., Hellerstein, M.K., Lee, H.-Y., Samuel, V.T., Shulman, G.I., Wang, Y., Duncan, R.E., Kang, C., Sul, H.S., 2011. Desnutrin/ATGL is Regulated by AMPK and is Required for a Brown Adipose Phenotype. *Cell Metab.* 13, 739–748. <https://doi.org/10.1016/j.cmet.2011.05.002>
- Alarcón, P., Manosalva, C., Conejeros, I., Carretta, M.D., Muñoz-Caro, T., Silva, L.M.R., Taubert, A., Hermosilla, C., Hidalgo, M.A., Burgos, R.A., 2017. d(-) Lactic Acid-Induced Adhesion of Bovine Neutrophils onto Endothelial Cells Is Dependent on Neutrophils Extracellular Traps Formation and CD11b Expression. *Front. Immunol.* 8. <https://doi.org/10.3389/fimmu.2017.00975>
- Alba, G., El Bekay, R., Álvarez-Maqueda, M., Chacón, P., Vega, A., Monteseirín, J., Santa María, C., Pintado, E., Bedoya, F.J., Bartrons, R., Sobrino, F., 2004. Stimulators of AMP-activated protein kinase inhibit the respiratory burst in human neutrophils. *FEBS Lett.* 573, 219–225. <https://doi.org/10.1016/j.febslet.2004.07.077>
- Alexandre, M., Brette, M.-D., Pascal, F., Tsianakas, P., Fraitag, S., Doan, S., Caux, F., Dupuy, A., Heller, M., Lièvre, N., Lepage, V., Dubertret, L., Laroche, L., Prost-Squarcioni, C., 2006. A Prospective Study of Upper Aerodigestive Tract Manifestations of Mucous Membrane Pemphigoid. *Medicine (Baltimore)* 85, 239–252. <https://doi.org/10.1097/01.md.0000231954.08350.52>
- American Diabetes Association, 2020. 9. Pharmacologic Approaches to Glycemic Treatment: Standards of Medical Care in Diabetes—2020. *Diabetes Care* 43, S98–S110. <https://doi.org/10.2337/dc20-S009>
- An, H., He, L., 2016. Current Understanding of Metformin Effect on the Control of Hyperglycemia in Diabetes. *J. Endocrinol.* 228, R97-106. <https://doi.org/10.1530/JOE-15-0447>
- Andersen, L.W., Mackenhauer, J., Roberts, J.C., Berg, K.M., Cocchi, M.N., Donnino, M.W., 2013. Etiology and therapeutic approach to elevated lactate. *Mayo Clin. Proc.* 88, 1127–1140. <https://doi.org/10.1016/j.mayocp.2013.06.012>
- Angiari, S., Runtsch, M.C., Sutton, C.E., Palsson-McDermott, E.M., Kelly, B., Rana, N., Kane, H., Papadopoulou, G., Pearce, E.L., Mills, K.H.G., O'Neill, L.A.J., 2020. Pharmacological Activation of Pyruvate Kinase M2 Inhibits CD4+ T Cell Pathogenicity and Suppresses Autoimmunity. *Cell Metab.* 31, 391-405.e8. <https://doi.org/10.1016/j.cmet.2019.10.015>
- Asfour, L., Chong, H., Mee, J., Groves, R., Singh, M., 2017. Epidermolysis Bullosa Acquisita (Brunsting-Perry Pemphigoid Variant) Localized to the Face and Diagnosed With Antigen Identification Using Skin Deficient in Type VII Collagen: *Am. J. Dermatopathol.* 39, e90–e96. <https://doi.org/10.1097/DAD.0000000000000829>
- Assmann, N., Finlay, D.K., n.d. Metabolic regulation of immune responses: therapeutic opportunities. *J. Clin. Invest.* 126, 2031–2039. <https://doi.org/10.1172/JCI83005>
- Awasthi, D., Nagarkoti, S., Sadaf, S., Chandra, T., Kumar, S., Dikshit, M., 2019. Glycolysis dependent lactate formation in neutrophils: A metabolic link between NOX-dependent

- and independent NETosis. *Biochim. Biophys. Acta BBA - Mol. Basis Dis.* 1865, 165542. <https://doi.org/10.1016/j.bbadis.2019.165542>
- Bailey, C., Day, C., 2004. Metformin: its botanical background. *Pract. Diabetes Int.* 21, 115–117. <https://doi.org/10.1002/pdi.606>
- Bando, H., Atsumi, T., Nishio, T., Niwa, H., Mishima, S., Shimizu, C., Yoshioka, N., Bucala, R., Koike, T., 2005. Phosphorylation of the 6-Phosphofructo-2-Kinase/Fructose 2,6-Bisphosphatase/PFKFB3 Family of Glycolytic Regulators in Human Cancer. *Clin. Cancer Res.* 11, 5784–5792. <https://doi.org/10.1158/1078-0432.CCR-05-0149>
- Baroudjian, B., Le Roux-Villet, C., Bréchnignac, S., Alexandre, M., Caux, F., Prost-Squarcioni, C., Laroche, L., 2012. Long-term efficacy of extracorporeal photochemotherapy in a patient with refractory epidermolysis bullosa acquisita. *Eur. J. Dermatol.* 22, 795–797. <https://doi.org/10.1684/ejd.2012.1840>
- Batandier, C., Guigas, B., Detaille, D., El-Mir, M., Fontaine, E., Rigoulet, M., Leverve, X.M., 2006. The ROS Production Induced by a Reverse-Electron Flux at Respiratory-Chain Complex 1 is Hampered by Metformin. *J. Bioenerg. Biomembr.* 38, 33–42. <https://doi.org/10.1007/s10863-006-9003-8>
- Beisswenger, C., Honecker, A., Kamyschnikow, A., Bischoff, M., Tschernig, T., Bals, R., 2014. Moxifloxacin modulates inflammation during murine pneumonia. *Respir. Res.* 15, 82. <https://doi.org/10.1186/1465-9921-15-82>
- Bertram, F., Bröcker, E.-B., Zillikens, D., Schmidt, E., 2009. Prospective analysis of the incidence of autoimmune bullous disorders in Lower Franconia, Germany. *JDDG J. Dtsch. Dermatol. Ges.* 7, 434–439. <https://doi.org/10.1111/j.1610-0387.2008.06976.x>
- Bettencourt, I.A., Powell, J.D., 2017. Targeting metabolism as a novel therapeutic approach to autoimmunity, inflammation and transplantation. *J. Immunol. Baltim. Md 1950* 198, 999–1005. <https://doi.org/10.4049/jimmunol.1601318>
- Bieber, K., Koga, H., Nishie, W., 2017a. In vitro and in vivo models to investigate the pathomechanisms and novel treatments for pemphigoid diseases. *Exp. Dermatol.* 26, 1163–1170. <https://doi.org/10.1111/exd.13415>
- Bieber, K., Sun, S., Witte, M., Kasprick, A., Beltsiou, F., Behnen, M., Laskay, T., Schulze, F.S., Pippi, E., Reichhelm, N., Pagel, R., Zillikens, D., Schmidt, E., Sparwasser, T., Kalies, K., Ludwig, R.J., 2017b. Regulatory T Cells Suppress Inflammation and Blistering in Pemphigoid Diseases. *Front. Immunol.* 8. <https://doi.org/10.3389/fimmu.2017.01628>
- Bieber, K., Witte, M., Sun, S., Hundt, J.E., Kalies, K., Dräger, S., Kasprick, A., Twelkmeyer, T., Manz, R.A., König, P., Köhl, J., Zillikens, D., Ludwig, R.J., 2016. T cells mediate autoantibody-induced cutaneous inflammation and blistering in epidermolysis bullosa acquisita. *Sci. Rep.* 6. <https://doi.org/10.1038/srep38357>
- Boothby, M., Rickert, R.C., 2017. Metabolic regulation of the immune humoral response. *Immunity* 46, 743–755. <https://doi.org/10.1016/j.immuni.2017.04.009>
- Brake, L.H.M., van den Heuvel, J.J.M.W., Buaben, A.O., van Crevel, R., Bilos, A., Russel, F.G., Aarnoutse, R.E., Koenderink, J.B., 2016. Moxifloxacin Is a Potent In Vitro Inhibitor of OCT- and MATE-Mediated Transport of Metformin and Ethambutol. *Antimicrob. Agents Chemother.* 60, 7105–7114. <https://doi.org/10.1128/AAC.01471-16>
- Brinkmann, V., 2004. Neutrophil Extracellular Traps Kill Bacteria. *Science* 303, 1532–1535. <https://doi.org/10.1126/science.1092385>
- Buck, M.D., Sowell, R.T., Kaech, S.M., Pearce, E.L., 2017. Metabolic Instruction of Immunity. *Cell* 169, 570–586. <https://doi.org/10.1016/j.cell.2017.04.004>
- Buijsrogge, J.J.A., Diercks, G.F.H., Pas, H.H., Jonkman, M.F., 2011. The many faces of epidermolysis bullosa acquisita after serration pattern analysis by direct immunofluorescence microscopy: Serration pattern analysis of EBA. *Br. J. Dermatol.* 165, 92–98. <https://doi.org/10.1111/j.1365-2133.2011.10346.x>
- Bultot, L., Guigas, B., Von Wilamowitz-Moellendorff, A., Maisin, L., Vertommen, D., Hussain, N., Beullens, M., Guinovart, J.J., Foretz, M., Viollet, B., Sakamoto, K., Hue, L., Rider, M.H.,

2012. AMP-activated protein kinase phosphorylates and inactivates liver glycogen synthase. *Biochem. J.* 443, 193–203. <https://doi.org/10.1042/BJ20112026>
- Burness, C.B., Deeks, E.D., 2014. Dimethyl fumarate: a review of its use in patients with relapsing-remitting multiple sclerosis. *CNS Drugs* 28, 373–387. <https://doi.org/10.1007/s40263-014-0155-5>
- Cantó, C., Gerhart-Hines, Z., Feige, J.N., Lagouge, M., Noriega, L., Milne, J.C., Elliott, P.J., Puigserver, P., Auwerx, J., 2009. AMPK regulates energy expenditure by modulating NAD⁺ metabolism and SIRT1 activity. *Nature* 458, 1056–1060. <https://doi.org/10.1038/nature07813>
- Carestia, A., Kaufman, T., Rivadeneyra, L., Landoni, V.I., Pozner, R.G., Negrotto, S., D’Atri, L.P., Gómez, R.M., Schattner, M., 2016. Mediators and molecular pathways involved in the regulation of neutrophil extracellular trap formation mediated by activated platelets. *J. Leukoc. Biol.* 99, 153–162. <https://doi.org/10.1189/jlb.3A0415-161R>
- Carling, D., Clarke, P.R., Zammit, V.A., Hardie, D.G., 1989. Purification and characterization of the AMP-activated protein kinase. Copurification of acetyl-CoA carboxylase kinase and 3-hydroxy-3-methylglutaryl-CoA reductase kinase activities. *Eur. J. Biochem.* 186, 129–136. <https://doi.org/10.1111/j.1432-1033.1989.tb15186.x>
- Ceolotto, Gallo Alessandra, Papparella Italia, Franco Lorenzo, Murphy Ellen, Iori Elisabetta, Pagnin Elisa, Fadini Gian Paolo, Albiero Mattia, Semplicini Andrea, Avogaro Angelo, 2007. Rosiglitazone Reduces Glucose-Induced Oxidative Stress Mediated by NAD(P)H Oxidase via AMPK-Dependent Mechanism. *Arterioscler. Thromb. Vasc. Biol.* 27, 2627–2633. <https://doi.org/10.1161/ATVBAHA.107.155762>
- Chavez, J.A., Roach, W.G., Keller, S.R., Lane, W.S., Lienhard, G.E., 2008. Inhibition of GLUT4 Translocation by Tbc1d1, a Rab GTPase-activating Protein Abundant in Skeletal Muscle, Is Partially Relieved by AMP-activated Protein Kinase Activation. *J. Biol. Chem.* 283, 9187–9195. <https://doi.org/10.1074/jbc.M708934200>
- Chen, E.C., Liang, X., Yee, S.W., Geier, E.G., Stocker, S.L., Chen, L., Giacomini, K.M., 2015. Targeted Disruption of Organic Cation Transporter 3 Attenuates the Pharmacologic Response to Metformin. *Mol. Pharmacol.* 88, 75–83. <https://doi.org/10.1124/mol.114.096776>
- Chen, M., O’Toole, E.A., Sanghavi, J., Woodley, D.T., Mahmud, N., Kelleher, D., Weir, D., Fairley, J.A., 2002. The Epidermolysis Bullosa Acquisita Antigen (Type VII Collagen) is Present in Human Colon and Patients with Crohn’s Disease have Autoantibodies to Type VII Collagen. *J. Invest. Dermatol.* 118, 1059–1064. <https://doi.org/10.1046/j.1523-1747.2002.01772.x>
- Chiriac, M., Roesler, J., Sindrilaru, A., Scharffetter-Kochanek, K., Zillikens, D., Sitaru, C., 2007. NADPH oxidase is required for neutrophil-dependent autoantibody-induced tissue damage. *J. Pathol.* 212, 56–65. <https://doi.org/10.1002/path.2157>
- Chiriac, M.T., Roesler, J., Sindrilaru, A., Scharffetter-Kochanek, K., Zillikens, D., Sitaru, C., 2007. NADPH oxidase is required for neutrophil-dependent autoantibody-induced tissue damage. *J. Pathol.* 212, 56–65. <https://doi.org/10.1002/path.2157>
- Chou, R.C., Kim, N.D., Sadik, C.D., Seung, E., Lan, Y., Byrne, M.H., Haribabu, B., Iwakura, Y., Luster, A.D., 2010. Lipid-Cytokine-Chemokine Cascade Drives Neutrophil Recruitment in a Murine Model of Inflammatory Arthritis. *Immunity* 33, 266–278. <https://doi.org/10.1016/j.immuni.2010.07.018>
- Chung, H.J., Uitto, J., 2010. Type VII Collagen: The Anchoring Fibril Protein at Fault in Dystrophic Epidermolysis Bullosa. *Dermatol. Clin.* 28, 93–105. <https://doi.org/10.1016/j.det.2009.10.011>
- Corton, J.M., Gillespie, J.G., Hawley, S.A., Hardie, D.G., 1995. 5-Aminoimidazole-4-Carboxamide Ribonucleoside. A Specific Method for Activating AMP-Activated Protein Kinase in Intact Cells? *Eur. J. Biochem.* 229, 558–565. <https://doi.org/10.1111/j.1432-1033.1995.tb20498.x>

- Crowley, L.C., Marfell, B.J., Scott, A.P., Waterhouse, N.J., 2016. Quantitation of Apoptosis and Necrosis by Annexin V Binding, Propidium Iodide Uptake, and Flow Cytometry. *Cold Spring Harb. Protoc.* 2016, pdb.prot087288. <https://doi.org/10.1101/pdb.prot087288>
- Cuartero, Ballesteros Iván, Moraga Ana, Nombela Florentino, Vivancos José, Hamilton John A., Corbí Ángel L., Lizasoain Ignacio, Moro María A., 2013. N2 Neutrophils, Novel Players in Brain Inflammation After Stroke. *Stroke* 44, 3498–3508. <https://doi.org/10.1161/STROKEAHA.113.002470>
- Cunningham, B.B., Kirchmann, T.T.T., Woodley, D., 1996. Colchicine for epidermolysis bullosa acquisita. *J. Am. Acad. Dermatol.* 34, 781–784. [https://doi.org/10.1016/S0190-9622\(96\)90013-4](https://doi.org/10.1016/S0190-9622(96)90013-4)
- Damoiseaux, J., 2013. Bullous Skin Diseases: Classical Types of Autoimmune Diseases. *Scientifica* 2013. <https://doi.org/10.1155/2013/457982>
- Delgado, L., Aoki, V., Santi, C., Gabbi, T., Sotto, M., Maruta, C., 2011. Clinical and immunopathological evaluation of epidermolysis bullosa acquisita: Clinical and immunopathological evaluation of EBA. *Clin. Exp. Dermatol.* 36, 12–18. <https://doi.org/10.1111/j.1365-2230.2010.03845.x>
- Divakaruni, A.S., Paradyse, A., Ferrick, D.A., Murphy, A.N., Jastroch, M., 2014. Analysis and Interpretation of Microplate-Based Oxygen Consumption and pH Data, in: *Methods in Enzymology*. Elsevier, pp. 309–354. <https://doi.org/10.1016/B978-0-12-801415-8.00016-3>
- Douda, D.N., Khan, M.A., Grasmann, H., Palaniyar, N., 2015. SK3 channel and mitochondrial ROS mediate NADPH oxidase-independent NETosis induced by calcium influx. *Proc. Natl. Acad. Sci. U. S. A.* 112, 2817–2822. <https://doi.org/10.1073/pnas.1414055112>
- Egan, D.F., Shackelford, D.B., Mihaylova, M.M., Gelino, S.R., Kohnz, R.A., Mair, W., Vasquez, D.S., Joshi, A., Gwinn, D.M., Taylor, R., Asara, J.M., Fitzpatrick, J., Dillin, A., Viollet, B., Kundu, M., Hansen, M., Shaw, R.J., 2011. Phosphorylation of ULK1 (hATG1) by AMP-activated protein kinase connects energy sensing to mitophagy. *Science* 331, 456–461. <https://doi.org/10.1126/science.1196371>
- El-Benna, J., Dang, P.M.-C., Gougerot-Pocidallo, M.-A., 2008. Priming of the neutrophil NADPH oxidase activation: role of p47phox phosphorylation and NOX2 mobilization to the plasma membrane. *Semin. Immunopathol.* 30, 279–289. <https://doi.org/10.1007/s00281-008-0118-3>
- Ellebrecht, C.T., Srinivas, G., Bieber, K., Banczyk, D., Kalies, K., Künzel, S., Hammers, C.M., Baines, J.F., Zillikens, D., Ludwig, R.J., Westermann, J., 2016. Skin microbiota-associated inflammation precedes autoantibody induced tissue damage in experimental epidermolysis bullosa acquisita. *J. Autoimmun.* 68, 14–22. <https://doi.org/10.1016/j.jaut.2015.08.007>
- Engineer, L., Ahmed, A.R., 2001. Emerging treatment for epidermolysis bullosa acquisita. *J. Am. Acad. Dermatol.* 44, 818–828. <https://doi.org/10.1067/mjd.2001.113693>
- Farabegoli, F., Vettraino, M., Manerba, M., Fiume, L., Roberti, M., Di Stefano, G., 2012. Galloflavin, a new lactate dehydrogenase inhibitor, induces the death of human breast cancer cells with different glycolytic attitude by affecting distinct signaling pathways. *Eur. J. Pharm. Sci.* 47, 729–738. <https://doi.org/10.1016/j.ejps.2012.08.012>
- Foretz, M., Guigas, B., Bertrand, L., Pollak, M., Viollet, B., 2014. Metformin: From Mechanisms of Action to Therapies. *Cell Metab.* 20, 953–966. <https://doi.org/10.1016/j.cmet.2014.09.018>
- Furue, M., Iwata, M., Yoon, H.-I., Kubota, Y., Ohto, H., Kawashima, M., Tsuchida, T., Oohara, K., Tamaki, K., Kukita, A., 1986. Epidermolysis bullosa acquisita: Clinical response to plasma exchange therapy and circulating anti-basement membrane zone antibody titer. *J. Am. Acad. Dermatol.* 14, 873–878. [https://doi.org/10.1016/S0190-9622\(86\)70103-5](https://doi.org/10.1016/S0190-9622(86)70103-5)
- Gaber, T., Strehl, C., Buttgereit, F., 2017. Metabolic regulation of inflammation. *Nat. Rev. Rheumatol.* 13, 267–279. <https://doi.org/10.1038/nrrheum.2017.37>
- Gammon, W.R., Heise, E.R., Burke, W.A., Fine, J.-D., Woodley, D.T., Briggaman, R.A., 1988. Increased Frequency of HLA-DR2 in Patients with Autoantibodies to Epidermolysis Bullosa

- Acquisita Antigen: Evidence that the Expression of Autoimmunity to Type VII Collagen Is HLA Class II Allele Associated. *J. Invest. Dermatol.* 91, 228–232. <https://doi.org/10.1111/1523-1747.ep12470317>
- Golubitzky, A., Dan, P., Weissman, S., Link, G., Wikstrom, J.D., Saada, A., 2011. Screening for Active Small Molecules in Mitochondrial Complex I Deficient Patient's Fibroblasts, Reveals AICAR as the Most Beneficial Compound. *PLoS ONE* 6. <https://doi.org/10.1371/journal.pone.0026883>
- Gordon, K.B., Chan, L.S., Woodley, D.T., 1997. Treatment of refractory epidermolysis bullosa acquisita with extracorporeal photochemotherapy. *Br. J. Dermatol.* 136, 415–420. <https://doi.org/10.1046/j.1365-2133.1997.5771549.x>
- Grigorash, B.B., Suvorova, I.I., Pospelov, V.A., 2018. [AICAR-Dependent Activation of AMPK Kinase Is Not Accompanied by G1/S Block in Mouse Embryonic Stem Cells]. *Mol. Biol. (Mosk.)* 52, 489–500. <https://doi.org/10.7868/S0026898418030126>
- Guigas, B., Taleux, N., Foretz, M., Demaille, D., Andreelli, F., Viollet, B., Hue, L., 2007. AMP-activated protein kinase-independent inhibition of hepatic mitochondrial oxidative phosphorylation by AICA riboside. *Biochem. J.* 404, 499–507. <https://doi.org/10.1042/BJ20070105>
- Gupta, R., Woodley, D.T., Chen, M., 2012. Epidermolysis Bullosa Acquisita. *Clin. Dermatol.* 30, 60–69. <https://doi.org/10.1016/j.clindermatol.2011.03.011>
- Gwinn, D.M., Shackelford, D.B., Egan, D.F., Mihaylova, M.M., Mery, A., Vasquez, D.S., Turk, B.E., Shaw, R.J., 2008. AMPK phosphorylation of raptor mediates a metabolic checkpoint. *Mol. Cell* 30, 214–226. <https://doi.org/10.1016/j.molcel.2008.03.003>
- Haas, R., Smith, J., Rocher-Ros, V., Nadkarni, S., Montero-Melendez, T., D'Acquisto, F., Bland, E.J., Bombardieri, M., Pitzalis, C., Perretti, M., Marelli-Berg, F.M., Mauro, C., 2015. Lactate Regulates Metabolic and Pro-inflammatory Circuits in Control of T Cell Migration and Effector Functions. *PLoS Biol.* 13. <https://doi.org/10.1371/journal.pbio.1002202>
- Habets, D.D.J., Coumans, W.A., El Hasnaoui, M., Zarrinpashneh, E., Bertrand, L., Viollet, B., Kiens, B., Jensen, T.E., Richter, E.A., Bonen, A., 2009. Crucial role for LKB1 to AMPK α 2 axis in the regulation of CD36-mediated long-chain fatty acid uptake into cardiomyocytes☆. *Biochim. Biophys. Acta BBA - Mol. Cell Biol. Lipids* 1791, 212–219. <https://doi.org/10.1016/j.bbalip.2008.12.009>
- Haeberle, S., Wei, X., Bieber, K., Goletz, S., Ludwig, R.J., Schmidt, E., Enk, A.H., Hadaschik, E.N., 2018. Regulatory T-cell deficiency leads to pathogenic bullous pemphigoid antigen 230 autoantibody and autoimmune bullous disease. *J. Allergy Clin. Immunol.* 142, 1831–1842.e7. <https://doi.org/10.1016/j.jaci.2018.04.006>
- Halliwell, B., 2006. Reactive Species and Antioxidants. Redox Biology Is a Fundamental Theme of Aerobic Life. *Plant Physiol.* 141, 312–322. <https://doi.org/10.1104/pp.106.077073>
- Hammers, C.M., Bieber, K., Kalies, K., Banczyk, D., Ellebrecht, C.T., Ibrahim, S.M., Zillikens, D., Ludwig, R.J., Westermann, J., 2011. Complement-Fixing Anti-Type VII Collagen Antibodies Are Induced in Th1-Polarized Lymph Nodes of Epidermolysis Bullosa Acquisita-Susceptible Mice. *J. Immunol.* 187, 5043–5050. <https://doi.org/10.4049/jimmunol.1100796>
- Han, X., Sheng, X., Jones, H.M., Jackson, A.L., Kilgore, J., Stine, J.E., Schointuch, M.N., Zhou, C., Bae-Jump, V.L., 2015. Evaluation of the anti-tumor effects of lactate dehydrogenase inhibitor galloflavin in endometrial cancer cells. *J. Hematol. Oncol. J Hematol Oncol* 8, 2. <https://doi.org/10.1186/s13045-014-0097-x>
- Hancock, J.T., Desikan, R., Neill, S.J., 2001. Role of reactive oxygen species in cell signalling pathways. *Biochem. Soc. Trans.* 29, 345–349. <https://doi.org/10.1042/bst0290345>
- Hardie, D.G., 2011. AMP-activated protein kinase—an energy sensor that regulates all aspects of cell function. *Genes Dev.* 25, 1895–1908. <https://doi.org/10.1101/gad.17420111>
- Hardie, D.G., 2004. The AMP-activated protein kinase pathway – new players upstream and downstream. *J. Cell Sci.* 117, 5479–5487. <https://doi.org/10.1242/jcs.01540>

- Hardie, D.G., Pan, D.A., 2002. Regulation of fatty acid synthesis and oxidation by the AMP-activated protein kinase. *Biochem. Soc. Trans.* 30, 1064–1070. <https://doi.org/10.1042/bst0301064>
- Hardie, D.G., Ross, F.A., Hawley, S.A., 2012. AMPK - a nutrient and energy sensor that maintains energy homeostasis. *Nat. Rev. Mol. Cell Biol.* 13, 251–262. <https://doi.org/10.1038/nrm3311>
- Heiden, M.G.V., Cantley, L.C., Thompson, C.B., 2009. Understanding the Warburg Effect: The Metabolic Requirements of Cell Proliferation. *Science* 324, 1029–1033. <https://doi.org/10.1126/science.1160809>
- Hellberg, L., Samavedam, U.K.S.R.L., Holdorf, K., Hänsel, M., Recke, A., Beckmann, T., Steinhorst, K., Boehncke, W.-H., Kirchner, T., Möckel, N., Solbach, W., Zillikens, D., Schmidt, E., Ludwig, R.J., Laskay, T., 2013. Methylprednisolone Blocks Autoantibody-Induced Tissue Damage in Experimental Models of Bullous Pemphigoid and Epidermolysis Bullosa Acquisita through Inhibition of Neutrophil Activation. *J. Invest. Dermatol.* 133, 2390–2399. <https://doi.org/10.1038/jid.2013.91>
- Hirose, M., Brandolini, L., Zimmer, D., Götz, J., Westermann, J., Allegretti, M., Moriconi, A., Recke, A., Zillikens, D., Kalies, K., Ludwig, R.J., 2013. The Allosteric CXCR1/2 Inhibitor DF2156A Improves Experimental Epidermolysis Bullosa Acquisita. *J. Genet. Syndr. Gene Ther.* s3. <https://doi.org/10.4172/2157-7412.S3-005>
- Hirose, M., Kasprick, A., Beltsiou, F., Dieckhoff, K.S., Schulze, F.S., Samavedam, U.K., Hundt, J.E., Pas, H.H., Jonkman, M.F., Schmidt, E., Kalies, K., Zillikens, D., Ludwig, R.J., Bieber, K., 2016. Reduced Skin Blistering in Experimental Epidermolysis Bullosa Acquisita After Anti-TNF Treatment. *Mol. Med.* 22, 918–926. <https://doi.org/10.2119/molmed.2015.00206>
- Hirose, Misa, Kasprick, A., Beltsiou, F., Dieckhoff, K.S., Schulze, F.S., Samavedam, U.K., Hundt, J.E., Pas, H.H., Jonkman, M.F., Schmidt, E., Kalies, K., Zillikens, D., Ludwig, R.J., Bieber, K., 2016. Reduced Skin Blistering in Experimental Epidermolysis Bullosa Acquisita After Anti-TNF Treatment. *Mol. Med.* 22, 918–926. <https://doi.org/10.2119/molmed.2015.00206>
- Hirose, M., Tiburzy, B., Ishii, N., Pipi, E., Wende, S., Rentz, E., Nimmerjahn, F., Zillikens, D., Manz, R.A., Ludwig, R.J., Kasperkiewicz, M., 2015. Effects of Intravenous Immunoglobulins on Mice with Experimental Epidermolysis Bullosa Acquisita. *J. Invest. Dermatol.* 135, 768–775. <https://doi.org/10.1038/jid.2014.453>
- Hirose, M., Vafia, K., Kalies, K., Groth, S., Westermann, J., Zillikens, D., Ludwig, R.J., Collin, M., Schmidt, E., 2012. Enzymatic autoantibody glycan hydrolysis alleviates autoimmunity against type VII collagen. *J. Autoimmun.* 39, 304–314. <https://doi.org/10.1016/j.jaut.2012.04.002>
- Hoppe, S., Bierhoff, H., Cado, I., Weber, A., Tiebe, M., Grummt, I., Voit, R., 2009. AMP-activated protein kinase adapts rRNA synthesis to cellular energy supply. *Proc. Natl. Acad. Sci. U. S. A.* 106, 17781–17786. <https://doi.org/10.1073/pnas.0909873106>
- Hu, S.C.-S., Yu, H.-S., Yen, F.-L., Lin, C.-L., Chen, G.-S., Lan, C.-C.E., 2016. Neutrophil extracellular trap formation is increased in psoriasis and induces human β -defensin-2 production in epidermal keratinocytes. *Sci. Rep.* 6, 31119. <https://doi.org/10.1038/srep31119>
- Huang, J., Liu, K., Zhu, S., Xie, M., Kang, R., Cao, L., Tang, D., 2018. AMPK regulates immunometabolism in sepsis. *Brain. Behav. Immun.* 72, 89–100. <https://doi.org/10.1016/j.bbi.2017.11.003>
- Huang, N., Perl, A., 2018. Metabolism as a Target for Modulation in Autoimmune Diseases. *Trends Immunol.* 39, 562–576. <https://doi.org/10.1016/j.it.2018.04.006>
- Hübner, F., Recke, A., Zillikens, D., Linder, R., Schmidt, E., 2016. Prevalence and Age Distribution of Pemphigus and Pemphigoid Diseases in Germany. *J. Invest. Dermatol.* 136, 2495–2498. <https://doi.org/10.1016/j.jid.2016.07.013>
- Hundorfean, G., Neurath, M.F., Sitaru, C., 2010. Autoimmunity against type VII collagen in inflammatory bowel disease. *J. Cell. Mol. Med.* 14, 2393–2403. <https://doi.org/10.1111/j.1582-4934.2009.00959.x>

- Injarabian, L., Devin, A., Ransac, S., Marteyn, B.S., 2019. Neutrophil Metabolic Shift during Their Lifecycle: Impact on Their Survival and Activation. *Int. J. Mol. Sci.* 21. <https://doi.org/10.3390/ijms21010287>
- Inoki, K., Zhu, T., Guan, K.-L., 2003. TSC2 Mediates Cellular Energy Response to Control Cell Growth and Survival. *Cell* 115, 577–590. [https://doi.org/10.1016/S0092-8674\(03\)00929-2](https://doi.org/10.1016/S0092-8674(03)00929-2)
- Ishii, N., Hamada, T., Dainichi, T., Karashima, T., Nakama, T., Yasumoto, S., Zillikens, D., Hashimoto, T., 2010a. Epidermolysis bullosa acquisita: What's new? *J. Dermatol.* 37, 220–230. <https://doi.org/10.1111/j.1346-8138.2009.00799.x>
- Ishii, N., Hashimoto, T., Zillikens, D., Ludwig, R.J., 2010b. High-Dose Intravenous Immunoglobulin (IVIg) Therapy in Autoimmune Skin Blistering Diseases. *Clin. Rev. Allergy Immunol.* 38, 186–195. <https://doi.org/10.1007/s12016-009-8153-y>
- Ishii, N., Recke, A., Mihai, S., Hirose, M., Hashimoto, T., Zillikens, D., Ludwig, R.J., 2011. Autoantibody-induced intestinal inflammation and weight loss in experimental epidermolysis bullosa acquisita: Autoantibody-induced intestinal inflammation. *J. Pathol.* 224, 234–244. <https://doi.org/10.1002/path.2857>
- Iwata, H., Bieber, K., Tiburzy, B., Chrobok, N., Kalies, K., Shimizu, A., Leineweber, S., Ishiko, A., Vorobyev, A., Zillikens, D., Köhl, J., Westermann, J., Seeger, K., Manz, R., Ludwig, R.J., 2013. B Cells, Dendritic Cells, and Macrophages Are Required To Induce an Autoreactive CD4 Helper T Cell Response in Experimental Epidermolysis Bullosa Acquisita. *J. Immunol.* 191, 2978–2988. <https://doi.org/10.4049/jimmunol.1300310>
- Iwata, H., Pipi, E., Möckel, N., Sondermann, P., Vorobyev, A., Beek, N. van, Zillikens, D., Ludwig, R.J., 2015. Recombinant Soluble CD32 Suppresses Disease Progression in Experimental Epidermolysis Bullosa Acquisita. *J. Invest. Dermatol.* 135, 916–919. <https://doi.org/10.1038/jid.2014.451>
- Jäger, S., Handschin, C., St.-Pierre, J., Spiegelman, B.M., 2007. AMP-activated protein kinase (AMPK) action in skeletal muscle via direct phosphorylation of PGC-1 α . *Proc. Natl. Acad. Sci. U. S. A.* 104, 12017–12022. <https://doi.org/10.1073/pnas.0705070104>
- Jeon, S.-M., 2016. Regulation and function of AMPK in physiology and diseases. *Exp. Mol. Med.* 48, e245–e245. <https://doi.org/10.1038/emm.2016.81>
- Jorch, S.K., Kubes, P., 2017. An emerging role for neutrophil extracellular traps in noninfectious disease. *Nat. Med.* 23, 279–287. <https://doi.org/10.1038/nm.4294>
- Jose, C., Hébert-Chatelain, E., Bellance, N., Larendra, A., Su, M., Nouette-Gaulain, K., Rossignol, R., 2011. AICAR inhibits cancer cell growth and triggers cell-type distinct effects on OXPHOS biogenesis, oxidative stress and Akt activation. *Biochim. Biophys. Acta BBA - Bioenerg., Bioenergetics of Cancer* 1807, 707–718. <https://doi.org/10.1016/j.bbabi.2010.12.002>
- Kamaguchi, M., Iwata, H., 2019. The Diagnosis and Blistering Mechanisms of Mucous Membrane Pemphigoid. *Front. Immunol.* 10. <https://doi.org/10.3389/fimmu.2019.00034>
- Karsten, C.M., Köhl, J., 2012. The immunoglobulin, IgG Fc receptor and complement triangle in autoimmune diseases. *Immunobiology* 217, 1067–1079. <https://doi.org/10.1016/j.imbio.2012.07.015>
- Karsten, C.M., Pandey, M.K., Figge, J., Kilchenstein, R., Taylor, P.R., Rosas, M., McDonald, J.U., Orr, S.J., Berger, M., Petzold, D., Blanchard, V., Winkler, A., Hess, C., Reid, D.M., Majoul, I.V., Strait, R.T., Harris, N.L., Köhl, G., Wex, E., Ludwig, R., Zillikens, D., Nimmerjahn, F., Finkelman, F.D., Brown, G.D., Ehlers, M., Köhl, J., 2012. Anti-inflammatory activity of IgG1 mediated by Fc galactosylation and association of Fc γ RIIB and dectin-1. *Nat. Med.* 18, 1401–1406. <https://doi.org/10.1038/nm.2862>
- Kasperkiewicz, M., Nimmerjahn, F., Wende, S., Hirose, M., Iwata, H., Jonkman, M.F., Samavedam, U., Gupta, Y., Möller, S., Rentz, E., Hellberg, L., Kalies, K., Yu, X., Schmidt, E., Häslner, R., Laskay, T., Westermann, J., Köhl, J., Zillikens, D., Ludwig, R.J., 2012. Genetic identification and functional validation of Fc γ RIV as key molecule in autoantibody-induced tissue injury: Fc γ RIV in autoantibody-induced tissue injury. *J. Pathol.* 228, 8–19. <https://doi.org/10.1002/path.4023>

- Kasperkiewicz, M., Sadik, C.D., Bieber, K., Ibrahim, S.M., Manz, R.A., Schmidt, E., Zillikens, D., Ludwig, R.J., 2016. Epidermolysis Bullosa Acquisita: From Pathophysiology to Novel Therapeutic Options. *J. Invest. Dermatol.* 136, 24–33. <https://doi.org/10.1038/JID.2015.356>
- Keating, G.M., Scott, L.J., 2004. Moxifloxacin. *Drugs* 64, 2347–2377. <https://doi.org/10.2165/00003495-200464200-00006>
- Kemp, B.E., Stapleton, D., Campbell, D.J., Chen, Z.-P., Murthy, S., Walter, M., Gupta, A., Adams, J.J., Katsis, F., van Denderen, B., Jennings, I.G., Iseli, T., Michell, B.J., Witters, L.A., 2003. AMP-activated protein kinase, super metabolic regulator. *Biochem. Soc. Trans.* 31, 162–168. <https://doi.org/10.1042/bst0310162>
- Kerperien, J., Veening-Griffioen, D., Wehkamp, T., van Esch, B.C.A.M., Hofman, G.A., Cornelissen, P., Boon, L., Jeurink, P.V., Garssen, J., Knippels, L.M.J., Willemsen, L.E.M., 2018. IL-10 Receptor or TGF- β Neutralization Abrogates the Protective Effect of a Specific Nondigestible Oligosaccharide Mixture in Cow-Milk-Allergic Mice. *J. Nutr.* 148, 1372–1379. <https://doi.org/10.1093/jn/nxy104>
- Kim, J.H., Kim, S.-C., 2013. Epidermolysis bullosa acquisita. *J. Eur. Acad. Dermatol. Venereol.* 27, 1204–1213. <https://doi.org/10.1111/jdv.12096>
- Kim, J.H., Kim, Y.H., Kim, S., Noh, E.B., Kim, S.-E., Vorobyev, A., Schmidt, E., Zillikens, D., Kim, S.-C., 2013. Serum levels of anti-type VII collagen antibodies detected by enzyme-linked immunosorbent assay in patients with epidermolysis bullosa acquisita are correlated with the severity of skin lesions: A correlation of ELISA with disease severity in EBA. *J. Eur. Acad. Dermatol. Venereol.* 27, e224–e230. <https://doi.org/10.1111/j.1468-3083.2012.04617.x>
- Kimura, N., Masuda, S., Tanihara, Y., Ueo, H., Okuda, M., Katsura, T., Inui, K., 2005. Metformin is a Superior Substrate for Renal Organic Cation Transporter OCT2 rather than Hepatic OCT1. *Drug Metab. Pharmacokinet.* 20, 379–386. <https://doi.org/10.2133/dmpk.20.379>
- Klein Geltink, R.I., Kyle, R.L., Pearce, E.L., 2018. Unraveling the Complex Interplay Between T Cell Metabolism and Function. *Annu. Rev. Immunol.* 36, 461–488. <https://doi.org/10.1146/annurev-immunol-042617-053019>
- Koga, H., Kasprick, A., López, R., Aulí, M., Pont, M., Godessart, N., Zillikens, D., Bieber, K., Ludwig, R.J., Balagué, C., 2018. Therapeutic Effect of a Novel Phosphatidylinositol-3-Kinase δ Inhibitor in Experimental Epidermolysis Bullosa Acquisita. *Front. Immunol.* 9. <https://doi.org/10.3389/fimmu.2018.01558>
- Koga, H., Prost-Squarcioni, C., Iwata, H., Jonkman, M.F., Ludwig, R.J., Bieber, K., 2019. Epidermolysis Bullosa Acquisita: The 2019 Update. *Front. Med.* 5. <https://doi.org/10.3389/fmed.2018.00362>
- Koga, H., Recke, A., Vidarsson, G., Pas, H.H., Jonkman, M.F., Hashimoto, T., Kasprick, A., Ghorbanalipour, S., Tenor, H., Zillikens, D., Ludwig, R.J., 2016. PDE4 Inhibition as Potential Treatment of Epidermolysis Bullosa Acquisita. *J. Invest. Dermatol.* 136, 2211–2220. <https://doi.org/10.1016/j.jid.2016.06.619>
- Kolesnik, M., Becker, E., Reinhold, D., Ambach, A., Heim, M.U., Gollnick, H., Bonnekoh, B., 2014. Treatment of severe autoimmune blistering skin diseases with combination of protein A immunoadsorption and rituximab: a protocol without initial high dose or pulse steroid medication. *J. Eur. Acad. Dermatol. Venereol.* 28, 771–780. <https://doi.org/10.1111/jdv.12175>
- Kominsky, D.J., Campbell, E.L., Colgan, S.P., 2010. Metabolic Shifts in Immunity and Inflammation. *J. Immunol. Baltim. Md* 1950 184, 4062–4068. <https://doi.org/10.4049/jimmunol.0903002>
- Komorowski, L., Müller, R., Vorobyev, A., Probst, C., Recke, A., Jonkman, M.F., Hashimoto, T., Kim, S.-C., Groves, R., Ludwig, R.J., Zillikens, D., Stöcker, W., Schmidt, E., 2013. Sensitive and specific assays for routine serological diagnosis of epidermolysis bullosa acquisita. *J. Am. Acad. Dermatol.* 68, e89–e95. <https://doi.org/10.1016/j.jaad.2011.12.032>

- Koo, S.-H., Flechner, L., Qi, L., Zhang, X., Screaton, R.A., Jeffries, S., Hedrick, S., Xu, W., Boussouar, F., Brindle, P., Takemori, H., Montminy, M., 2005. The CREB coactivator TORC2 is a key regulator of fasting glucose metabolism. *Nature* 437, 1109–1114. <https://doi.org/10.1038/nature03967>
- Kopecki, Z., Arkell, R.M., Strudwick, X.L., Hirose, M., Ludwig, R.J., Kern, J.S., Bruckner-Tuderman, L., Zillikens, D., Murrell, D.F., Cowin, A.J., 2011. Overexpression of the *Flii* gene increases dermal-epidermal blistering in an autoimmune ColVII mouse model of epidermolysis bullosa acquisita: The role of Flightless in epidermolysis bullosa acquisita. *J. Pathol.* 225, 401–413. <https://doi.org/10.1002/path.2973>
- Kopecki, Z., Ruzehaji, N., Turner, C., Iwata, H., Ludwig, R.J., Zillikens, D., Murrell, D.F., Cowin, A.J., 2013. Topically Applied Flightless I Neutralizing Antibodies Improve Healing of Blistered Skin in a Murine Model of Epidermolysis Bullosa Acquisita. *J. Invest. Dermatol.* 133, 1008–1016. <https://doi.org/10.1038/jid.2012.457>
- Kopecki, Z., Yang, G.N., Arkell, R.M., Jackson, J.E., Melville, E., Iwata, H., Ludwig, R.J., Zillikens, D., Murrell, D.F., Cowin, A.J., 2014. Flightless I over-expression impairs skin barrier development, function and recovery following skin blistering: Flii regulation of skin barrier function. *J. Pathol.* 232, 541–552. <https://doi.org/10.1002/path.4323>
- Kornberg, M.D., 2020. The immunologic Warburg effect: Evidence and therapeutic opportunities in autoimmunity. *Wiley Interdiscip. Rev. Syst. Biol. Med.* 12. <https://doi.org/10.1002/wsbm.1486>
- Kornberg, M.D., Bhargava, P., Kim, P.M., Putluri, V., Snowman, A.M., Putluri, N., Calabresi, P.A., Snyder, S.H., 2018. Dimethyl fumarate targets GAPDH and aerobic glycolysis to modulate immunity. *Science* 360, 449–453. <https://doi.org/10.1126/science.aan4665>
- Kovács, M., Németh, T., Jakus, Z., Sitaru, C., Simon, E., Futosi, K., Botz, B., Helyes, Z., Lowell, C.A., Mócsai, A., 2014. The Src family kinases Hck, Fgr, and Lyn are critical for the generation of the in vivo inflammatory environment without a direct role in leukocyte recruitment. *J. Exp. Med.* 211, 1993–2011. <https://doi.org/10.1084/jem.20132496>
- Kramer, P.A., Ravi, S., Chacko, B., Johnson, M.S., Darley-Usmar, V.M., 2014. A review of the mitochondrial and glycolytic metabolism in human platelets and leukocytes: Implications for their use as bioenergetic biomarkers. *Redox Biol.* 2, 206–210. <https://doi.org/10.1016/j.redox.2013.12.026>
- Kubisch, I., Diessenbacher, P., Schmidt, E., Gollnick, H., Leverkus, M., 2010. Premonitory Epidermolysis Bullosa Acquisita Mimicking Eyelid Dermatitis: Successful Treatment with Rituximab and Protein A Immunoapheresis. *Am. J. Clin. Dermatol.* 1. <https://doi.org/10.2165/11533210-000000000-00000>
- Kulkarni, S., Sitaru, C., Jakus, Z., Anderson, K.E., Damoulakis, G., Davidson, K., Hirose, M., Juss, J., Oxley, D., Chessa, T.A.M., Ramadani, F., Guillou, H., Segonds-Pichon, A., Fritsch, A., Jarvis, G.E., Okkenhaug, K., Ludwig, R., Zillikens, D., Mocsai, A., Vanhaesebroeck, B., Stephens, L.R., Hawkins, P.T., 2011. PI3K Plays a Critical Role in Neutrophil Activation by Immune Complexes. *Sci. Signal.* 4, ra23–ra23. <https://doi.org/10.1126/scisignal.2001617>
- Kulkarni, U., Karsten, C.M., Kohler, T., Hammerschmidt, S., Bommert, K., Tiburzy, B., Meng, L., Thieme, L., Recke, A., Ludwig, R.J., Pollok, K., Kalies, K., Bogen, B., Boettcher, M., Kamradt, T., Hauser, A.E., Langer, C., Huber-Lang, M., Finkelman, F.D., Köhl, J., Wong, D.M., Manz, R.A., 2016. IL-10 mediates plasmacytosis-associated immunodeficiency by inhibiting complement-mediated neutrophil migration. *J. Allergy Clin. Immunol.* 137, 1487–1497.e6. <https://doi.org/10.1016/j.jaci.2015.10.018>
- Kumar, S., Dikshit, M., 2019. Metabolic Insight of Neutrophils in Health and Disease. *Front. Immunol.* 10. <https://doi.org/10.3389/fimmu.2019.02099>
- Kuo, T.T., Baker, K., Yoshida, M., Qiao, S.-W., Aveson, V.G., Lencer, W.I., Blumberg, R.S., 2010. Neonatal Fc Receptor: From Immunity to Therapeutics. *J. Clin. Immunol.* 30, 777–789. <https://doi.org/10.1007/s10875-010-9468-4>

- Le Bourgeois, T., Strauss, L., Aksoylar, H.-I., Daneshmandi, S., Seth, P., Patsoukis, N., Boussiotis, V.A., 2018. Targeting T Cell Metabolism for Improvement of Cancer Immunotherapy. *Front. Oncol.* 8. <https://doi.org/10.3389/fonc.2018.00237>
- Leclerc, I., Lenzner, C., Gourdon, L., Vaulont, S., Kahn, A., Viollet, B., 2001. Hepatocyte Nuclear Factor-4 α Involved in Type 1 Maturity-Onset Diabetes of the Young Is a Novel Target of AMP-Activated Protein Kinase. *Diabetes* 50, 1515–1521. <https://doi.org/10.2337/diabetes.50.7.1515>
- Lee, C.W., 1998. Letters to Dermatology. *Dermatology* 197, 187–196. <https://doi.org/10.1159/000017997>
- Lee, S.-Y., Moon, S.-J., Kim, E.-K., Seo, H.-B., Yang, E.-J., Son, H.-J., Kim, J.-K., Min, J.-K., Park, S.-H., Cho, M.-L., 2017. Metformin Suppresses Systemic Autoimmunity in Roquinsan/san Mice through Inhibiting B Cell Differentiation into Plasma Cells via Regulation of AMPK/mTOR/STAT3. *J. Immunol. Author Choice* 198, 2661–2670. <https://doi.org/10.4049/jimmunol.1403088>
- Leprivier, G., Remke, M., Rotblat, B., Dubuc, A., Mateo, A.-R.F., Kool, M., Agnihotri, S., El-Naggar, A., Yu, B., Somasekharan, S.P., Faubert, B., Bridon, G., Tognon, C.E., Mathers, J., Thomas, R., Li, A., Barokas, A., Kwok, B., Bowden, M., Smith, S., Wu, X., Korshunov, A., Hielscher, T., Northcott, P.A., Galpin, J.D., Ahern, C.A., Wang, Y., McCabe, M.G., Collins, V.P., Jones, R.G., Pollak, M., Delattre, O., Gleave, M.E., Jan, E., Pfister, S.M., Proud, C.G., Derry, W.B., Taylor, M.D., Sorensen, P.H., 2013. The eEF2 Kinase Confers Resistance to Nutrient Deprivation by Blocking Translation Elongation. *Cell* 153, 1064–1079. <https://doi.org/10.1016/j.cell.2013.04.055>
- Li, Y., Xu, S., Mihaylova, M., Zheng, B., Hou, X., Jiang, B., Park, O., Luo, Z., Lefai, E., Shyy, J.Y.-J., Gao, B., Wierzbicki, M., Verbeuren, T.J., Shaw, R.J., Cohen, R.A., Zang, M., 2011. AMPK Phosphorylates and Inhibits SREBP Activity to Attenuate Hepatic Steatosis and Atherosclerosis in Diet-induced Insulin Resistant Mice. *Cell Metab.* 13, 376–388. <https://doi.org/10.1016/j.cmet.2011.03.009>
- Li, Z., Li, D., Tsun, A., Li, B., 2015. FOXP3⁺ regulatory T cells and their functional regulation. *Cell. Mol. Immunol.* 12, 558–565. <https://doi.org/10.1038/cmi.2015.10>
- Liberti, M.V., Dai, Z., Wardell, S.E., Baccile, J.A., Liu, X., Gao, X., Baldi, R., Mehrmohamadi, M., Johnson, M.O., Madhukar, N.S., Shestov, A.A., Christine Chio, I.I., Elemento, O., Rathmell, J.C., Schroeder, F.C., McDonnell, D.P., Locasale, J.W., 2017. Metabolic Control Analysis Uncovers a Predictive Model for Selective Targeting of the Warburg Effect through GAPDH Inhibition with a Natural Product. *Cell Metab.* 26, 648-659.e8. <https://doi.org/10.1016/j.cmet.2017.08.017>
- Liu, R.-T., Zhang, M., Yang, C.-L., Zhang, P., Zhang, N., Du, T., Ge, M.-R., Yue, L.-T., Li, X.-L., Li, H., Duan, R.-S., 2018. Enhanced glycolysis contributes to the pathogenesis of experimental autoimmune neuritis. *J. Neuroinflammation* 15, 51. <https://doi.org/10.1186/s12974-018-1095-7>
- Loftus, R.M., Finlay, D.K., 2016. Immunometabolism: Cellular Metabolism Turns Immune Regulator. *J. Biol. Chem.* 291, 1–10. <https://doi.org/10.1074/jbc.R115.693903>
- Ludwig, R.J., 2013. Clinical Presentation, Pathogenesis, Diagnosis, and Treatment of Epidermolysis Bullosa Acquisita. *ISRN Dermatol.* 2013. <https://doi.org/10.1155/2013/812029>
- Ludwig, R.J., Müller, S., Marques, A. d C., Recke, A., Schmidt, E., Zillikens, D., Möller, S., Ibrahim, S.M., 2012. Identification of Quantitative Trait Loci in Experimental Epidermolysis Bullosa Acquisita. *J. Invest. Dermatol.* 132, 1409–1415. <https://doi.org/10.1038/jid.2011.466>
- Ludwig, R.J., Recke, A., Bieber, K., Müller, S., Marques, A. de C., Banczyk, D., Hirose, M., Kasperkiewicz, M., Ishii, N., Schmidt, E., Westermann, J., Zillikens, D., Ibrahim, S.M., 2011. Generation of Antibodies of Distinct Subclasses and Specificity Is Linked to H2s in an Active Mouse Model of Epidermolysis Bullosa Acquisita. *J. Invest. Dermatol.* 131, 167–176. <https://doi.org/10.1038/jid.2010.248>

- Luke, M.C., Darling, T.N., Hsu, R., Summers, R.M., Smith, J.A., Solomon, B.I., Thomas, G.R., Yancey, K.B., 1999. Mucosal Morbidity in Patients With Epidermolysis Bullosa Acquisita. *Arch. Dermatol.* 135, 954–959. <https://doi.org/10.1001/archderm.135.8.954>
- Luo, F., Das, A., Chen, J., Wu, P., Li, X., Fang, Z., 2019. Metformin in patients with and without diabetes: a paradigm shift in cardiovascular disease management. *Cardiovasc. Diabetol.* 18, 54. <https://doi.org/10.1186/s12933-019-0860-y>
- Macheda, M.L., Rogers, S., Best, J.D., 2005. Molecular and cellular regulation of glucose transporter (GLUT) proteins in cancer. *J. Cell. Physiol.* 202, 654–662. <https://doi.org/10.1002/jcp.20166>
- Maher, J.C., Savaraj, N., Priebe, W., Liu, H., Lampidis, T.J., 2005. Differential Sensitivity to 2-Deoxy-D-glucose Between Two Pancreatic Cell Lines Correlates With GLUT-1 Expression: Pancreas 30, e34–e39. <https://doi.org/10.1097/01.mpa.0000153327.46945.26>
- Maianski, N.A., Geissler, J., Srinivasula, S.M., Alnemri, E.S., Roos, D., Kuijpers, T.W., 2004. Functional characterization of mitochondria in neutrophils: a role restricted to apoptosis. *Cell Death Differ.* 11, 143–153. <https://doi.org/10.1038/sj.cdd.4401320>
- Makowski, L., Chaib, M., Rathmell, J.C., 2020. Immunometabolism: From basic mechanisms to translation. *Immunol. Rev.* 295, 5–14. <https://doi.org/10.1111/imr.12858>
- Manerba, M., Vettriano, M., Fiume, L., Di Stefano, G., Sartini, A., Giacomini, E., Buonfiglio, R., Roberti, M., Recanatini, M., 2012. Galloflavin (CAS 568-80-9): A Novel Inhibitor of Lactate Dehydrogenase. *ChemMedChem* 7, 311–317. <https://doi.org/10.1002/cmdc.201100471>
- Marsin, A.-S., Bertrand†, L., Rider, M.H., Deprez, J., Beauloye, C., Vincent‡, M.F., Berghe‡, G.V. den, Carling, D., Hue, L., 2000. Phosphorylation and activation of heart PFK-2 by AMPK has a role in the stimulation of glycolysis during ischaemia. *Curr. Biol.* 10, 1247–1255. [https://doi.org/10.1016/S0960-9822\(00\)00742-9](https://doi.org/10.1016/S0960-9822(00)00742-9)
- Marzano, A.V., Cozzani, E., Biasin, M., Russo, I., Alaibac, M., 2016. The use of Biochip immunofluorescence microscopy for the serological diagnosis of epidermolysis bullosa acquisita. *Arch. Dermatol. Res.* 308, 273–276. <https://doi.org/10.1007/s00403-016-1632-0>
- Mathis, D., Shoelson, S.E., 2011. Immunometabolism: an emerging frontier. *Nat. Rev. Immunol.* 11, 81–83. <https://doi.org/10.1038/nri2922>
- Menegazzo, L., Scattolini, V., Cappellari, R., Bonora, B.M., Albiero, M., Bortolozzi, M., Romanato, F., Ceolotto, G., Vigili de Kreutzberg, S., Avogaro, A., Fadini, G.P., 2018. The antidiabetic drug metformin blunts NETosis in vitro and reduces circulating NETosis biomarkers in vivo. *Acta Diabetol.* 55, 593–601. <https://doi.org/10.1007/s00592-018-1129-8>
- Mihai, S., Chiriac, M.T., Takahashi, K., Thurman, J.M., Holers, V.M., Zillikens, D., Botto, M., Sitaru, C., 2007. The Alternative Pathway of Complement Activation Is Critical for Blister Induction in Experimental Epidermolysis Bullosa Acquisita. *J. Immunol.* 178, 6514–6521. <https://doi.org/10.4049/jimmunol.178.10.6514>
- Mihai, S., Hirose, M., Wang, Y., Thurman, J.M., Holers, V.M., Morgan, B.P., Köhl, J., Zillikens, D., Ludwig, R.J., Nimmerjahn, F., 2018. Specific Inhibition of Complement Activation Significantly Ameliorates Autoimmune Blistering Disease in Mice. *Front. Immunol.* 9. <https://doi.org/10.3389/fimmu.2018.00535>
- Mihaylova, M.M., Vasquez, D.S., Ravnskjaer, K., Denechaud, P.-D., Yu, R.T., Alvarez, J.G., Downes, M., Evans, R.M., Montminy, M., Shaw, R.J., 2011. Class IIa Histone Deacetylases are Hormone-activated regulators of FOXO and Mammalian Glucose Homeostasis. *Cell* 145, 607–621. <https://doi.org/10.1016/j.cell.2011.03.043>
- Miller, R.A., Birnbaum, M.J., 2010. An energetic tale of AMPK-independent effects of metformin. *J. Clin. Invest.* 120, 2267–2270. <https://doi.org/10.1172/JCI43661>
- Mohammad, G.H., Vassileva, V., Acedo, P., Olde Damink, S.W.M., Malago, M., Dhar, D.K., Pereira, S.P., 2019. Targeting Pyruvate Kinase M2 and Lactate Dehydrogenase A Is an Effective Combination Strategy for the Treatment of Pancreatic Cancer. *Cancers* 11. <https://doi.org/10.3390/cancers11091372>

- Morgan, M.J., Liu, Z., 2011. Crosstalk of reactive oxygen species and NF- κ B signaling. *Cell Res.* 21, 103–115. <https://doi.org/10.1038/cr.2010.178>
- Mortaz, E., Alipoor, S.D., Adcock, I.M., Mumby, S., Koenderman, L., 2018. Update on Neutrophil Function in Severe Inflammation. *Front. Immunol.* 9. <https://doi.org/10.3389/fimmu.2018.02171>
- Müller, R., Dahler, C., Möbs, C., Wenzel, E., Eming, R., Messer, G., Niedermeier, A., Hertl, M., 2010. T and B cells target identical regions of the non-collagenous domain 1 of type VII collagen in epidermolysis bullosa acquisita. *Clin. Immunol.* 135, 99–107. <https://doi.org/10.1016/j.clim.2009.12.010>
- Müller, S., Behnen, M., Bieber, K., Möller, S., Hellberg, L., Witte, M., Hänsel, M., Zillikens, D., Solbach, W., Laskay, T., Ludwig, R.J., 2016. Dimethylfumarate Impairs Neutrophil Functions. *J. Invest. Dermatol.* 136, 117–126. <https://doi.org/10.1038/JID.2015.361>
- Muoio, D.M., Seefeld, K., Witters, L.A., Coleman, R.A., 1999. AMP-activated kinase reciprocally regulates triacylglycerol synthesis and fatty acid oxidation in liver and muscle: evidence that sn-glycerol-3-phosphate acyltransferase is a novel target. *Biochem. J.* 338, 783–791.
- Muramatsu, K., Ujiie, H., Kobayashi, I., Nishie, W., Izumi, K., Ito, T., Yoshimoto, N., Natsuga, K., Iwata, H., Shimizu, H., 2018. Regulatory T-cell dysfunction induces autoantibodies to bullous pemphigoid antigens in mice and human subjects. *J. Allergy Clin. Immunol.* 142, 1818-1830.e6. <https://doi.org/10.1016/j.jaci.2018.03.014>
- Nakamaru, K., Matsumoto, K., Taguchi, T., Suefuji, M., Murata, Y., Igata, M., Kawashima, J., Kondo, T., Motoshima, H., Tsuruzoe, K., Miyamura, N., Toyonaga, T., Araki, E., 2005. AICAR, an activator of AMP-activated protein kinase, down-regulates the insulin receptor expression in HepG2 cells. *Biochem. Biophys. Res. Commun.* 328, 449–454. <https://doi.org/10.1016/j.bbrc.2005.01.004>
- Nath, N., Giri, S., Prasad, R., Salem, M.L., Singh, A.K., Singh, I., 2005. 5-Aminoimidazole-4-Carboxamide Ribonucleoside: A Novel Immunomodulator with Therapeutic Efficacy in Experimental Autoimmune Encephalomyelitis. *J. Immunol.* 175, 566–574. <https://doi.org/10.4049/jimmunol.175.1.566>
- Nath, N., Khan, M., Paintlia, M.K., Hoda, M.N., Giri, S., 2009. Metformin Attenuated the Autoimmune Disease of the Central Nervous System in Animal Models of Multiple Sclerosis. *J. Immunol. Baltim. Md 1950* 182, 8005–8014. <https://doi.org/10.4049/jimmunol.0803563>
- Németh, T., Futosi, K., Sitaru, C., Ruland, J., Mócsai, A., 2016. Neutrophil-specific deletion of the CARD9 gene expression regulator suppresses autoantibody-induced inflammation in vivo. *Nat. Commun.* 7. <https://doi.org/10.1038/ncomms11004>
- Nguyen, G.T., Green, E.R., Meccas, J., 2017. Neutrophils to the ROScUE: Mechanisms of NADPH Oxidase Activation and Bacterial Resistance. *Front. Cell. Infect. Microbiol.* 7. <https://doi.org/10.3389/fcimb.2017.00373>
- Nguyen, T.T., Ung, T.T., Li, S., Lian, S., Xia, Y., Park, S.Y., Do Jung, Y., 2019. Metformin inhibits lithocholic acid-induced interleukin 8 upregulation in colorectal cancer cells by suppressing ROS production and NF- κ B activity. *Sci. Rep.* 9, 2003. <https://doi.org/10.1038/s41598-019-38778-2>
- Niedermeier, A., Eming, R., Pfütze, M., Neumann, C.R., Happel, C., Reich, K., Hertl, M., 2007. Clinical Response of Severe Mechanobullous Epidermolysis Bullosa Acquisita to Combined Treatment With Immunoabsorption and Rituximab (Anti-CD20 Monoclonal Antibodies). *Arch. Dermatol.* 143, 192–198. <https://doi.org/10.1001/archderm.143.2.192>
- Nieman, D.C., Lila, M.A., Gillitt, N.D., 2019. Immunometabolism: A Multi-Omics Approach to Interpreting the Influence of Exercise and Diet on the Immune System. *Annu. Rev. Food Sci. Technol.* 10, 341–363. <https://doi.org/10.1146/annurev-food-032818-121316>
- Nimmerjahn, F., Ravetch, J.V., 2008. Fc γ receptors as regulators of immune responses. *Nat. Rev. Immunol.* 8, 34–47. <https://doi.org/10.1038/nri2206>
- Noe, M.H., Chen, M., Woodley, D.T., Fairley, J.A., 2008. Familial epidermolysis bullosa acquisita. *Dermatol. Online J.* 14.

- O'Neill, L.A.J., Hardie, D.G., 2013. Metabolism of inflammation limited by AMPK and pseudo-starvation. *Nature* 493, 346–355. <https://doi.org/10.1038/nature11862>
- O'Neill, L.A.J., Kishton, R.J., Rathmell, J., 2016. A guide to immunometabolism for immunologists. *Nat. Rev. Immunol.* 16, 553–565. <https://doi.org/10.1038/nri.2016.70>
- Owen, M.R., Doran, E., Halestrap, A.P., 2000. Evidence that metformin exerts its anti-diabetic effects through inhibition of complex 1 of the mitochondrial respiratory chain. *Biochem. J.* 348, 607–614.
- Pålsson-McDermott, E.M., O'Neill, L.A.J., 2020. Targeting immunometabolism as an anti-inflammatory strategy. *Cell Res.* 30, 300–314. <https://doi.org/10.1038/s41422-020-0291-z>
- Pearce, E.J., Pearce, E.L., 2018. Driving immunity: all roads lead to metabolism. *Nat. Rev. Immunol.* 18, 81–82. <https://doi.org/10.1038/nri.2017.139>
- Pike Winer, L.S., Wu, M., 2014. Rapid Analysis of Glycolytic and Oxidative Substrate Flux of Cancer Cells in a Microplate. *PLoS ONE* 9. <https://doi.org/10.1371/journal.pone.0109916>
- Prost-Squarcioni, C., Caux, F., Schmidt, E., Jonkman, M.F., Vassileva, S., Kim, S.C., Iranzo, P., Daneshpazhooch, M., Terra, J., Bauer, J., Fairley, J., Hall, R., Hertl, M., Lehman, J.S., Marinovic, B., Patsatsi, A., Zillikens, D., Werth, V., Woodley, D.T., Murrell, D.F., 2018. International Bullous Diseases Group: consensus on diagnostic criteria for epidermolysis bullosa acquisita. *Br. J. Dermatol.* 179, 30–41. <https://doi.org/10.1111/bjd.16138>
- Rao, X., Zhong, J., Sun, Q., 2014. The heterogenic properties of monocytes/macrophages and neutrophils in inflammatory response in diabetes. *Life Sci.* 116, 59. <https://doi.org/10.1016/j.lfs.2014.09.015>
- Ray, P.D., Huang, B.-W., Tsuji, Y., 2012. Reactive oxygen species (ROS) homeostasis and redox regulation in cellular signaling. *Cell. Signal.* 24, 981–990. <https://doi.org/10.1016/j.cellsig.2012.01.008>
- Recke, A., Sitaru, C., Vidarsson, G., Evensen, M., Chiriac, M.T., Ludwig, R.J., Zillikens, D., 2010. Pathogenicity of IgG subclass autoantibodies to type VII collagen: Induction of dermal-epidermal separation. *J. Autoimmun.* 34, 435–444. <https://doi.org/10.1016/j.jaut.2009.11.003>
- Rego, A.C., Vesce, S., Nicholls, D.G., 2001. The mechanism of mitochondrial membrane potential retention following release of cytochrome c in apoptotic GT1-7 neural cells. *Cell Death Differ.* 8, 995–1003. <https://doi.org/10.1038/sj.cdd.4400916>
- Rena, G., Hardie, D.G., Pearson, E.R., 2017. The mechanisms of action of metformin. *Diabetologia* 60, 1577–1585. <https://doi.org/10.1007/s00125-017-4342-z>
- Rice, C.M., Davies, L.C., Subleski, J.J., Maio, N., Gonzalez-Cotto, M., Andrews, C., Patel, N.L., Palmieri, E.M., Weiss, J.M., Lee, J.-M., Annunziata, C.M., Rouault, T.A., Durum, S.K., McVicar, D.W., 2018. Tumour-elicited neutrophils engage mitochondrial metabolism to circumvent nutrient limitations and maintain immune suppression. *Nat. Commun.* 9, 5099. <https://doi.org/10.1038/s41467-018-07505-2>
- Rosales, C., 2018. Neutrophil: A Cell with Many Roles in Inflammation or Several Cell Types? *Front. Physiol.* 9. <https://doi.org/10.3389/fphys.2018.00113>
- Russell, R.C., Tian, Y., Yuan, H., Park, H.W., Chang, Y.-Y., Kim, J., Kim, H., Neufeld, T.P., Dillin, A., Guan, K.-L., 2013. ULK1 induces autophagy by phosphorylating Beclin-1 and activating Vps34 lipid kinase. *Nat. Cell Biol.* 15, 741–750. <https://doi.org/10.1038/ncb2757>
- Sadeghi, H., Gupta, Y., Möller, S., Samavedam, U.K., Behnen, M., Kasprick, A., Bieber, K., Müller, S., Kalies, K., de Castro Marques, A., Recke, A., Schmidt, E., Zillikens, D., Laskay, T., Mariani, J., Ibrahim, S.M., Ludwig, R.J., 2015a. The retinoid-related orphan receptor alpha is essential for the end-stage effector phase of experimental epidermolysis bullosa acquisita: ROR α in EBA. *J. Pathol.* 237, 111–122. <https://doi.org/10.1002/path.4556>
- Sadeghi, H., Lockmann, A., Hund, A.-C., Samavedam, U.K.S.R.L., Pipi, E., Vafia, K., Hauenschild, E., Kalies, K., Pas, H.H., Jonkman, M.F., Iwata, H., Recke, A., Schön, M.P., Zillikens, D., Schmidt, E., Ludwig, R.J., 2015b. Caspase-1–Independent IL-1 Release Mediates Blister Formation in Autoantibody-Induced Tissue Injury through Modulation of Endothelial

- Adhesion Molecules. *J. Immunol.* 194, 3656–3663.
<https://doi.org/10.4049/jimmunol.1402688>
- Sadik, C.D., Miyabe, Y., Sezin, T., Luster, A.D., 2018. The critical role of C5a as an initiator of neutrophil-mediated autoimmune inflammation of the joint and skin. *Semin. Immunol.* 37, 21–29. <https://doi.org/10.1016/j.smim.2018.03.002>
- Saleh, M.A., Ishii, K., Kim, Y.-J., Murakami, A., Ishii, N., Hashimoto, T., Schmidt, E., Zillikens, D., Shirakata, Y., Hashimoto, K., Kitajima, Y., Amagai, M., 2011. Development of NC1 and NC2 domains of Type VII collagen ELISA for the diagnosis and analysis of the time course of epidermolysis bullosa acquisita patients. *J. Dermatol. Sci.* 62, 169–175.
<https://doi.org/10.1016/j.jdermsci.2011.03.003>
- Samavedam, U.K., Mitschker, N., Kasprick, A., Bieber, K., Schmidt, E., Laskay, T., Recke, A., Goletz, S., Vidarsson, G., Schulze, F.S., Armbrust, M., Schulze Dieckhoff, K., Pas, H.H., Jonkman, M.F., Kalies, K., Zillikens, D., Gupta, Y., Ibrahim, S.M., Ludwig, R.J., 2018. Whole-Genome Expression Profiling in Skin Reveals SYK As a Key Regulator of Inflammation in Experimental Epidermolysis Bullosa Acquisita. *Front. Immunol.* 9.
<https://doi.org/10.3389/fimmu.2018.00249>
- Samavedam, U.K.S.R.L., Iwata, H., Müller, S., Schulze, F.S., Recke, A., Schmidt, E., Zillikens, D., Ludwig, R.J., 2014. GM-CSF Modulates Autoantibody Production and Skin Blistering in Experimental Epidermolysis Bullosa Acquisita. *J. Immunol.* 192, 559–571.
<https://doi.org/10.4049/jimmunol.1301556>
- Samavedam, U.K.S.R.L., Kalies, K., Scheller, J., Sadeghi, H., Gupta, Y., Jonkman, M.F., Schmidt, E., Westermann, J., Zillikens, D., Rose-John, S., Ludwig, R.J., 2013. Recombinant IL-6 treatment protects mice from organ specific autoimmune disease by IL-6 classical signalling-dependent IL-1ra induction. *J. Autoimmun.* 40, 74–85.
<https://doi.org/10.1016/j.jaut.2012.08.002>
- Saraiva, M., O’Garra, A., 2010. The regulation of IL-10 production by immune cells. *Nat. Rev. Immunol.* 10, 170–181. <https://doi.org/10.1038/nri2711>
- Saschenbrecker, S., Karl, I., Komorowski, L., Probst, C., Dähnrich, C., Fechner, K., Stöcker, W., Schlumberger, W., 2019. Serological Diagnosis of Autoimmune Bullous Skin Diseases. *Front. Immunol.* 10. <https://doi.org/10.3389/fimmu.2019.01974>
- Schilf, P., Schmitz, M., Derenda-Hell, A., Thieme, M., Bremer, T., Väh, M., Zillikens, D., Sadik, C.D., 2021. Inhibition of glucose metabolism abrogates the effector phase of bullous pemphigoid-like epidermolysis bullosa acquisita. *J. Invest. Dermatol.* 0.
<https://doi.org/10.1016/j.jid.2021.01.014>
- Schmidt, E., Benoit, S., Bröcker, E.-B., Zillikens, D., Goebeler, M., 2006. Successful Adjuvant Treatment of Recalcitrant Epidermolysis Bullosa Acquisita With Anti-CD20 Antibody Rituximab. *Arch. Dermatol.* 142, 147–150. <https://doi.org/10.1001/archderm.142.2.147>
- Schmidt, E., Zillikens, D., 2013. Pemphigoid diseases. *The Lancet* 381, 320–332.
[https://doi.org/10.1016/S0140-6736\(12\)61140-4](https://doi.org/10.1016/S0140-6736(12)61140-4)
- Schmidt, E., Zillikens, D., 2011. The Diagnosis and Treatment of Autoimmune Blistering Skin Diseases (10.06.2011) [WWW Document]. *Dtsch. Ärztebl.* URL
<https://www.aerzteblatt.de/int/archive/article?id=93032> (accessed 8.10.20).
- Seelig, E., Meyer, S., Timper, K., Nigro, N., Bally, M., Pernicova, I., Schuetz, P., Müller, B., Korbonits, M., Christ-Crain, M., 2017. Metformin prevents metabolic side effects during systemic glucocorticoid treatment. *Eur. J. Endocrinol.* 176, 349–358.
<https://doi.org/10.1530/EJE-16-0653>
- Seo, M., Crochet, R.B., Lee, Y.-H., 2014. Targeting Altered Metabolism—Emerging Cancer Therapeutic Strategies, in: *Cancer Drug Design and Discovery*. Elsevier, pp. 427–448.
<https://doi.org/10.1016/B978-0-12-396521-9.00014-0>
- Sesarman, A., Sitaru, A.G., Oлару, F., Zillikens, D., Sitaru, C., 2008. Neonatal Fc receptor deficiency protects from tissue injury in experimental epidermolysis bullosa acquisita. *J. Mol. Med.* 86, 951–959. <https://doi.org/10.1007/s00109-008-0366-7>

- Sezin, T., Ferreirós, N., Jennrich, M., Ochirbold, K., Seutter, M., Attah, C., Mousavi, S., Zillikens, D., Geisslinger, G., Sadik, C.D., 2020. 12/15-Lipoxygenase choreographs the resolution of IgG-mediated skin inflammation. *J. Autoimmun.* 115, 102528. <https://doi.org/10.1016/j.jaut.2020.102528>
- Sezin, T., Krajewski, M., Wutkowski, A., Mousavi, S., Chakievska, L., Bieber, K., Ludwig, R.J., Dahlke, M., Rades, D., Schulze, F.S., Schmidt, E., Kalies, K., Gupta, Y., Schilf, P., Ibrahim, S.M., König, P., Schwudke, D., Zillikens, D., Sadik, C.D., 2017. The Leukotriene B4 and its Receptor BLT1 Act as Critical Drivers of Neutrophil Recruitment in Murine Bullous Pemphigoid-Like Epidermolysis Bullosa Acquisita. *J. Invest. Dermatol.* 137, 1104–1113. <https://doi.org/10.1016/j.jid.2016.12.021>
- Sezin, T., Murthy, S., Attah, C., Seutter, M., Holtsche, M.M., Hammers, C.M., Schmidt, E., Meshrkey, F., Mousavi, S., Zillikens, D., Nunn, M.A., Sadik, C.D., 2019. Dual inhibition of complement factor 5 and leukotriene B₄ synergistically suppresses murine pemphigoid disease. *JCI Insight* 4. <https://doi.org/10.1172/jci.insight.128239>
- Shchepina, L.A., Pletjushkina, O.Y., Avetisyan, A.V., Bakeeva, L.E., Fetisova, E.K., Izyumov, D.S., Saprunova, V.B., Vysokikh, M.Y., Chernyak, B.V., Skulachev, V.P., 2002. Oligomycin, inhibitor of the F₀ part of H⁺-ATP-synthase, suppresses the TNF-induced apoptosis. *Oncogene* 21, 8149–8157. <https://doi.org/10.1038/sj.onc.1206053>
- Shehata, H.M., Murphy, A.J., Lee, M. Kit S., Gardiner, C.M., Crowe, S.M., Sanjabi, S., Finlay, D.K., Palmer, C.S., 2017. Sugar or Fat?—Metabolic Requirements for Immunity to Viral Infections. *Front. Immunol.* 8. <https://doi.org/10.3389/fimmu.2017.01311>
- Shimanovich, I., Mihai, S., Oostingh, G.J., Ilenchuk, T.T., Bröcker, E.-B., Opendakker, G., Zillikens, D., Sitaru, C., 2004. Granulocyte-derived elastase and gelatinase B are required for dermal–epidermal separation induced by autoantibodies from patients with epidermolysis bullosa acquisita and bullous pemphigoid. *J. Pathol.* 204, 519–527. <https://doi.org/10.1002/path.1674>
- Singh, D., Banerji, A.K., Dwarakanath, B.S., Tripathi, R.P., Gupta, J.P., Mathew, T.L., Ravindranath, T., Jain, V., 2005. Optimizing Cancer Radiotherapy with 2-Deoxy-D-Glucose. *Strahlenther. Onkol.* 181, 507–514. <https://doi.org/10.1007/s00066-005-1320-z>
- Singh, S., Pandey, S., Bhatt, A.N., Chaudhary, R., Bhuria, V., Kalra, N., Soni, R., Roy, B.G., Saluja, D., Dwarakanath, B.S., 2015. Chronic Dietary Administration of the Glycolytic Inhibitor 2-Deoxy-D-Glucose (2-DG) Inhibits the Growth of Implanted Ehrlich’s Ascites Tumor in Mice. *PLoS ONE* 10. <https://doi.org/10.1371/journal.pone.0132089>
- Sitaru, C., 2007. Experimental models of epidermolysis bullosa acquisita. *Exp. Dermatol.* 16, 520–531. <https://doi.org/10.1111/j.1600-0625.2007.00564.x>
- Sitaru, C., Chiriac, M.T., Mihai, S., Büning, J., Gebert, A., Ishiko, A., Zillikens, D., 2006. Induction of Complement-Fixing Autoantibodies against Type VII Collagen Results in Subepidermal Blistering in Mice. *J. Immunol.* 177, 3461–3468. <https://doi.org/10.4049/jimmunol.177.5.3461>
- Sitaru, C., Mihai, S., Otto, C., Chiriac, M.T., Hausser, I., Dotterweich, B., Saito, H., Rose, C., Ishiko, A., Zillikens, D., 2005. Induction of dermal–epidermal separation in mice by passive transfer of antibodies specific to type VII collagen. *J. Clin. Invest.* 115, 870–878. <https://doi.org/10.1172/JCI200521386>
- Son, H.-J., Lee, J., Lee, S.-Y., Kim, E.-K., Park, M.-J., Kim, K.-W., Park, S.-H., Cho, M.-L., 2014. Metformin Attenuates Experimental Autoimmune Arthritis through Reciprocal Regulation of Th17/Treg Balance and Osteoclastogenesis. *Mediators Inflamm.* 2014. <https://doi.org/10.1155/2014/973986>
- Spangenburg, E.E., Jackson, K.C., Schuh, R.A., 2013. AICAR inhibits oxygen consumption by intact skeletal muscle cells in culture. *J. Physiol. Biochem.* 69, 909–917. <https://doi.org/10.1007/s13105-013-0269-0>
- Srinivas, G., Möller, S., Wang, J., Künzel, S., Zillikens, D., Baines, J.F., Ibrahim, S.M., 2013. Genome-wide mapping of gene–microbiota interactions in susceptibility to autoimmune skin blistering. *Nat. Commun.* 4. <https://doi.org/10.1038/ncomms3462>

- Stienstra, R., Netea-Maier, R.T., Riksen, N.P., Joosten, L.A.B., Netea, M.G., 2017. Specific and Complex Reprogramming of Cellular Metabolism in Myeloid Cells during Innate Immune Responses. *Cell Metab.* 26, 142–156. <https://doi.org/10.1016/j.cmet.2017.06.001>
- Sun, M., Wang, R., Han, Q., 2017. Inhibition of leukotriene B4 receptor 1 attenuates lipopolysaccharide-induced cardiac dysfunction: role of AMPK-regulated mitochondrial function. *Sci. Rep.* 7. <https://doi.org/10.1038/srep44352>
- Sun, Y., Tian, T., Gao, J., Liu, X., Hou, H., Cao, R., Li, B., Quan, M., Guo, L., 2016. Metformin ameliorates the development of experimental autoimmune encephalomyelitis by regulating T helper 17 and regulatory T cells in mice. *J. Neuroimmunol.* 292, 58–67. <https://doi.org/10.1016/j.jneuroim.2016.01.014>
- Suwa, M., Nakano, H., Radak, Z., Kumagai, S., 2015. A comparison of chronic AICAR treatment-induced metabolic adaptations in red and white muscles of rats. *J. Physiol. Sci.* 65, 121–130. <https://doi.org/10.1007/s12576-014-0349-0>
- Swamydas, M., Lionakis, M.S., 2013. Isolation, purification and labeling of mouse bone marrow neutrophils for functional studies and adoptive transfer experiments. *J. Vis. Exp. JoVE* e50586. <https://doi.org/10.3791/50586>
- Tanaka, N., Dainichi, T., Ohyama, B., Yasumoto, S., Oono, T., Iwatsuki, K., Elfert, S., Fritsch, A., Bruckner-Tuderman, L., Hashimoto, T., 2009. A case of epidermolysis bullosa acquisita with clinical features of Brunsting-Perry pemphigoid showing an excellent response to colchicine. *J. Am. Acad. Dermatol.* 61, 715–719. <https://doi.org/10.1016/j.jaad.2008.12.020>
- TeSlaa, T., Teitell, M.A., 2014. Techniques to Monitor Glycolysis. *Methods Enzymol.* 542, 91–114. <https://doi.org/10.1016/B978-0-12-416618-9.00005-4>
- The Jackson Laboratory, n.d. Mouse physiological data. Summary – C57BL/6J (000664).
- Tiburzy, B., Szyska, M., Iwata, H., Chrobok, N., Kulkarni, U., Hirose, M., Ludwig, R.J., Kalies, K., Westermann, J., Wong, D., Manz, R.A., 2013. Persistent Autoantibody-Production by Intermediates between Short-and Long-Lived Plasma Cells in Inflamed Lymph Nodes of Experimental Epidermolysis Bullosa Acquisita. *PLoS ONE* 8. <https://doi.org/10.1371/journal.pone.0083631>
- Tsuji, G., Hashimoto-Hachiya, A., Yen, V.H., Takemura, M., Yumine, A., Furue, K., Furue, M., Nakahara, T., 2020. Metformin inhibits IL-1 β secretion via impairment of NLRP3 inflammasome in keratinocytes: implications for preventing the development of psoriasis. *Cell Death Discov.* 6, 1–11. <https://doi.org/10.1038/s41420-020-0245-8>
- Tukaj, S., Bieber, K., Kleszczyński, K., Witte, M., Cames, R., Kalies, K., Zillikens, D., Ludwig, R.J., Fischer, T.W., Kasperkiewicz, M., 2017. Topically Applied Hsp90 Blocker 17AAG Inhibits Autoantibody-Mediated Blister-Inducing Cutaneous Inflammation. *J. Invest. Dermatol.* 137, 341–349. <https://doi.org/10.1016/j.jid.2016.08.032>
- Tukaj, S., Bieber, K., Witte, M., Ghorbanalipour, S., Schmidt, E., Zillikens, D., Ludwig, R.J., Kasperkiewicz, M., 2018. Calcitriol Treatment Ameliorates Inflammation and Blistering in Mouse Models of Epidermolysis Bullosa Acquisita. *J. Invest. Dermatol.* 138, 301–309. <https://doi.org/10.1016/j.jid.2017.09.009>
- Tukaj, S., Hellberg, L., Ueck, C., Hänsel, M., Samavedam, U., Zillikens, D., Ludwig, R.J., Laskay, T., Kasperkiewicz, M., 2015a. Heat shock protein 90 is required for ex vivo neutrophil-driven autoantibody-induced tissue damage in experimental epidermolysis bullosa acquisita. *Exp. Dermatol.* 24, 471–473. <https://doi.org/10.1111/exd.12680>
- Tukaj, S., Zillikens, D., Kasperkiewicz, M., 2015b. Heat shock protein 90: a pathophysiological factor and novel treatment target in autoimmune bullous skin diseases. *Exp. Dermatol.* 24, 567–571. <https://doi.org/10.1111/exd.12760>
- Ursini, F., Russo, E., Pellino, G., D’Angelo, S., Chiaravalloti, A., De Sarro, G., Manfredini, R., De Giorgio, R., 2018. Metformin and Autoimmunity: A “New Deal” of an Old Drug. *Front. Immunol.* 9. <https://doi.org/10.3389/fimmu.2018.01236>

- Vincent, E.E., Coelho, P.P., Blagih, J., Griss, T., Viollet, B., Jones, R.G., 2015. Differential effects of AMPK agonists on cell growth and metabolism. *Oncogene* 34, 3627–3639. <https://doi.org/10.1038/onc.2014.301>
- Vincent, M.F., Bontemps, F., Van den Berghe, G., 1992. Inhibition of glycolysis by 5-amino-4-imidazolecarboxamide riboside in isolated rat hepatocytes. *Biochem. J.* 281, 267–272.
- Vodegel, R.M., de Jong, M.C.J.M., Pas, H.H., Jonkman, M.F., 2002. IgA-mediated epidermolysis bullosa acquisita: Two cases and review of the literature. *J. Am. Acad. Dermatol.* 47, 919–925. <https://doi.org/10.1067/mjd.2002.125079>
- Vorobyev, A., Ludwig, R.J., Schmidt, E., 2017. Clinical features and diagnosis of epidermolysis bullosa acquisita. *Expert Rev. Clin. Immunol.* 13, 157–169. <https://doi.org/10.1080/1744666X.2016.1221343>
- Wang, D.-S., Jonker, J.W., Kato, Y., Kusuhara, H., Schinkel, A.H., Sugiyama, Y., 2002. Involvement of Organic Cation Transporter 1 in Hepatic and Intestinal Distribution of Metformin. *J. Pharmacol. Exp. Ther.* 302, 510–515. <https://doi.org/10.1124/jpet.102.034140>
- Wang, J., Li, Z., Gao, L., Qi, Y., Zhu, H., Qin, X., 2018. The regulation effect of AMPK in immune related diseases. *Sci. China Life Sci.* 61, 523–533. <https://doi.org/10.1007/s11427-017-9169-6>
- Wang, J.-P., Raung, S.-L., Huang, L.-J., Kuo, S.-C., 1998. Involvement of cyclic AMP generation in the inhibition of respiratory burst by 2-phenyl-4-quinolone (YT-1) in rat neutrophils. *Biochem. Pharmacol.* 56, 1505–1514. [https://doi.org/10.1016/S0006-2952\(98\)00265-2](https://doi.org/10.1016/S0006-2952(98)00265-2)
- Wannick, M., Assmann, J.C., Vielhauer, J.F., Offermanns, S., Zillikens, D., Sadik, C.D., Schwaninger, M., 2018. The Immunometabolomic Interface Receptor Hydroxycarboxylic Acid Receptor 2 Mediates the Therapeutic Effects of Dimethyl Fumarate in Autoantibody-Induced Skin Inflammation. *Front. Immunol.* 9. <https://doi.org/10.3389/fimmu.2018.01890>
- Wendt, E.H.U., Schoenrogge, M., Vollmar, B., Zechner, D., 2020. Galloflavin Plus Metformin Treatment Impairs Pancreatic Cancer Cells. *Anticancer Res.* 40, 153–160. <https://doi.org/10.21873/anticancerres.13936>
- Wilcock, C., Bailey, C.J., 1994. Accumulation of metformin by tissues of the normal and diabetic mouse. *Xenobiotica* 24, 49–57. <https://doi.org/10.3109/00498259409043220>
- Wing, J.B., Sakaguchi, S., 2012. Multiple treg suppressive modules and their adaptability. *Front. Immunol.* 3. <https://doi.org/10.3389/fimmu.2012.00178>
- Witte, M., Koga, H., Hashimoto, T., Ludwig, R.J., Bieber, K., 2016. Discovering potential drug-targets for personalized treatment of autoimmune disorders - what we learn from epidermolysis bullosa acquisita. *Expert Opin. Ther. Targets* 20, 985–998. <https://doi.org/10.1517/14728222.2016.1148686>
- Witte, M., Zillikens, D., Schmidt, E., 2018. Diagnosis of Autoimmune Blistering Diseases. *Front. Med.* 5. <https://doi.org/10.3389/fmed.2018.00296>
- Wong, H.-S., Dighe, P.A., Mezera, V., Monternier, P.-A., Brand, M.D., 2017. Production of superoxide and hydrogen peroxide from specific mitochondrial sites under different bioenergetic conditions. *J. Biol. Chem.* 292, 16804–16809. <https://doi.org/10.1074/jbc.R117.789271>
- Woo, C.-H., You, H.-J., Cho, S.-H., Eom, Y.-W., Chun, J.-S., Yoo, Y.-J., Kim, J.-H., 2002. Leukotriene B4 Stimulates Rac-ERK Cascade to Generate Reactive Oxygen Species That Mediates Chemotaxis. *J. Biol. Chem.* 277, 8572–8578. <https://doi.org/10.1074/jbc.M104766200>
- Woodley, Briggaman, R.A., O’Keefe, E.J., Inman, A.O., Queen, L.L., Gammon, W.R., 1984. Identification of the Skin Basement-Membrane Autoantigen in Epidermolysis Bullosa Acquisita. *N. Engl. J. Med.* 310, 1007–1013. <https://doi.org/10.1056/NEJM198404193101602>
- Woodley, Burgeson, R.E., Lunstrum, G., Bruckner-Tuderman, L., Reese, M.J., Briggaman, R.A., 1988. Epidermolysis bullosa acquisita antigen is the globular carboxyl terminus of type VII procollagen. [WWW Document]. <https://doi.org/10.1172/JCI113373>
- Woodley, D.T., Chang, C., Saadat, P., Ram, R., Liu, Z., Chen, M., 2005. Evidence that Anti-Type VII Collagen Antibodies Are Pathogenic and Responsible for the Clinical, Histological, and

- Immunological Features of Epidermolysis Bullosa Acquisita. *J. Invest. Dermatol.* 124, 958–964. <https://doi.org/10.1111/j.0022-202X.2005.23702.x>
- Woodley, D.T., Ram, R., Doostan, A., Bandyopadhyay, P., Huang, Y., Remington, J., Hou, Y., Keene, D.R., Liu, Z., Chen, M., 2006. Induction of Epidermolysis Bullosa Acquisita in Mice by Passive Transfer of Autoantibodies from Patients. *J. Invest. Dermatol.* 126, 1323–1330. <https://doi.org/10.1038/sj.jid.5700254>
- Wu, N., Zheng, B., Shaywitz, A., Dagon, Y., Tower, C., Bellinger, G., Shen, C.-H., Wen, J., Asara, J., McGraw, T.E., Kahn, B.B., Cantley, L.C., 2013. AMPK-dependent degradation of TXNIP upon energy stress leads to enhanced glucose uptake via GLUT1. *Mol. Cell* 49, 1167–1175. <https://doi.org/10.1016/j.molcel.2013.01.035>
- Yan, Y., Kover, K.L., Moore, W.V., 2020. New Insight into Metformin Mechanism of Action and Clinical Application. *Metformin*. <https://doi.org/10.5772/intechopen.91148>
- Yin, Y., Choi, S.-C., Xu, Z., Perry, D.J., Seay, H., Croker, B.P., Sobel, E.S., Brusko, T.M., Morel, L., 2015. Normalization of CD4+ T Cell Metabolism Reverses Lupus. *Sci. Transl. Med.* 7, 274ra18. <https://doi.org/10.1126/scitranslmed.aaa0835>
- Yu, X., Akbarzadeh, R., Pieper, M., Scholzen, T., Gehrig, S., Schultz, C., Zillikens, D., König, P., Petersen, F., 2018. Neutrophil Adhesion Is a Prerequisite for Antibody-Mediated Proteolytic Tissue Damage in Experimental Models of Epidermolysis Bullosa Acquisita. *J. Invest. Dermatol.* 138, 1990–1998. <https://doi.org/10.1016/j.jid.2018.03.1499>
- Zaba, L.C., Fuentes-Duculan, J., Eungdamrong, N.J., Abello, M.V., Novitskaya, I., Pierson, K.C., Gonzalez, J., Krueger, J.G., Lowes, M.A., 2009. Psoriasis is characterized by accumulation of immunostimulatory and Th1/Th17 cell polarizing myeloid dendritic cells. *J. Invest. Dermatol.* 129, 79–88. <https://doi.org/10.1038/jid.2008.194>
- ZHENG, J., 2012. Energy metabolism of cancer: Glycolysis versus oxidative phosphorylation (Review). *Oncol. Lett.* 4, 1151–1157. <https://doi.org/10.3892/ol.2012.928>
- Zhu, L., Zhao, Q., Yang, T., Ding, W., Zhao, Y., 2015. Cellular Metabolism and Macrophage Functional Polarization. *Int. Rev. Immunol.* 34, 82–100. <https://doi.org/10.3109/08830185.2014.969421>
- Zumelzu, C., Roux-Villet, C.L., Loiseau, P., Busson, M., Heller, M., Aucouturier, F., Pendaries, V., Lièvre, N., Pascal, F., Brette, M.-D., Doan, S., Charron, D., Caux, F., Laroche, L., Petit, A., Prost-Squarcioni, C., 2011. Black Patients of African Descent and HLA-DRB1*15:03 Frequency Overrepresented in Epidermolysis Bullosa Acquisita. *J. Invest. Dermatol.* 131, 2386–2393. <https://doi.org/10.1038/jid.2011.231>

6 APPENDIX

6.1 Publications

* Equal contributing first authors

Parts of this work have been published in:

Schilf, P.*, Schmitz, M.*, **Derenda-Hell, A.***, Thieme, M., Bremer, T., Väh, M., Zillikens, D., Sadik, C.D., (2021). "Inhibition of glucose metabolism abrogates the effector phase of bullous pemphigoid-like epidermolysis bullosa acquisita". *Journal of Investigative Dermatology* DOI: <https://doi.org/10.1016/j.jid.2021.01.0142>

6.2 Approvals

All experiments were approved by the Ministerium für Energiewende, Landwirtschaft, Umwelt, Natur und Digitalisierung of the state Schleswig-Holstein with the permission number V 242-2034/2019 (15-2/19) from 22.02.2019 and V242-54182/2019 (15-2/19) from 24.01.2020.

7 ACKNOWLEDGEMENTS

First of all, I would like to thank my supervisor Prof. Dr. Christian Sadik for accepting me into his research group and for his support during the whole process.

I also thank Prof. Detlef Zillikens for giving me the opportunity to conduct my doctoral research at the Department of Dermatology, Lübeck.

Special thanks go to Dr. Paul Schilf for teaching me most of the techniques of performing the experiments and analyzing the data, for his kindness and endless patience.

I am also incredibly grateful to Dr. Sripriya Murthy for her teaching, guidance, and most importantly for her kind words which always motivated me to keep going. Together with Dr. Schilf "you're simply the best!".

Many thanks to Francesca Fagiani for the musical joy she brought into science and motivating each other to write our thesis.

Thanks also to Steffi Wichmann for her help and for the nice conversations during the incubation time.

Thanks to Tabea Bremer, who invited me to the fascinating world of neutrophil isolation and ROS and NETosis experiments.

Thanks to Heike Kross for interesting talks on very important aspects.

Thanks to Sadegh Mousavi for teaching me staining techniques.

Once again, I would like to thank all my colleagues from AG Sadik, you made my stay in Lübeck feel like home. I will never forget that.

I would like to thank Dr. Christian Reichert for giving this thesis the final touch.

I would also like to thank my parents in law, Christa and Günter, for their support, understanding and kindness.

Endless thanks and gratitude go to my parents, Gabriela and Kazimierz, and my sister Marta, for supporting me, pushing me forward, believing in me and loving me. And I know it hasn't always been easy. Dziękuję.

But the biggest appreciation goes to my husband, Sebastian, and to him I dedicate this work. Without his endless support, belief in me, motivating me, I wouldn't be today at this point in my life, and this work would have never been created.